Hinode-V

October 11-14, 2011

Local Organizing Committee:

Kathy Campbell • Jason Conry • Alisdair Davey
Kathy Reeves, Chair • Wendy Roberts • Jonathan Sattelberger

Science Organizing Committee:

Jose Luis Ballester • Thomas Berger • Fausto Cattaneo • Peng-Fei Chen
Ed DeLuca, Chair • Bernard Fleck • Leon Golub • Viggo Hansteen
Ryoko Ishikawa • Ryouhei Kano • Ineke De Moortel
Etienne Pariat • Toshi Shimizu • Harry Warren • David Williams

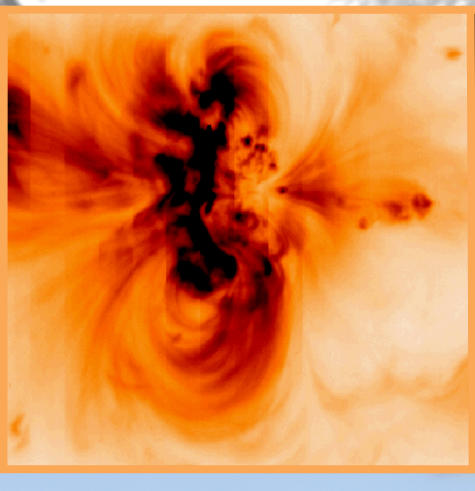

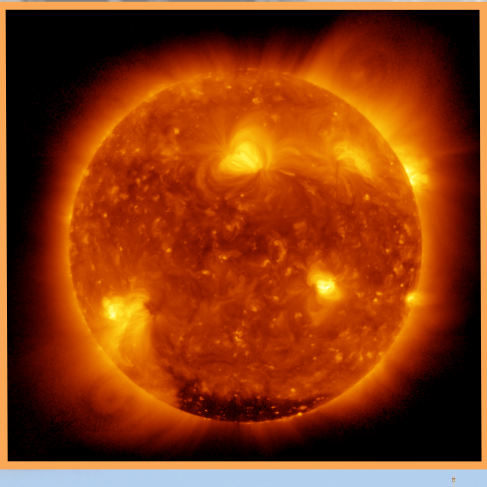

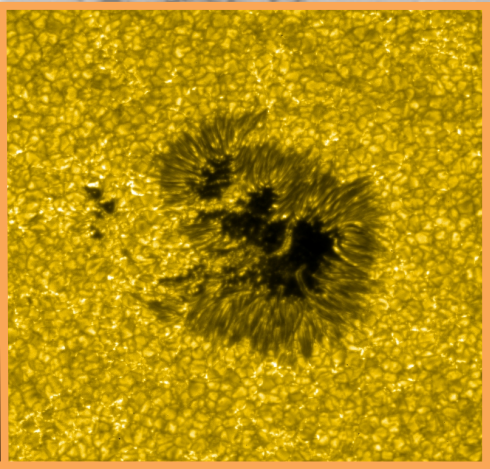

http://hinode5.cfa.harvard.edu

Smithsonian Astrophysical Observatory
NASA
CfA
esa
LUXEL
CMSO
e2v

Acknowledgements

The organizers of the Fifth Hinode Science Conference gratefully acknowledge financial support from the following corporations, institutions and organizations:

e2v Technologies
Chelmsford, Essex UK

ESA. Directorate of Science and Robotic Exploration
Paris France

Japan Society for the Promotion of Science - Core-to-Core Program 22001
Tokyo Japan

Luxel Corporation
Friday Harbor WA USA

NASA, Heliophysics Division
Washington DC, USA

Hinode 5
Exploring the Active Sun

Hinode, the 3rd Japanese led international solar mission, is improving our understanding of the mechanisms that power the solar atmosphere and drive solar eruptions. Launched in 2006, the Hinode satellite is an international collaboration of space agencies, industry and research organizations dedicated to measuring solar magnetic fields. The Hinode-5 meeting will bring scientists from all over the world together to discuss breakthroughs in our understanding of the Sun and the origins of space weather events as we approach the next maximum in solar activity.

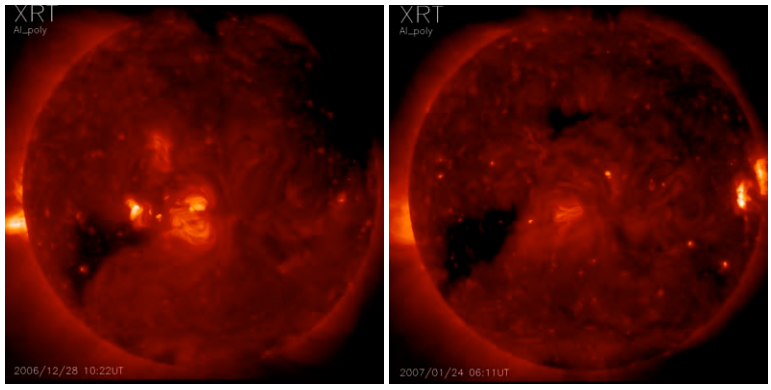

Caption: Two full disk images taken by the X-Ray Telescope aboard Hinode are taken one solar rotation apart. In the center of the left hand image are NOAA active regions 10931 and 10932. A rotation later the active regions have disappeared, but their effect is still noticeable in the long quiet sun loops. Yohkoh experts can comment on whether this was commonly seen by SXT. This type of evolution was seen in Skylab, though not this clearly (1982; ApJ 266, 359-365).

Table of Contents

Extended Table of Contents……...4

Meeting Schedule…..……..9
Monday……....9
Tuesday……...10
Wednesday……..11
Thursday……12
Friday……13
Saturday……..…14

Talk Abstracts……...…15
Invited Talks……....15
Contributed Talks……...29

Poster Abstracts……...…68

Index……..…184

Extended Table of Contents

Meeting Schedule

Acknowledgements **2**

Hinode 5 ..... **3**

Extended Table of Contents **4**

Meeting Schedule **4**

Monday, Oct. 10, 2011 ..... **9**
Tuesday, Oct. 11, 2011 ..... **10**
Wednesday, Oct. 12, 2011 ..... **11**
Thursday, Oct. 13, 2011 ..... **12**
Friday, Oct. 14, 2011 ..... **13**
Saturday, Oct. 15, 2011: Solar-C Meeting and Agenda **14**

Talk Abstracts **15**

Invited Talks **15**

Small-scale structure in the quiet solar atmosphere 16
Properties of transient horizontal magnetic fields; their implication to the origin of quiet-Sun magnetism 17
The Magnetic Diagnostics of the Quiet-Sun Chromosphere 18
Recent progress in observing the emergence of magnetic fields 19
Modeling the Solar Chromosphere 20
Ellerman bomb as a manifestation of chromospheric fine scale activity 21
The Magnetically Closed Corona: A Review of the Coronal Loops Workshop 22
Quantitative study of microflares 23
Coronal mass ejections as a result of magnetic helicity accumulation 24
Solar flares: Energy release, transport and radiation 25
Solar and stellar X-ray activity and the solar-stellar connection 26
The Interface Region Imaging Spectrograph (IRIS) NASA SMEX 27
Solar-C mission with Solar-D on the horizon 28

Talk Abstracts **29**

Contributed Talks **29**

Comparison Of Observations And Advanced Numerical Simulations Of Type II Spicules 30
Numerical Simulation and the SOT Magnetogram Analysis on the Small-scale Magnetic Elements on the Solar Emerging Flux Region 31
Non-thermal broadening of EUV lines in magnetic flux emergence 32
Statistical Study on the Nature of Solar Flux Emergence 33
A rainy day on the Sun 34
Precursor of sunspot penumbral formation discovered with Hinode SOT observations 35
3D Magnetic, Thermal and Velocity Structure of a Sunspot as Observed from Hinode (SOT/SP) 36
The Pre-eruption Behavior of an XRT Sigmoid - NLFFF models and an MHD simulation 37
Quantitative analyses of the 3-D coronal magnetic fields associated with the X3.4 flare event of the solar active region NOAA 10930 38
Polar Faculae: A Proxy for the Evolution of the Solar Polar Field During the Last 100 Years 39

Yearly Variation of Magnetic Field in the Polar Regions Observed with Hinode 40
Observations of supersonic downflows in pores 41
Propagating waves along spicules 42
Using Hinode/SOT to uncover the dynamics of spicules 43
Magnetohydrodynamics of the Partially-Ionized Solar Atmosphere 44
Statistical Study of Chromospheric Anemone Jets Observed With HINODE/SOT 45
Spectroscopic Diagnosis of Propagating disturbances in coronal loops: Waves or flows? 46
Two components of the coronal emission revealed by both spectroscopic and imaging observations 47
What determines coronal-loop temperature? 48
3D Simulations of Wave Heating; where is all the energy? 49
Cambridge Active Region Studies 50
MHD modeling of the heating of coronal loops 51
Non-equlibrium ionization in 3D numerical models 52
Active region plasma outflows and their contribution to the solar wind 53
Self-consistent reconstruction of the solar corona and the solar wind under the Alfvén wave scenario 54
Excitation of Low Frequency Electromagnetic Waves in Magnetic Reconnection Laboratory Experiment 55
Simulations of the magnetic Rayeigh-Taylor instability in the Kippenhahn-Schluter pominence model 56
Forecasting a CME by Spectroscopic Precursor 57
Observations and Magnetic Field Modeling of the Flare/CME Event on 2010 April 8 58
Spectral diagnostics of flare and active region plasma based on EUV spectra from SPIRIT spectroheliograph aboard CORONAS-F 59
Spectroscopic observations of a coronal Moreton wave 60
A New Look at a Classic Flare Structure 61
Observed Features of Magnetic Reconnection in 2007 May 19 Flare 62
Comparative Study of Solar Flare Onset Based on MHD Simulations and Hinode Observations 63
Imaging Spectroscopic Observation of Filament Eruptions by Hinode/EIS Flare Hunting Study 64
Current Sheet and Reconnection Inflow-Outflow Observations During Solar Eruptions 65
The Hanle Effect from Space for Measuring the Magnetic Fields of the Upper Chromosphere 66
The Chromospheric Lyman-Alpha SpectroPolarimeter (CLASP) 67

Poster Abstracts 68

Network boundary study in coronal hole and quiet Sun regions with HINODE/EIS data 69
Bayesian model comparison in spectropolarimetry 70
Pervasive linear polarization signals in the quiet Sun internetwork 71
Proto-sunspots at the beginning of Solar Cycle 24 observed by THEMIS/MTR and Hinode/SOT 72
MHD waves in magnetic bright points: The construction of magnetic waveguides using solar magneto-seismology 73
Net Circular Polarization as a tool to measure the gradient with height of the penumbral magnetic field 74
Visibility of solar prominences in SDO/AIA channels 75
Flux Dependence of cancellation occurrence in Quiet Sun 76
Vortex tubes as a source of acoustic emission in quiet Sun 77
Formation of multi-scale structures in solar magnetoconvection and their dynamics 78

Photospheric Signature of Granular-scale Flux Emergence and Cancellation 79
Multi-wavelength observation of EUV jet in AR 10960 80
A Case for Polar Magnetic Field Diagnostics from the Perspective of the Solar Dynamo 81
CME-related changes in line-of-sight magnetic field strength in dimming regions observed by Hinode on 14 December 2006 82
Magnetic field topology of pores and naked sunspot 83
Convective flows in a sunspot penumbra 84
Diagnosing the Prominence-Cavity Connection 85
Statistics of mass loading of quiescent prominences 86
Understanding chromospheric swirls in the solar corona 87
Spontaneous Pore Formation in Magneto-Convection Simulations 88
Structure and Dynamics of the Quiescent Prominence Eruption on 2010 December 6 89
Hemispheric Helicity Trend for Solar Cycle 24 90
Coronal structure and outflow velocities overlaying network and coronal holes 91
Partial Frequency Redistribution Effects on the Scattering Polarization Pattern of Ly-alpha 92
Time damping of non-adiabatic magnetohydrodynamic waves in a partially ionised prominence medium: Effect of a background flow 93
A high-resolution study of Ca II H time-series as observed with Hinode 94
Flux cancellation events in high-temporal, high-spatial resolution Hinode SOT quiet sun data 95
Comparisons of observed and simulated umbral dots 96
A comparison of flow patterns around coronal structures as observed by Hinode and SDO 97
Structure of the inverse-Evershed flow in sunspots observed by SOT 98
Overturning Convection in Sunspot Penumbra: Observation in Deep Photospheric Spectral Line C I 5380 99
Power spectra of the solar surface convection and implication to local dynamo 100
Comparing Photospheric Magnetic Fields and Subsurface Flows in the Quiet Sun 101
Temperature Structure of a Coronal Cavity 102
The AZAM Disambiguity Utility for the Hinode Spectro-Polarimeter 103
Emergence and disappearance of magnetic field in the quiet Sun at the photosphere 104
Time-distance helioseismology analyses of multi-wavelength datasets obtained with Hinode/SOT and SDO/HMI 105
High-resolution observations of type II spicules 106
On the nature of prominence bubbles and plumes 107
An abrupt magnetization in the upper chromosphere of the quiet Sun 108
Calculating Magnetic Free Energy Using the Minimum Current Corona Model in Evolving Active Regions: NOAA AR11158 109
Some dynamic analysis of the photosphere with HINODE/SOT and SDO 110
Comparison of multi-height observations with a 3D MHD sunspot model 111
Inversion of physical parameters in coronal magnetic structures 112
Differential Emission Measure Analysis of a Polar Coronal Hole During the Recent Solar Minimum 113
EVE non-detection of Doppler-shifted He II 304 Å 114
Power-law index of nanoflares in a coronal loop modified by observational conditions 115
Properties in the North and South Polar Coronal Holes in the Ascending Phase of Solar Cycle 24, and Comparison with the Associated Solar Wind 116
Statistical Analysis of EIS spectra in Active Regions 117
Heating of Flare Foops During a Two-ribbon Flare on 2011 March 07 118
Propagation of Polar Coronal Jets in the Fast Solar Wind 119
What Powers Coronal Heating and the Solar Wind According to Hinode 120

Diagnostics of coronal temperature based on the calibration result of X-Ray Telescope and further calibration 121
DEMs for EIS and AIA 122
Hot plasma detected in active regions by Hinode/XRT and SDO/AIA 123
Simultaneous observation of high temperature plasma of solar corona by TESIS/CORONAS-PHOTON and XRT/Hinode. 124
Elemental abundances, as a new source of uncertainty of the Hinode/XRT filter-ratio temperatures and emission measures of coronal structures. 125
Transverse kink oscillations in threads observed with Hinode 126
Temperature Diagnostics of a solar active region using a Single-filter observation of Hinode/XRT 127
A new model of TSI based on solar surface magnetic energy 128
Explaining observed red and blue-shifts using multi-stranded coronal loops 129
Plasma flows in active region fan loops 130
Signature of Alfvén waves energy deposition above polar coronal holes with Hinode/EIS 131
X-ray and EUV filter responses and AR emission model for the non-thermal kappa-distributions 132
Temperature diagnostic of an Active Region brightening observed by XRT 133
Thermal Evolution of a Coronal Bright Point 134
High-frequency Acoustic Waves in the Solar Atmosphere: Comparing Hinode/SP Observations with Numerical Simulations 135
The mass balance between the chromsphere and corona 136
Simulated vs observed emission measures of the solar corona 137
Propagation of Slow-Modes through the Transition Region in Network Magnetic Elements 138
Observation of Magnetic Fluctuations with Ion Cyclotron Frequency Range during Reconnection in Plasma Merging Experiment 139
Heating of Flare Loops During a Two-ribbon Flare on 2005 May 13 140
Coronal Heating and Magnetic Properties of Solar Active Regions: Confronting the Relationship with High Resolution Observations from Hinode SOT and XRT 141
Thermal properties and evolution of a coronal cavity as observed by the X-Ray Telescope on Hinode 142
Study of Small-Scale Chromospheric Plasmoid Ejections with Improved Hinode Ca II H Filtergrams 143
Laboratory Experiment on Plasma Heating During Magnetic Reconnection in Torus Plasma Merging Device TS-3 and TS-4 144
The role of the magnetic field in the formation of chromospheric spicules 145
High-speed Outflows on Plume-like Structures of the Quiet Sun and Coronal Holes 146
Evidence of magnetic heating of chromosphere 147
Slow-mode oscillations of hot coronal loops excited at flaring footpoints 148
Modeling Slow Speed Solar Wind Streams 149
Time series of synthetic spectra from prominence oscillations 150
Interactions and Eruptions of Two Filaments Observed by Hinode, SOHO, and STEREO 151
Distribution of the Sizes and Fluxes Produced in Patchy Reconnection 152
Asymmetric Magnetic Reconnection in Coronal Mass Ejection Current Sheets 153
X-ray jets and Bright Points: evidence for sympathetic activity 154
Hinode and SDO Observations of the Onset of a CME-Producing Eruption 155
A new view of the structure, evolution and eruption of a polar crown cavity 156
High-Temperature & High-Speed Downflows in an Impulsive Flare of 2011 March 12 157
Statistical Analyses of White-Light Flares observed by Hinode/SOT 158
A High-Velocity Motion of Active Region Loops Triggered by a 2011 Feb 18 Flare 159

The Rayleigh-Taylor Instability in Solar Prominences: a review of Hinode and SDO results .. 160
Differential Emission Measures from the Regularized Inversion of SDO and Hinode data 161
Confirmation of prominence oscillations by simultaneous observations from two remote sites 162
Small Scale Structures inside the Reconnecting Current Sheet: Observations and Theories .. 163
Flare detection in Hinode XRT lightcurves 164
Physical parameters of a blowout jet observed by Hinode XRT and Stereo SECCHI 165
Coronal Rotation from XBPs Observed with Hinode/XRT 166
Structure and Dynamics of Quiescent Prominence Eruptions 167
EUV spectroscopic observations of CME-related kinematics 168
Influence of static and stochastic electric fields on electron beams bombarding the chromosphere 169
RHD Modelling of Solar Flares 170
The Neupert Effect as a Function of Pitch Angle Distribution and Energy Budget in Simulated Flares 171
Study of Solar Flare Energetic Electrons by Using Synthesized Emission Based on Fokker-Planck Simulation Results 172
Solar coronal shocks and particle acceleration as deduced from EUV, radio, and in-situ observations 173
Photometric Uncertainties within XRT 174
The emergent technology of space-qualified liquid-crystal variable retarders for solar remote sensing 175
The X-ray Telescope & Spectrograph - Coronal Instrumentation for the Solar-C Mission 176
Instrument for the Chromospheric Lyman-Alpha SpectroPolarimeter (CLASP) program 177
Observing the Dynamic Sun with SPIES 178
Realistic simulations of the impact of partial ionization on the chromosphere 179
Warm Coronal Rain on Young Solar Analog, EK Draconis? 180
Calibrating the Solar-Stellar Coronal Connection: Using Hinode XRT to Measure Stellar Coronae 181
Mass and Energy Loss Due to CMEs Throughout the Sun's History 182
DEM analysis at impulsive phase footpoints 183

Index 184

Monday, Oct. 10, 2011

Location: University B&C

Start Time	Event
09:00 – 18:00	Hinode Science Working Group Meeting (restricted attendance)
17:00 – 19:30	Hinode-5 Registration
18:00 – 20:00	Reception

Tuesday, Oct. 11, 2011

Location of Talks: Grand Ballroom B

Chair	Start Time	Event
Bernhard Fleck	**08:00**	**Registration Opens**
	08:40 – 09:00	**Welcoming Remarks**
	Session 1	**Magnetic structuring of the Sun from beneath the photosphere through the corona**
	09:00 – 09:40	Invited Talk (1) O. Steiner: Small-scale structure in the quiet solar atmosphere
	09:40 – 10:00	Contributed Talk (1) J. Martinez-Sykora: Comparison Of Observations And Advanced Numerical Simulations Of Type II Spicules
	10:00 – 10:20	Contributed Talk (2) S. Toriumi: Numerical Simulation and the SOT Magnetogram Analysis on the Small-scale Magnetic Elements on the Solar Emerging Flux Region
	10:20 – 10:50	**BREAK/30 minutes**
	10:50 – 11:30	Invited Talk (2) R. Ishikawa: Properties of transient horizontal magnetic fields; their implication to the origin of quiet-Sun magnetism
	11:30 – 11:50	Contributed Talk (3) D. Williams: Non-thermal broadening of EUV lines in magnetic flux emergence
	11:50 – 12:10	Contributed Talk (4) K. Otsuji: Statistical Study on the Nature of Solar Flux Emergence
	12:10 – 13:30	**LUNCH/80 minutes**
Ineke De Moortel	**13:30 – 14:10**	Invited Talk (3) R. Casini: The Magnetic Diagnostics of the Quiet-Sun Chromosphere
	14:10 – 14:30	Contributed Talk (5) Patrick Antolin: A rainy day on the Sun
	14:30 – 14:50	**BREAK/20 minutes**
	14:50 – 16:20	**POSTERS/90 minutes**
	16:20 – 16:40	Contributed Talk (6) T. Shimizu: Precursor of sunspot penumbral formation discovered with Hinode SOT observations
	16:40 – 17:00	Contributed Talk (7) S.K. Tiwari: 3D Magnetic, Thermal and Velocity Structure of a Sunspot as Observed from Hinode (SOT/SP)
	17:00 – 17:20	Contributed Talk (8) A. Savcheva: The Pre-eruption Behavior of an XRT Sigmoid – NLFFF models and an MHD simulation
	17:20 – 17:40	Contributed Talk (9) H. He: Quantitative analyses of the 3-D coronal magnetic fields associated with the X3.4 flare event of the solar active region NOAA 10930
	17:40	**END OF DAY**

Wednesday, Oct. 12, 2011

Location of Talks: Grand Ballroom B

Chair	Start Time	Event
	08:00	**Registration Opens**
Masahito Kubo	**08:30 – 09:10**	Invited Talk (4) F. Hill: Recent progress in observing the emergence of magnetic fields
	09:10 – 09:30	Contributed Talk (10) A. Munoz-Jaramillo: Polar Faculae: A Proxy for the Evolution of the Solar Polar Field During the Last 100 Years
	09:30 – 09:50	Contributed Talk (11) D. Shiota: Yearly Variation of Magnetic Field in the Polar Regions Observed with Hinode
	09:50 – 10:10	Contributed Talk (12) A. Oritz: Observations of supersonic downflows in pores
	10:10 – 10:40	**BREAK/30 minutes**
	Session 2	**Energy transport and dissipation through the solar atmosphere and into the heliosphere**
	10:40 – 11:20	Invited Talk (5) M. Carlsson: Modeling the Solar Chromosphere
	11:20 – 11:40	Contributed Talk (13) J. Okamoto: Propagating waves along spicules
	11:40 – 12:00	Contributed Talk (14) T. Pereira: Using Hinode/SOT to uncover the dynamics of spicules
	12:00 – 13:20	**LUNCH/80 minutes**
Brigitte Schmieder	**13:20 – 14:00**	Invited Talk (6) R. Kitai: Ellerman bomb as a manifestation of chromospheric fine scale activity
	14:00 – 14:20	Contributed Talk (15) M. Cheung: Magnetohydrodynamics of the Partially-Ionized Solar Atmosphere
	14:20 – 14:40	Contributed Talk (16) N. Nishizuka: Statistical Study of Chromospheric Anemone Jets Observed With HINODE/SOT
	14:40 – 15:00	**BREAK/20 minutes**
	15:00 – 16:30	**POSTERS/90 minutes**
	16:30 – 16:50	Contributed Talk (17) T. Wang: Spectroscopic Diagnosis of Propagating disturbances in coronal loops: Waves or flows?
	16:50 – 17:10	Contributed Talk (18) H. Tian: Two components of the coronal emission revealed by both spectroscopic and imaging observations
	17:10 – 17:30	Contributed Talk (19) R. Kano: What determines coronal-loop temperature?
	17:30	**END OF DAY**

Thursday, Oct. 13, 2011

Location of Talks: Grand Ballroom B

Chair	Start Time	Event
	08:00	**Registration Opens**
Harry Warren	**08:30 – 09:10**	Invited Talk (7) A. Winebarger: The Magnetically Closed Corona: A Review of the Coronal Loops Workshop
	09:10 – 09:30	Contributed Talk (20) I. De Moortel: 3D Simulations of Wave Heating; where is all the energy?
	09:30 – 09:50	Contributed Talk (21) H. Mason: Cambridge Active Region Studies
	09:50 – 10:10	Contributed Talk (22) M. Guarrasi: MHD modeling of the heating of coronal loops
	10:10 – 10:40	**BREAK/30 minutes**
	10:40 – 11:20	Invited Talk (8) S. Kamio: Quantitative study of microflares
	11:20 – 11:40	Contributed Talk (23) K. Olluri: Non-equlibrium ionization in 3D numerical models
	11:40 – 12:00	Contributed Talk (24) L. Culhane: Active region plasma outflows and their contribution to the solar wind
	12:00 – 13:20	**LUNCH/80 minutes**
Paola Testa	**13:20 – 13:40**	Contributed Talk (25) T. Matsumoto: Self-consistent reconstruction of the solar corona and the solar wind under the Alfven wave scenario
	Session 3	**Instabilities, Transients and Eruptions**
	13:40 – 14:20	Invited Talk (9) M. Zhang: Coronal mass ejections as a result of magnetic helicity accumulation
	14:20 – 14:40	Contributed Talk (26) M. Inomoto: Excitation of Low Frequency Electromagnetic Waves in Magnetic Reconnection Laboratory Experiment
	14:40 – 15:00	**BREAK/20 minutes**
	15:00 – 16:30	**POSTERS/90 minutes**
	16:30 – 16:50	Contributed Talk (27) A. Hillier: Simulations of the magnetic Rayeigh-Taylor instability in the Kippenhahn-Schluter pominence model
	16:50 – 17:10	Contributed Talk (28) D. Baker: Forecasting a CME by Spectroscopic Precursor
	17:10 – 17:30	Contributed Talk (29) Y. Su: Observations and Magnetic Field Modeling of the Flare/CME Event on 2010 April 8
	17:30	**END OF DAY**
	18:30 – 21:10	**Conference Dinner**

Friday, Oct. 14, 2011

Location of Talks: Grand Ballroom B

Chair	Start Time	Event
	08:00	**Registration Opens**
Tom Berger	**08:30 – 08:50**	Contributed Talk (30) S. Shestov: Spectral diagnostics of flare and active region plasma based on EUV spectra from SPIRIT spectroheliograph aboard CORONAS-F
	08:50 – 09:30	Invited Talk (10) L. Fletcher: Solar flares: Energy release, transport and radiation
	09:30 – 09:50	Contributed Talk (31) L. Harra: Spectroscopic observations of a coronal Moreton wave
	09:50 – 10:10	**BREAK/20 minutes**
	10:10 – 11:40	**POSTERS/90 minutes**
	11:40 – 13:00	**LUNCH/80 munutes**
Kathy Reeves	**13:00 – 13:20**	Contributed Talk (32) S. Guidoni: A New Look at a Classic Flare Structure
	13:20 – 13:40	Contributed Talk (33) H. Hara: Observed Features of Magnetic Reconnection in 2007 May 19 Flare
	13:40 – 14:00	Contributed Talk (34) K. Kusano: Comparative Study of Solar Flare Onset Based on MHD Simulations and Hinode Observations
	14:00 – 14:20	Contributed Talk (35) S. Imada: Imaging Spectroscopic Observation of Filament Eruptions by Hinode/EIS Flare Hunting Study
	14:20 – 14:40	Contributed Talk (36) S. Savage: Current Sheet and Reconnection Inflow-Outflow Observations During Solar Eruptions
	Session 4	**Solar-Stellar Connections**
	14:40 – 15:20	Invited Talk (11) P. Testa: Solar and stellar X-ray activity and the solar-stellar connection
	15:20 – 15:40	**BREAK/20 minutes**
	Session 5	**Future Needs - Observational, Theoretical and Computational**
	15:40 – 16:00	Invited Talk (12) B. De Pontieu: The Interface Region Imaging Spectrograph (IRIS) NASA SMEX
	16:00 – 16:20	Invited Talk (13) S. Tsuneta: Solar-C mission with Solar-D on the horizon
	16:20 – 16:40	Contributed Talk (37) J. Trujillo Bueno: The Hanle Effect from Space for Measuring the Magnetic Fields of the Upper Chromosphere
	16:40 – 17:00	Contributed Talk (38) K. Kobayashi: The Chromospheric Lyman-Alpha SpectroPolarimeter (CLASP)
	17:00	**END OF DAY**

Saturday, Oct. 15, 2011: Solar-C Meeting and Agenda

Location: Charles Suites

Start Time	Event
09:00	Solar-C status and Science Goals overview (Tsuneta, JAXA Solar-C SWG chair)
09:30	SUVIT overview (Ichimoto)
09:45	EUV instrument overview (Shimizu)
10:00	X-ray instrument overview (Sakao)
10:15	Coffee
10:30	Spacecraft overview (Katsukawa)
10:45 – 11:05	Structural connection talk (Dan Longcope)
11:15 – 11:35	Energy transport from Chromosphere to corona (Phil Judge)
11:45 – 12:05	Coronal energy release-observational evidence (Harry Warren)
12:15 – 12:35	The entire atmosphere (Spiro Antiochos)
12:40	**LUNCH**
14:00	Panel discussion on mission science objectives
16:00	Agency discussions (**closed**)
17:30	**END OF MEETING**

Talk Abstracts

Invited Talks

Small-scale structure in the quiet solar atmosphere

Abstract Author(s): Steiner, O.
Institution(s): Kiepenheuer-Institut für Sonnenphysik
Email: steiner@kis.uni-freiburg.de
Session: Magnetic structuring of the Sun from beneath the photosphere through the corona
Presentation: IT-1

Abstract:

With ever increasing spatial resolution due to larger telescope apertures, more powerful adaptive optics, refined image-restoration techniques, and observations from the space and the stratosphere, more and more substructure of the quiet Sun atmosphere becomes visible. At the same time, three-dimensional MHD-simulations have become more numerous and refined in spatial resolution, and a greater variety of initial and boundary conditions are considered. Magnetoconvection simulations are now also used for carrying out numerical experiments targeted at specific processes like the conversion of wave modes or seismic wave propagation.

A recent focus of interest concerns vortical flows. Signatures of various vortical flows have been discovered by feature tracking and spectroscopic observations in the photosphere and the chromosphere. These discoveries are complemented with analyses of numerical simulations, which lead to new insights and predictions.

With respect to the magnetic field, observations with the Solar Optical Telescope of the Hinode space observatory have revealed parts of the hitherto so-called ‘hidden’ magnetic flux and made it accessible to Zeeman polarimetry. It was found that the magnetic field of the quiet Sun atmosphere is not homogeneously turbulent but that it shows structure in the form of tiny loops and flux concentrations and that it points predominantly in the horizontal direction. The origin of this field remains enigmatic. Is it all generated by the surface dynamo? To what extent does it consist of recycled field of decaying active regions? The propagation of magnetoacoustic waves in such a magnetically complex structured atmosphere has just started to become subject of intense research. It seems that conversion from slow, predominantly acoustic waves to fast, predominantly magnetic waves near the surface of plasma-beta unity is responsible for the measured reduction of wave travel-time in magnetic areas and for the so called magnetic shadow.

Properties of transient horizontal magnetic fields; their implication to the origin of quiet-Sun magnetism

Abstract Author(s): Ishikawa, R.
Institution(s): National Astronomical Observatory of Japan
Email: ryoko.ishikawa@nao.ac.jp
Session: Magnetic structuring of the Sun from beneath the photosphere through the corona
Presentation Type: IT-2

Abstract:

The origin and evolution of the quiet-Sun magnetic fields are not well understood. Hinode/SOT with high spatial resolution and high polarization sensitivity reveals that there are a lot of transient horizontal magnetic fields in the internetwork region and provides us with new insight to better understand the quiet-Sun magnetism. Exploiting the SOT data with careful treatment of photon noise, we reveal the enigmatic properties of these horizontal magnetic fields such as lifetime, size, position in terms of granular structure, occurrence rate, three-dimensional structure and so on. Comparing the properties of these horizontal fields between the quiet Sun and plage region, we conclude that they are generated by the local dynamo process due to the granular convective motion. Furthermore, we broaden our scope to clarify the origin and the properties of the internetwork magnetic fields, both vertical and horizontal, in a unified way, and reveal the clear positional association between the vertical and horizontal magnetic fields. We also investigate the relationship of these magnetic fields with the meso- and super-granulations. Based on the observational results, we conjecture that internetwork magnetic fields are formed by the emergence of small-scale horizontal magnetic fields with bipolar footpoints, and the vertical magnetic fields of the footpoints are advected by the supergranular flow, and eventually form the network fields.

The Magnetic Diagnostics of the Quiet-Sun Chromosphere

Abstract Author(s): Casini, R.
Institution(s): High Altitude Observatory (HAO)
Email: casini@hao.ucar.edu
Session: Magnetic structuring of the Sun from beneath the photosphere through the corona
Presentation: IT-3

Abstract:

This decade will offer tremendous new opportunities to deepen our understanding of the Sun's magnetism. Both ground-based and space-borne instruments currently being developed (ATST, EST, Solar-C) are specifically designed to deliver spectro-polarimetric data of unprecedented quality. The spatial and temporal resolutions offered by these instruments will be adequate to attain critical observations that can realistically constrain the sophisticated modelings of the time-varying solar atmosphere, which are also being developed at this time. In particular, the magnetic diagnostics of the quiet-sun chromosphere represents the next big challenge, in order to bridge our picture of the Sun's magnetism from the deep layers of the photosphere into the lower solar corona. In this talk we focus our attention on the identification of target spectral lines in the solar chromosphere, the magnetic regimes that they would help unveil, and the diagnostic tools needed for their interpretation.

Recent progress in observing the emergence of magnetic fields

Abstract Author(s): Hill, F.
Institution(s): National Solar Observatory
Email: fhill@noao.edu
Session: Magnetic structuring of the Sun from beneath the photosphere through the corona
Presentation: IT-4

Abstract:
Helioseismology allows us to probe below the visible photosphere, holding out the hope that we can forecast surface magnetic field behavior. If possible, such forecasts would be valuable for space weather and could help to mitigate the adverse effects of geomagnetic storms on society and technology. In this talk I will present four approaches that could lead to useful predictions. The first study uses global helioseismology to detect the large-scale zonal and meridional flows below the surface that appear to be intimately linked with the long-term behavior of the solar cycle. The second study uses local helioseismology to observe the temporal evolution of vorticity below active regions and associated flare production. The third study uses acoustic holography to detect active regions that emerge on the farside of the sun, which can be compared to STEREO observations. The final line of research uses local helioseismology to detect changes in vertical velocity and p-mode travel times associated with active regions before they emerge on the solar surface. The current status and prospects for these methods will be presented.

Modeling the Solar Chromosphere

Abstract Author(s): Carlsson, M., Hansteen, V. H., Gudiksen, B.V.
Institution(s): Institute of Theoretical Astrophysics, University of Oslo
Email: mats.carlsson@astro.uio.no
Session: Energy transport and dissipation through the solar atmosphere and into the heliosphere
Presentation: IT-5

Abstract:

The enigmatic chromosphere is the transition between the solar surface and the eruptive outer solar atmosphere. The chromosphere harbors and constrains the mass and energy loading processes that define the heating of the corona, the acceleration and the composition of the solar wind, and the energetics and triggering of solar outbursts. In spite of its importance, the chromosphere is arguably the least understood domain of solar physics. All at once it represents the transition from optically thick to thin radiation escape, from gas-pressure to magnetic-pressure domination, from neutral to ionised state, from MHD to plasma physics, and from near-equilibrium ("LTE") to non-equilibrium conditions. Its physics is so complex that traditional methods relying on analytic analysis or simplified mechanisms do not work. It has become abundantly clear that only ab-initio numerical simulation, built on the same fundamental non-linear physics equations that the Sun obeys, and explicitly accompanied by sufficiently deep subsequent analysis of what occurs within each simulation, can deliver physical insight to understand how the chromosphere works. We here report on recent results from such numerical simulations with the Bifrost code. The 3D radiation MHD equations are solved for a computational region extending from the convection zone into the corona for various initial magnetic field configurations. We include conduction along magnetic field lines, optically thin radiative losses in the corona, non-LTE radiative losses in the chromosphere, heating from incoming radiation from the corona and full radiative transfer including scattering in the photosphere. Effects of the hydrogen ionization balance being out of equilibrium are also discussed.

Ellerman bomb as a manifestation of chromospheric fine scale activity

Abstract Author(s): Kitai, R.
Institution(s): Kwasan and Hida Observatories, Kyoto University
Email: kitai@kwasan.kyoto-u.ac.jp
Session: Energy transport and dissipation through the solar atmosphere and into the heliosphere
Presentation Type: IT-6

Abstract:

Since their findings in 1917, Ellerman bombs have been studied as one of the small-scale chromospheric activities in active regions. As their wide H-alpha emission profiles resemble those of flare kernels, these bombs have been believed to be driven by similar mechanism as solar flares. However, the atmospheric structure and dynamic state of these fine scale structure have not observationally been cleared due to the atmospheric degradation in ground-based observations. Recent instrumental developments in ground-based and space observations, such as SOT/Hinode, have considerably advanced our understanding of the magnetohydrodynamic states in Ellerman bombs. With spectroscopic and monochromatic imaging observations, we now have a view that Ellerman bombs are driven by intermittent magnetic reconnection in upper photosphere or in lower chromosphere. A review of our study and present understanding of Ellerman bombs will be given in this paper.

The Magnetically Closed Corona: A Review of the Coronal Loops Workshop

Abstract Author(s): Winebarger, A.
Institution(s): NASA MSFC
Email: amy.r.winebarger@nasa.gov
Session: Energy transport and dissipation through the solar atmosphere and into the heliosphere
Presentation: IT-7

Abstract:

Coronal loops are the magnetically closed structures that direct the flow of hot plasma in the solar atmosphere. The observational properties of loops, including their lifetime, evolution, and temperature indicate that there are different classes of loops and that the different classes have different heating magnitudes and timescales. The classes of loops can be related to the loop length and magnetic field strength, with shorter loops associated with stronger magnetic field being hotter and steadier than longer loops associated with weaker field. There has been significant effort to model the observational properties of loops with both 1-D and 3-D hydrodynamic models and 3-D magneto-hydrodynamic models, however no model has been able to well reproduce all the observations. In this talk, I will review the latest observations, simulations, and theoretical models of coronal loops presented at the Fifth Coronal Loops workshop held in Palma Mallorca, Spain in June 2011.

Quantitative study of microflares

Abstract Author(s): Kamio, S.
Institution(s): MPS
Email: skamio@spd.aas.org
Session: Energy transport and dissipation through the solar atmosphere and into the heliosphere
Presentation: IT-8

Abstract:
Microflares are small transient brightenings in the corona, which are often observed in X-ray and EUV. Although the scale is different, they share common characteristics with ordinary flares in active regions. One of the advantages of studying these small-scale events is that they are frequently observed and show simple structure. First, we review the properties of microflares observed by X-ray and EUV telescopes. We also present the temporal evolution of flaring bright points captured by EIS and XRT. The lightcurves at different temperatures can be interpreted as a cooling of small flare loops. Coronal jets and dimmings associated with the bright points reflects the magnetic field structures in the surrounding.

Coronal mass ejections as a result of magnetic helicity accumulation

Abstract Author(s): Zhang, M.
Institution(s): National Astronomical Observatory of China
Email: zhangmei@bao.ac.cn
Session: Instabilities, Transients and Eruptions
Presentation: IT-9

Abstract:
Coronal mass ejections (CMEs) are a major form of solar activities. A CME takes away a body of plasma from the low corona into the solar wind and disturbs the near-Earth space if the CME is earth-directed. Here we summarize our understandings and reasoning that lead us to conclude that CMEs are the unavoidable products of magnetic helicity accumulation in the corona. Our study puts the formation of magnetic flux rope and CME eruption as the natural results of solar coronal evolution. Our study also gives insights into the observed associations of CMEs with the magnetic features at their solar surface origins.

Solar flares: Energy release, transport and radiation

Abstract Author(s): Fletcher, L.
Institution(s): School of Physics and Astronomy, University of Glasgow
Email: lyndsay.fletcher@glasgow.ac.uk
Session: Instabilities, Transients and Eruptions
Presentation: IT-10

Abstract:

Magnetic free energy in a flaring active region is built up over timescales of many hours to days, and stored on large spatial scales. It is released on much shorter timescales during a rapid restructuring of the field and converted primarily into the kinetic energy of non-thermal particles and chromospheric radiation in the flare impulsive phase. The observationally determined properties of solar flares such as overall energy budget and distribution in space, time and energy of flare radiation, have improved enormously over the last cycle. This has enabled precision diagnostics of flare plasmas and nonthermal particles, informing and driving new theoretical modeling. The theoretical challenges in understanding this process are considerable, involving MHD and kinetic processes operating in an environment that is far from equilibrium, but progress is being made. New observations have also provided some challenges to long-standing models of flare energy release and transport. This talk will overview recent solar flare observational and theoretical developments, and highlight some important questions for the future.

Solar and stellar X-ray activity and the solar-stellar connection

Abstract Author(s): Testa, P.
Institution(s): Harvard-Smithsonian Center for Astrophysics
Email: ptesta@cfa.harvard.edu
Session: Solar-Stellar Connections
Presentation: IT-11

Abstract:

Magnetic activity similar to that of the Sun is observed in solar-like stars. The corona of our Sun is, to date, the only stellar corona that can be spatially resolved and studied at a high level of detail, and it is therefore often used as paradigm for the interpretation of the X-ray activity of other solar-like stars. Stellar astrophysics, on the other hand, allows us to place the Sun in a more general stellar context, and, by providing access to a wide range of stellar parameters (e.g., mass, age, rotation period, multiplicity), it allows us to investigate the characteristics of dynamo mechanisms in very different regimes, and the consequent differences in the properties of coronal emission. I will discuss recent advances and outstanding questions concerning our understanding of the Sun as a star and how far the solar analogy can be extended to other stars, with particular focus on the X-ray emission from the Sun and other stars, activity cycles, solar and stellar flares, and chemical fractionation in stellar outer atmospheres.

The Interface Region Imaging Spectrograph (IRIS) NASA SMEX

Abstract Author(s): De Pontieu, B. (1), Title, A. (1), Lemen, J. (1), Schrijver, C.J. (1), Tarbell, T.D. (1), Wuelser, J.-P. (1), Golub, L. (2), Kankelborg, C. (3), Carlsson, M. (4), Hansteen, V., (4)
Institution(s): (1) Lockheed Martin Solar & Astrophysics Laboratory, Palo Alto, CA, (2), Harvard Smithsonian Center for Astrophysics, Cambridge, MA, (3), Montana State University, Bozeman, MT, (4) Institute of Theoretical Astrophysics, University of Oslo, Norway
Email: bdp@lmsal.com
Session: Future Needs - Observational, Theoretical and Computational
Presentation: IT-12

Abstract:

The solar chromosphere and transition region (TR) form a highly structured and dynamic interface region between the photosphere and the corona. This region not only acts as the conduit of all mass and energy feeding into the corona and solar wind, it also requires an order of magnitude more energy to heat than the corona. Nevertheless, the chromosphere remains poorly understood, because of the complexity of the required observational and analytical tools: the interface region is highly complex with transitions from optically thick to optically thin radiation, from pressure to magnetic field domination, and large density and temperature contrasts on small spatial scales. The Interface Region Imaging Spectrograph (IRIS) was selected for a NASA SMEX mission in 2009 and is scheduled to launch in December 2012. IRIS addresses critical questions: (1) Which types of non-thermal energy dominate in the chromosphere and beyond? (2) How does the chromosphere regulate mass and energy supply to the corona and heliosphere? (3) How do magnetic flux and matter rise through the lower atmosphere, and what role does flux emergence play in flares and mass ejections? These questions are addressed with a high-resolution near and far UV imaging spectrometer sensitive to emission from plasma at temperatures between 5,000 K and 10 MK. IRIS has a field-of-view of 120 arcsec, a spatial resolution of 0.4 arcsec, and velocity resolution of 0.5 km/s. The IRIS investigation includes a strong numerical modeling component based on advanced radiative MHD codes to facilitate interpretation of observations. We will highlight some of the issues that IRIS is expected to help resolve, describe the IRIS instrumentation and numerical modeling, and present the status of the IRIS observatory development.

Solar-C mission with Solar-D on the horizon

Abstract Author(s): Tsuneta, S. (1), Solar-C Working Group (2)
Institution(s): (1) National Astronomical Observatory of Japan, (2) ISAS/JAXA
Email: saku.tsuneta@nao.ac.jp
Session: Future Needs - Observational, Theoretical and Computational
Presentation: IT-13

Abstract:

The purpose of the Solar-C mission is to reveal the magnetic and plasma structures of the whole solar atmosphere from the photosphere throughout the corona, and understand the mechanisms of chromospheric and coronal heating/dynamism and acceleration of the solar wind as a system. It is our understanding that small scale processes related to waves, shocks and reconnection play an important role in the global phenomena of the Sun and the heliosphere.

Our approach to implement this science goal is through high resolution imaging spectroscopy for the entire solar atmosphere without gaps in temperature coverage where plasma might escape detection because of lack of instrumental sensitivity. Hinode clearly showed that the combination of high spatial resolution and spectroscopy (including spectro-polarimetry) is critically important both in the photosphere and in the corona. The strawman instruments for the Solar-C satellite include a larger visible light telescope, which obtains magnetic and velocity maps for the chromosphere and the photosphere, a high-throughput UV imaging spectrometer covering the chromosphere through the corona, and an X-ray/EUV imaging spectrometer. The three instruments will seamlessly cover the photosphere through the corona. Such a wide spectroscopic coverage with high resolution is not available with any mission so far launched. The Solar-C instruments are characterized by high spatial and spectral resolution, high throughput, wide temperature coverage, and high time resolution, better than available from any existing missions.

An Interim Report of the mission is available now. The document describes the current state of development for the Solar-C mission concept. As the program progresses we will continue to solicit new ideas and improvements to the mission definitions, especially from our colleagues outside Japan. We recognize that Solar-C will only be realized with the enthusiastic participation of NASA and ESA in all phases of its development from the conceptual design of the instruments, through their construction, and in the science operation of the Solar-C mission.

Since plan A is as important as Solar-C for our future and it will require a long time to be ready for one mission, we desire to continue activities for plan A as a Solar-D program. This includes preparation of a mission called DESTINY (PI: Dr. Y. Kawakatsu, kawakatsu.yasuhiro@jaxa.jp, Department of Space Systems and Astronautics, ISAS/JAXA) for the ISAS small satellite announcement of opportunity to be expected in 2012: it is essentially a technology demonstration satellite for a large ion engine, a ultra-light weight solar paddle, autonomous onboard operation, and advanced orbit design and control, all to be used in Solar-D program. The plan is to launch DESTINY to L2 in 2016-2017 time frame. In parallel with the Solar-C development, ISAS/JAXA may allocate some resources to run the basic development program for the Solar-D mission.

Talk Abstracts

Contributed Talks

Comparison Of Observations And Advanced Numerical Simulations Of Type II Spicules

Abstract Author(s): Martinez-Sykora, J. (1,2) De Pontieu, B. (1) Hansteen, V. H. (2) Moreno-Insertis, F. (3) Pereira, T. M. D. (1)
Institution(s): (1) Lockheed Martin Solar & Astrophysics Lab, Palo Alto, CA, USA, (2) Institute of theoretical astrohpysics, University of Oslo, Norway, (3) Instituto Astrofisico de canarias, La Laguna, Tenerife, Spain
Email: juanms@lmsal.com
Session: Magnetic structuring of the Sun from beneath the photosphere through the corona
Presentation: CT-1

Abstract:

We have performed realistic 3D radiation MHD simulations of the solar atmosphere. These simulations show jet-like features that are similar to the type II spicules discovered with Hinode's Solar Optical Telescope. These type II spicules have been associated with so-called rapid blueshifted events (RBE's) on the solar disk, and with significant blueward asymmetries in transition region and coronal lines at the footpoints of coronal loops (discovered with Hinode's EIS). These observational results and their ubiquity suggest they may play a significant role in providing the corona with hot plasma. We will present a detailed comparison of the properties of the simulated jets, with those of type II spicules (observed with Hinode) and RBE's (with ground-based instruments). We will present analysis of a wide variety of synthetic emission lines from the simulations covering temperatures from 10,000K to several million K, and compare their intensities, velocities, line widths and asymmetry with those of the observed phenomena. We will also show how the formation mechanism of these jets complicates efforts to establish a firm link between observations of magnetic fields and of chromospheric flows, and suggests that magnetic field observations at chromospheric heights may be crucial to establish from observations how these jets are formed.

Numerical Simulation and the SOT Magnetogram Analysis on the Small-scale Magnetic Elements on the Solar Emerging Flux Region

Abstract Author(s): Toriumi, S., Yokoyama, T.
Institution(s): The University of Tokyo
Email: toriumi@eps.s.u-tokyo.ac.jp
Session: Magnetic structuring of the Sun from beneath the photosphere through the corona
Presentation: CT-2

Abstract:
It is thought that solar active regions are formed by the risings of flux tubes from the convection zone. In this study, we aim to figure out the flux emergence from the interior to the atmosphere through the surface, by conducting a numerical simulation and a Hinode/SOT observation. First, we performed a three-dimensional magnetohydrodynamic (MHD) simulation on the flux tube emergence from -20,000 km of the convective layer. The initial tube has a field strength of 2.0x10^4 G, a total flux of 6.3x10^20 Mx, and a twist of 5.0x10^-4 km^-1. As a result, the rising tube expands sideways beneath the surface to create a flat structure. As time goes on, the subphotospheric field rises again into the corona due to the Parker mode of the magnetic buoyancy instability. We newly found that the photopsheric magnetogram showed multiple separation events as well as shearing motions, which reflects the Parker instability of the subphotospheric field. This situation agrees well with Strous & Zwaan (1999)'s model: each emergence event occurs in a vertical sheet, while the sheets are aligned in a parallel fashion. We also confirmed that the wavelength perpendicular to the separations (the distance between vertical sheets) is approximately a few times the tube's initial radius. Secondly, we analyzed an SOT/FG magnetogram of an active region (AR 10926), and observed that the small-scale magnetic elements among the major sunspots make alignments with a certain orientation. The wavelength perpendicular to the alignments (the distance between the sheets) was found to be ~3,000 km. Comparing with the numerical results, we speculate that this active region observed by the SOT is created by the rising flux tube with a radius of the order of 1,000 km in the deeper convection zone.

Non-thermal broadening of EUV lines in magnetic flux emergence

Abstract Author(s): Williams, D. R. (1), Lee, E. (2), Lapenta, G. (2)
Institution(s): (1) Mullard Space Science Laboratory, University College London, Holmury St Mary, Surrey, RH5 6NT, UK, (2) Centrum voor Plasma-Astrofysica, Katholieke Universiteit Leuven, Belgium
Email: drw@mssl.ucl.ac.uk
Session: Magnetic structuring of the Sun from beneath the photosphere through the corona
Presentation: CT-3

Abstract:

Understanding both large- and small-scale dynamics of the solar corona is a prime driver behind the use of spectrometers on modern solar missions; but an important mystery remains unsolved in the understanding of spectroscopic data. In coronal plasmas, if the ion kinetic energy distribution can be described by a Maxwellian (at least along the line of sight), then this Maxwellian will produce a Gaussian distribution of particle velocities about some mean, leading to the commonly-fit profile. This Gaussian has a standard deviation that is predictable from the characteristic temperature, but almost all EUV coronal emission lines exhibit a larger width than this prediction, even when instrumental effects are taken into account. This is even more true in active regions than in the quiet Sun. It is difficult to know how the population of electrons behaves, since we only directly measure emission from ions, but it cannot be ruled out that the former plays a key role in the energy transport.

In an effort to understand the source of this line broadening, this work builds on initial findings that show growth of a high-energy tail of non-thermal velocities in the core of an active region, following a case of flux emergence. We investigate a further case of flux emergence from its early phase, and examine in detail the variation of this tail over several days of observation. We do this at multiple coronal temperatures and multiple sites within the active region, and find that there is appreciable variation in behaviour with both of these variables, that the shape of the non-thermal distribution is time-dependent, and that this shape is not easily predicted from other observables.

Statistical Study on the Nature of Solar Flux Emergence

Abstract Author(s): Otsuji, K. (1), Kitai, R. (2), Ichimoto, K. (2), Shibata, K. (2)
Institution(s): (1) National Astronomical Observatory of Japan, (2) Kwasan and Hida Observatory, Kyoto University
Email: otsuji@solar.mtk.nao.ac.jp
Session: Magnetic structuring of the Sun from beneath the photosphere through the corona
Presentation: CT-4

Abstract:

We studied 101 flux emergence events ranging from small ephemeral regions to large emerging flux regions which were observed with Hinode Solar Optical Telescope filtergram. We investigated how the total magnetic flux of the emergence event controls the nature of emergence. To determine the modes of emergences, horizontal velocity fields of global motion of the magnetic patches in the flux emerging sites were measured by the local correlation tracking. Between two main polarities of the large emerging flux regions with more than around 2x10^19 Mx, there were the converging flows of anti-polarity magnetic patches. On the other hand, small ephemeral regions showed no converging flow but simple diverging pattern. When we looked into the detailed features in the emerging sites, irrespective of the total flux and the spatial size, all the emergence events were observed to consist of single or multiple elementary emergence unit(s). The typical size of unitary emergence is 4 Mm and consistent with the simulation results.

From the statistical study of the flux emergence events, the maximum spatial distance between two main polarities, the magnetic flux growth rate and the mean separation speed were found to follow the power-law functions of the total magnetic flux with the indices of 0.27, 0.57, and -0.16, respectively. From the discussion on the observed power-law relations, we got a physical view of solar flux emergence that emerging magnetic fields float and evolve balancing to the surrounding turbulent atmosphere.

A rainy day on the Sun

Abstract Author(s): Antolin, P., Rouppe van der Voort, L., Verwichte, E.
Institution(s): Institute of Theoretical Astrophysics, University of Oslo
Email: antolin@astro.uio.no
Session: Magnetic structuring of the Sun from beneath the photosphere through the corona
Presentation: CT-5

Abstract:

Observed in cool chromospheric lines such as Hα or Ca II H, coronal rain corresponds to cool and dense plasma falling from coronal heights. Considered rather as a peculiar sporadic phenomenon of active regions, it has not received much attention since its discovery more than 40 years ago. Yet, it has been shown recently that a close relationship exists between this phenomenon and the coronal heating mechanism. Indeed, numerical simulations have shown that this phenomenon is most likely due to a loss of thermal equilibrium ensuing from a heating mechanism acting mostly towards the footpoints of loops. In this work we show the important role it can play in the understanding of the coronal magnetic field. We start by presenting Hinode/SOT observations in the Ca II H line where in-phase transverse oscillations of multiple strand- like structures in a loop are put in evidence by coronal rain. Estimates of the coronal magnetic field and the energy flux of the waves are given through helioseismology techniques. We then present the first multi-wavelength high-resolution spectroscopic observations of coronal rain, performed by the CRISP instrument at the Swedish Solar Telescope. The condensations composing coronal rain are observed to elongate and separate as they fall down to sizes as small as the diffraction limit resolution of the SST. At this resolution, coronal rain is observed to literally invade the entire field of view, implying that coronal rain may be a common phenomenon, and thus that thermal non-equilibrium is important for coronal heating. A large statistical set is obtained in which temperatures and dynamics of the condensations are derived. Simultaneous observations obtained with SDO provide a complementary picture of the ambient corona, thus allowing further insight into the local and global physical conditions.

Precursor of sunspot penumbral formation discovered with Hinode SOT observations

Abstract Author(s): Shimizu, T. (1), Ichimoto, K. (2), Suematsu, Y. (3)
Institution(s): (1) ISAS/JAXA, Japan, (2) Kyoto University, Japan, (3) NAOJ, Japan
Email: shimizu@solar.isas.jaxa.jp
Session: Magnetic structuring of the Sun from beneath the photosphere through the corona
Presentation: CT-6

Abstract:

Formation of sunspot penumbra and the period before its moment is poorly understood due to lack of high resolution, continuous observations on the early phase of sunspot formation. Particularly, the moments of penumbra formation have been reported only in a few papers (Leka & Skumanich 1998, Yang et al. 2003, Schlichenmaier et al. 2010), because the formation of a penumbra is a rapid phenomenon.

We succeeded to continuously monitor the development of an emerging flux region in 30-31 December, 2009, with Hinode SOT magnetogram and Ca II H observations. The observations cover from the start of emergence to the formation of a large well-developed sunspot pair, including the moment of the penumbral formation. We discovered a remarkable dark ring-like structure (3-5 arcsec in radial direction) surrounding the spot in Ca II H, which appeared soon after the pore formation and existed until the appearance of penumbra at the photosphere. Magnetic signal is fairly weak in the ring. The network flux pre-existed before the flux emergence (same polarity with the sunspot) were swept out to the outer boundary of the ring, and they kept 3-5 arcsec distance from the pore (umbra), although the umbra moved outward slowly as the flux emerged. Finally, the penumbra was formed to fill in the ring-like region.

What is this Ca II H ring before the penumbral formation? It is completely different from the moat, in which moving magnetic features move outward in radial direction. The ring can be well seen in chromospheric Ca II H images, whereas normal granules are only visible in photospheric G-band images. We infer that a canopy structure is already formed around the umbra in the chromospheric level, much before the formation of the penumbra at the photospheric level. The magnetic pressure by the canopy structure may act to keep the 3-5 arcsec distance from the pre-existing network elements. Therefore, the remarkable Ca II H ring structure is a chromospheric precursor of penumbral formation and, with this "precursory chromospheric penumbra," we can predict the size and area where the penumbra will be formed at the photosphere.

3D Magnetic, Thermal and Velocity Structure of a Sunspot as Observed from Hinode (SOT/SP)

Abstract Author(s): Tiwari, S. K., Lagg, A., Solanki, S. K.
Institution(s): Max-Planck Institute for Solar System Research, Katlenburg-Lindau, 37191, Germany
Email: tiwari@mps.mpg.de
Session: Magnetic structuring of the Sun from beneath the photosphere through the corona
Presentation: CT-7

Abstract:

Three dimensional (3D) structure of sunspots has been extensively studied for the last two decades by using advanced inversion codes on polarimetric observations. Reliable height dependent inversions of polarimetric observations are essential to understand the three-dimensional magnetic, thermal and velocity structure of sunspots. We perform such an inversion of a complete sunspot to retrieve magnetic, thermal and velocity parameters in three dimensions. The spectro-polarimetric observations of the sunspot, NOAA AR 10933, was taken from SOT/SP onboard the Hinode spacecraft. The sunspot was observed on the solar disk center during a normal scan mode of SOT/SP. We used the inversion code SPINOR to obtain the height stratification of magnetic field vector, temperature and velocity throughout the umbra and penumbra. The inversion is optimized to obtain the best solutions for the umbra (including umbral dots, light bridges and dark background), the penumbra (including dark and bright fibrils) and quiet Sun. Here, we present some of these results obtained at different optical depths. The excellent Hinode/SOT/SP data allow both the 3D large-scale and the 3D fine structure to be simultaneously determined. The spatially averaged magnetic field strength increases with depth in umbra and inner penumbra, and decreases in outer penumbra. Field inclination is almost constant with depth in umbra and inner penumbra and increases as one goes towards outer penumbra. Temperature shows its expected behavior: it increases with depth but the slope is significantly flatter in the umbra, in good agreement with umbral model atmospheres in the literature. Upflows in inner penumbra and downflows in outer penumbra are seen with increasing depth. The azimuth shows a global twist that increases outwards from center of spot. In addition, we also obtain the fine scale structure in umbra and penumbra as a function of depth.

The Pre-eruption Behavior of an XRT Sigmoid - NLFFF models and an MHD simulation

Abstract Author(s): Savcheva, A., Pariat, E., DeLuca, E., van Ballegooijen, A., Aulanier, G.
Institution(s): Boston University
Email: asavchev@cfa.harvard.edu
Session: Magnetic structuring of the Sun from beneath the photosphere through the corona
Presentation: CT-8

Abstract:

Sigmoidal regions are known to be great storage places for magnetic free energy, which they can later release in a flare or CME event. The field of a sigmoid is characterized by highly sheared and twisted magnetic fields held down by a potential arcade. We present topological analysis of the 3D magnetic field structure of a sigmoid observed with Hinode/XRT in Feb 2007. The field is derived from a Non-Linear Force Free Field (NLFFF) model, based on the flux rope insertion method. We compare the results of the NLFFF model with the dynamical MHD simulation of Aulanier at al. (2010). The comparison is based on quasi-separatrix layer maps and current distributions. We point out the similarities in the field line structure. We discuss the implications of the observed flux cancellation and conditions for the torus instability that are observed both in the NLFFF model and the MHD simulation. We show the presence of a hyperbolic flux tube at the flare location. All of the above point to a single coherent picture about the pre-eruption behavior of this sigmoid, which is also reproduced in the MHD simulation.

Quantitative analyses of the 3-D coronal magnetic fields associated with the X3.4 flare event of the solar active region NOAA 10930

Abstract Author(s): He, H., Wang, H., Yan, Y.
Institution(s): National Astronomical Observatories, Chinese Academy of Sciences, Beijing, China.
Email: hehan@nao.cas.cn
Session: Magnetic structuring of the Sun from beneath the photosphere through the corona
Presentation: CT-9

Abstract:

The X3.4 flare event of the solar active region NOAA 10930 happened on 13 December 2006, which was captured by many space and ground telescopes. Based on the nonlinear force-free field (NLFFF) model and the photospheric vector magnetograms obtained by the Spectro-Polarimete (SP) of the Solar Optical Telescope (SOT) aboard the Hinode satellite, the 3-D coronal magnetic field distributions of NOAA 10930 before and after the X3.4 flare eruption were calculated by using the upward boundary integration computational scheme of the direct boundary integral equation (DBIE) NLFFF extrapolation method (He and Wang, 2008; He et al., 2011). To analyze the time series evolution of the 3-D coronal magnetic structures, six magnetograms within the time interval of 25 hours were selected for the NLFFF modeling, three for pre-flare and three for post-flare. Projection effect in the photospheric vector magnetograms was corrected prior to the extrapolation calculations, and the corrected magnetograms were co-aligned and cropped to a uniform 300" x 160" field of view (FOV). The pixel scale of the calculated 3-D coronal magnetic fields is 1"/pixel. The quantitative analyses of the 3-D coronal magnetic fields associated with the X3.4 flare event show that: (1) There exists a magnetic connectivity in the lower layers of the corona just before the flare eruption, the direction of the connectivity is parallel to the direction of the polarity inversion line (PIL) in the photospheric magnetograms. This connectivity is totally disconnected and separated after the flare eruption. (2) The total magnetic energy conserved in the modeling volume of the corona decreases remarkably after the flare eruption, the order of magnitude of the magnetic energy loss is 10^{32} erg. By comparing the 3-D magnetic energy density distributions before and after the flare eruption, it is found that the region of magnetic energy density decrease is located in the relatively higher layers of the corona, and the projection site of the energy density decrease region on the solar surface coincides with the location of the flare eruption.

Polar Faculae: A Proxy for the Evolution of the Solar Polar Field During the Last 100 Years

Abstract Author(s): Munoz-Jaramillo, A., DeLuca, E.
Institution(s): Harvard-Smithsonian Center for Astrophysics
Email: amunoz@cfa.harvard.edu
Session: Magnetic structuring of the Sun from beneath the photosphere through the corona
Presentation: CT-10

Abstract:

Apart from its mean 11-year periodicity, the solar cycle presents long-term modulations of its amplitude and period which remain poorly understood. However, grasping the mechanisms behind these changes becomes more important as more efforts are made to disentangle the role of solar variability on climate and predict solar cycle properties. Unfortunately, aside from sunspot properties, there are very few data-sets spanning the timescales necessary to understand long-term solar variability. Here we show how can we alleviate this deficiency by consolidating polar faculae data from four observational campaigns (1906-1964, Sheeley 1966; 1960-1975, Sheeley 1976; 1975-1990, Sheeley 1991; 1985-2007, Sheeley 2008) and combine it with polar field measurements taken by the Wilcox Solar Observatory (1977-2011) to estimate the polar field evolution since 1906. These data nicely complement polar field measurements using Hinode (Ito et al. 2010) and can be expanded by using SOHO/MDI and SDO/HMI magnetograms.

This research is supported by NASA Living With a Star Grant NNX08AW53G to Montana State University/Harvard-Smithsonian Center for Astrophysics and the NASA Living With a Star Jack Eddy Postdoctoral Fellowship Program, administered by the UCAR Visiting Scientist Programs.

Yearly Variation of Magnetic Field in the Polar Regions Observed with Hinode

Abstract Author(s): Shiota, D. (1), Tsuneta, S. (2), Orozco Suarez, D. (2), Shimojo, M. (3), Sako, N. (4)
Institution(s): (1) RIKEN, Wako, Saitama, Japan, (2) National Astronomical Observatory of Japan, Mitaka, Tokyo, Japan, (3) Nobeyama Solar Radio Observatory, NAOJ, Nobeyama, Nagano, Japan (4) The Graduate University for Advanced Studies, Mitaka, Tokyo, Japan
Email: shiotad@gmail.com
Session: Magnetic structuring of the Sun from beneath the photosphere through the corona
Presentation: CT-11

Abstract:

The magnetic polarity of the global magnetic field of the Sun reverses during the solar cycle maximum. The understanding of the magnetic field evolution in the polar region is important for the solar dynamo process, because the magnetic flux may be transported into the solar interior due to the meridional circulation of the solar convection zone and then become the seed of the magnetic flux in following solar cycles in some solar dynamo models. To make clear the process, we monitored the polar region (HOP 81) since September 2008. We have investigated the properties of the photospheric magnetic fields of the polar regions using data taken with the spectropolarimeter of the Solar Optical Telescope aboard the Hinode satellite. The magnetic field vector was inferred from the observed Stokes profiles using a Milne-Eddington inversion code. We resolve the 180-degree ambiguity of the transverse magnetic fields assuming that the magnetic field is either vertical or horizontal. Then, we identified all the strong magnetic flux concentrations observed within the field-of-view and investigated the variation of their magnetic properties with solar cycle. The main results will be summarized in this contribution. Among them, we found that there exist a strong variation with the solar cycle of the distribution of the vertical magnetic flux elements in the North polar region. The variation is smoother in the South polar region.

Observations of supersonic downflows in pores

Abstract Author(s): Ortiz, A. (1), Bellot Rubio, L. (2) Rouppe van der Voort, L. (1)
Institution(s): (1) Institute of Theoretical Astrophysics, University of Oslo, Norway, (2) Instituto de Astrofisica de Andalucia-CSIC, Spain
Email: ada@astro.uio.no
Session: Magnetic structuring of the Sun from beneath the photosphere through the corona
Presentation: CT-12

Abstract:

We have investigated the velocity field of pores at a resolution of 0.14". Our analysis is based on full Stokes spectropolarimetric measurements taken with the CRISP instrument at the Swedish 1m Solar Telescope. We find localized patches of supersonic downflows in some parts of the pore edges, with velocities reaching up to 7-8 km/s. We have determined the velocities and magnetic properties of these regions from a two-component Stokes inversion of the photospheric Fe I lines at 630 nm. The observations are compatible with inclined magnetic fields containing the strong downflows above a normal, field-free granulation pattern. In addition we performed full Stokes spectropolarimetric measurements in the Ca II 854.2 nm line, with a cadence of 1 minute. These observations reveal the presence of very strong chromospheric downflows at the position of the photospheric supersonic flows. Some of them show brightenings in Ca 854.2 nm and Ca II H line core images.

Propagating waves along spicules

Abstract Author(s): Okamoto, T. J. (1), De Pontieu, B. (2)
Institution(s): (1) NAOJ, (2) LMSAL
Email: joten.okamoto@nao.ac.jp
Session: Energy transport and dissipation through the solar atmosphere and into the heliosphere
Presentation: CT-13

Abstract:
Propagating Alfvenic waves in the corona are thought to play an important role in coronal heating and acceleration of solar wind. Recent observations have shown the existence of such waves along chromospheric spicules, jets of plasma that protrude into the corona. Here we investigated the detailed and statistical properties of Alfvenic waves along spicules in the polar coronal hole using very high cadence observations of the Solar Optical Telescope onboard Hinode. We developed a technique for the automated detection of spicules and high-frequency waves in a time series of images. We detected 89 spicules, and obtained the following observational results: (1) We found a mix of upward propagating, downward propagating, as well as standing waves (i.e., with a phase speed of more than 500 km/s). The ratio is 59%, 21%, and 20%, respectively. (2) A gradual increase with height of the phase speed was observed. (3) Upward waves were dominant at lower altitudes, while standing waves were dominant at higher altitudes. (4) Standing waves were dominant in the early and late phases of each spicule, while upward waves were dominant in the middle phase. (5) In some spicules, we found direct observational evidence for a scenario in which waves along one spicule propagate upward (from the bottom of the spicule) and downward (from the top of the spicule) to form, through superposition, a standing wave in the middle of the spicule. (6) The medians of the (displacement) amplitude, period, and velocity amplitude were 55 km, 45 s, and 7.4 km/s, respectively. Assuming a plasma number density of 10^10 /cm^3, we would roughly estimate the Poynting flux to be 2.5x10^5 erg/cm^2/s, if the filling factor were 1.

We speculate that upward propagating waves are produced near the solar surface (below the spicule) and downward propagating waves are caused by reflection of (initially) upward propagating waves off the transition region at the spicule top. The mix of upward and downward propagating waves implies that exploiting these waves to perform seismology of the spicular environment requires careful analysis and may be problematic.

Using Hinode/SOT to uncover the dynamics of spicules

Abstract Author(s): M. D. Pereira, T. (1), De Pontieu, B. (2), Carlsson, M. (3)
Institution(s): (1) NASA Ames Research Center; (2) Lockheed-Martin Solar & Astrophysics Lab; (3) Institute of Theoretical Astrophysics, University of Oslo
Email: tiago.pereira@nasa.gov
Session: Energy transport and dissipation through the solar atmosphere and into the heliosphere
Presentation: CT-14

Abstract:

Understanding the dynamic solar chromosphere is of paramount importance in solar physics. Spicules are an important feature of the chromosphere, connecting the photosphere to the corona, potentially mediating the transfer of energy and mass. While it is generally accepted that there is more than one type of spicule, their quick motions, small spatial scales, and short lifetimes have prevented a systematic study of their properties over different solar regions. In the present work we undertake such a study, using the unique view of Hinode/SOT's Ca H filtergrams to detect spicules at the solar limb. Looking at different magnetic field configurations (quiet Sun, coronal holes, active regions), we discuss how the properties of the spicules change, how the two spicule populations (type I and type II) are connected, and how spicules are related to other chromospheric phenomena such as dynamic fibrils.

Magnetohydrodynamics of the Partially-Ionized Solar Atmosphere

Abstract Author(s): Cheung, M. C. M. (1), Cameron, R. H. (2)
Institution(s): (1) Lockheed Martin Solar & Astrophysics Laboratory, Palo Alto, CA, (2) Max Planck Institute for Solar System Research, Katlenburg-Lindau, Germany
Email: cheung@lmsal.com
Session: Energy transport and dissipation through the solar atmosphere and into the heliosphere
Presentation: CT-15

Abstract:

By incorporating important physical processes such as radiative transfer and magnetoconvection, recent numerical magnetohydrodynamics (MHD) simulations have provided key insights into the mechanisms underlying a plethora of solar atmospheric phenomena. Until now, however, such simulations have treated the plasma in the photosphere and chromosphere as fully ionized. When one takes into account that photospheric and chromospheric plasma are weakly ionized, new effects such as the Hall drift and ambipolar diffusion need to be taken into account. We present MHD simulations that use a generalized Ohm's law in the induction equation to take into account neutral-ion coupling in the solar photosphere. Ambipolar diffusion is responsible for the collapse of current sheets in weakly ionized plasma and the Hall effect is responsible for rotation of the plane of polarization of Alfven waves. The relative importance of these respective effects under certain thermodynamic regimes will be discussed.

Statistical Study of Chromospheric Anemone Jets Observed With HINODE/SOT

Abstract Author(s): Nishizuka, N. (1, 2), Nakamura, T. (2), Kawate, T. (2), Singh, K. A. P. (2), Shibata, K. (2)
Institution(s): (1) ISAS/JAXA, (2) Kwasan and Hida Observatories, Kyoto University
Email: nishizuka.naoto@jaxa.jp
Session: Energy transport and dissipation through the solar atmosphere and into the heliosphere
Presentation: CT-16

Abstract:

The Solar Optical Telescope on board Hinode has revealed numerous tiny jets in all regions of the chromosphere outside of sunspots. A typical chromospheric anemone jet has a cusp-shaped structure and bright footpoint, similar to the shape of an X-ray anemone jet observed previously with SXT/Yohkoh. In Ca II H broadband and Fe I 6302A narrowband filter images, chromospheric anemone jets are associated with the mixed polarity regions which are either small-scale emerging flux regions or moving magnetic features. This configuration has been well explained by the emerging flux-reconnection model. We examine various chromospheric anemone jets in the active region near the limb and the disk center, and study the typical features (e.g., length, width, lifetime, and velocity) of the chromospheric anemone jets. Statistical studies find that chromospheric anemone jets have: (1) a typical length 1.0-4.0 Mm, (2) a width 100-400 km, (3) a lifetime 100-500 s, and (4) a velocity 5-20 km/s. The velocity of the chromospheric anemone jets is comparable to the local Alfvén speed in the lower chromosphere (about 10 km/s). The observed relationship between the velocity and length of chromospheric anemone jets shows that the jets do not follow ballistic motion but are more likely accelerated by some other mechanism, e.g. shock acceleration. This is consistent with numerical simulations of chromospheric anemone jets and may give some model to explain coronal heating. The timescale of chromospheric anemone jets indicates faster reconnection than expected from the Sweet-Parker theory. Since the current sheet in the low Reynolds number atmosphere (10^6 in the lower chromosphere) is hard to get thin enough for microscopic instability to trigger localized anomalous resistivity, magnetic reconnection in weakly ionized plasma, i.e. the role of neutral particles and macroscopic dynamics such as turbulence, plasmoid ejections and fractal structure in the current sheet will be also discussed in this presentation.

Spectroscopic Diagnosis of Propagating disturbances in coronal loops: Waves or flows?

Abstract Author(s): Wang, T. (1, 2), Ofman, L. (1, 2), Davila, J. M. (2)
Institution(s): (1) Catholic University of America, Washington, DC, USA, (2) NASA's Goddard Space Flight Center, Greenbelt, MD, USA
Email: tongjiang.wang@nasa.gov
Session: Energy transport and dissipation through the solar atmosphere and into the heliosphere
Presentation: CT-17

Abstract:

Quasi-periodic intensity disturbances propagating upward along the coronal structure have been studied with EUV imaging observations for a long time. They were mostly interpreted as slow mode magnetoacoustic waves. However, it was recently argued that they are actually caused by a faint highly blueshifted quasi-periodic upflowing component of the order of 50-150 km/s. Here we present the analysis of multi-wavelength spectral properties of propagating disturbances (PDs) using the Hinode/EIS sit-and-stare observations. First we test the forward modeling of the Red-Blue (RB) asymmetry profiles for 6 EIS coronal lines for different Doppler velocities of the secondary Gaussian, and found that the derived velocity by the RB analysis is saturated when the secondary component is centered at offset velocities equivalent to the line width. This effect leads to a detection limitation of upflow velocity by the RB method to be above 50-60 km/s due to the broad instrumental width for EIS spectra (especially for the short-wavelength band). We then developed a different method to examine the spectral features for the PDs. By assuming that the excessive emission of the PD profile against the background (taken as the one prior to the PD) is caused by the hypothetic upflow, we derived the LOS velocities of the order of 10-20 km/s for the warm (1-1.5 MK) loops, in which the PDs are most prominent. This velocity size is much smaller than those inferred from the RB asymmetry analysis, and did not support the interpretation of the PDs by intermittent high-speed upflows, and therefore confirms the previous wave interpretation. However, the PDs seen in higher (about 2 MK) temperature lines appear to show different features. We discuss their origin based on the double Gaussian fits.

Two components of the coronal emission revealed by both spectroscopic and imaging observations

Abstract Author(s): Tian, H. (1), McIntosh, S. W. (1), De Pontieu, B. (2), Martinez-Sykora, J. (2), Sechler, M. (1), Wang, X. (3)
Institution(s): (1) High Altitude Observatory, National Center for Atmospheric Research, (2) LMSAL, Palo Alto, USA, (3) School of Earth and Space Sciences, Peking University, China
Email: htian@ucar.edu
Session: Energy transport and dissipation through the solar atmosphere and into the heliosphere
Presentation: CT-18

Abstract:

Recent spectroscopic observations have revealed the ubiquitous presence of blueward asymmetries of emission lines formed in the solar corona and transition region. These asymmetries are most prominent in loop footpoint regions, where a clear correlation of the asymmetry with the Doppler shift and line width determined from the single Gaussian fit is found. Such asymmetries suggest at least two emission components: a primary component accounting for the background emission and a secondary component associated with high-speed upflows. The latter has been proposed to play a vital role in the coronal heating process and there is no agreement on its properties. Here we slightly modify the initially developed technique of Red-Blue (RB) asymmetry analysis and apply it to both artificial spectra and spectra observed by the EUV Imaging Spectrometer onboard Hinode, and demonstrate that the secondary component usually contributes a few percent of the total emission, has a velocity ranging from 50 to 150 km s−1 and a Gaussian width comparable to that of the primary one in loop footpoint regions. The results of the RB asymmetry analysis are then used to guide a double Gaussian fit and we find that the obtained properties of the secondary component are generally consistent with those obtained from the RB asymmetry analysis. Through a comparison of the location, relative intensity, and velocity distribution of the blueward secondary component with the properties of the upward propagating disturbances revealed in simultaneous images from the Atmospheric Imaging Assembly onboard the Solar Dynamics Observatory, we find a clear association of the secondary component with the propagating disturbances.

What determines coronal-loop temperature?

Abstract Author(s): Kano, R. (1), Tsuneta, S. (1), Ueda, K. (2)
Institution(s): (1) National Astronomical Observatory of Japan, Tokyo, Japan, (2) University of Tokyo, Tokyo, Japan
Email: ryouhei.kano@nao.ac.jp
Session: Energy transport and dissipation through the solar atmosphere and into the heliosphere
Presentation: CT-19

Abstract:
Magnetic loops in active regions have widespread distribution in temperature as indicated by distinct difference between SDO/AIA and XRT images. One way to tackle the coronal heating problem is to reveal why and how such loop-dependent difference in temperature occurs. Cool loops emanate from both sunspot regions (SS regions; i.e. umbrae, penumbrae and pores) and non-SS regions, while most of hot loops from non-SS regions. We identify the photospheric footpoints of the hot and cool loops in the SOT/SP images, and obtain the magnetic fields and the horizontal velocities. We confirm that the footpoints of the cool loops in SS regions have higher magnetic filling factors than the footpoints of the hot loops (Katsukawa and Tsuneta, 2005). However, we find no difference between the hot and cool loops in any photospheric property including the magnetic filling factors in the non-SS regions. There is little correlation between the position-dependent photospheric magnetic properties obtained with SOT/SP and the associated coronal temperatures. Instead, we discover a clear anti-correlation between the loop temperatures and the loop length estimated with potential field approximation: If the loop length is larger, lower the temperature. The loop length (i.e. volume for unit cross-section) is somehow related to the temperature, suggesting the uniform heat input from the footpoints.

3D Simulations of Wave Heating; where is all the energy?

Abstract Author(s): De Moortel, I., Pascoe, D. J.
Institution(s): University of St Andrews
Email: ineke@mcs.st-and.ac.uk
Session: Energy transport and dissipation through the solar atmosphere and into the heliosphere
Presentation: CT-20

Abstract:
Recently, observations have shown that transverse oscillations are present in a multitude of coronal structures. It is generally assumed these oscillations are driven by (sub)surface footpoint motions. Using fully 3D MHD simulations, we show that these footpoint perturbations generate propagating kink modes which couple very entireciently into Alfvén waves. We investigate the energy budget contained within such oscillations in various ways. We compare the footpoint energy with the energy budget at higher altitudes and show the distribution of the temperature resulting from the phasemixing of the Alfvén waves. Using an ensemble of randomly distributed loops, driven by footpoint motions with random periods and amplitudes, we compare the absolute energy in the numerical domain with the energy that is 'visible' when integrating along the line of sight. We show that this 'LOS energy' is only a small fraction of the actual energy provided by the footpoint motions.

Cambridge Active Region Studies

Abstract Author(s): Mason, H. (1), Tripathi, D. (1), Klimchuk, J. (2), Del Zanna, G. (1), O'Dwyer, B. (1)
Institution(s): (1) University of Cambridge, UK, (2) NASA Goddard Space Flight Center, USA
Email: hm11@damtp.cam.ac.uk
Session: Energy transport and dissipation through the solar atmosphere and into the heliosphere
Presentation: CT-21

Abstract:
The Hinode EUV Imaging Spectrometer (EIS) provides us with an opportunity to determine the plasma properties of solar active regions, and hence to attempt to distinguish between different coronal heating mechanisms. Recent work by the Cambridge (UK!) group of moss and hot core loops favours the impulsive (nanoflare) models.

MHD modeling of the heating of coronal loops

Abstract Author(s): Guarrasi, M. (1, 2), Reale, F. (1, 2), Orlando, S. (2), Mignone, A. (3)
Institution(s): (1) Universita degli Studi Di Palermo, Palermo, Italy, (2) INAF Osservatorio Astronomico di Palermo, Palermo, Italy, (3) Dipartimento di Fisica Generale, Università di Torino, Torino, Italy
Email: guarrasi@astropa.unipa.it
Session: Energy transport and dissipation through the solar atmosphere and into the heliosphere
Presentation: CT-22

Abstract:
It has been recognized that magnetic flux tubes must expand rapidly in the region between the high beta photosphere and the low beta corona. This loop expansion needs to be accounted in modeling the moss intensities. Anyway, this cross section variation with loop position is not included in a large part of numerical models of coronal loops. In all these models the emission measure from the transition region and from the lower corona is much higher than what is observed. We present a 2D MHD loop model that naturally accounts for loop expansion through the variation of the magnetic field from the chromosphere to the corona. Our model consistently includes plasma fluid and thermodynamic behavior, in particular the plasma thermal conduction along the magnetic field lines and the radiative losses. We present some 2D MHD simulations of the ignition and evolution of a loop under different kinds of heating and analyze the plasma structure and feedback on the loop expansion.

Non-equlibrium ionization in 3D numerical models

Abstract Author(s): Olluri, K., Gudiksen, B., Hansteen, V.
Institution(s): Institute of Theoretical Astrophysics, University of Oslo
Email: kosovare.olluri@astro.uio.no
Session: Energy transport and dissipation through the solar atmosphere and into the heliosphere
Presentation: CT-23

Abstract:
The chromosphere and transition region have for the last 20 years been shown to be quite dynamic layers of the solar atmosphere with timescales shorter then the equilibration timescales of many of the ions observed in the solar atmosphere. The fast change in the properties of the atmosphere and the long ionization- and recombination times, result in ions being unable to reach equilibration with their surroundings. A number of the spectral lines we observe can therefore no longer be expected to give us any information about the local density or temperature, since ions can now be found far from their equilibrium temperatures. Numerical modeling is essential to interpret the observations. Modeling of the ionization balance has earlier been done in 1D simulations, but due to many free parameters inherent in such modeling, led to incomplete results. We have studied the ionization balance closer by implementing the rate equations in the 3D numerical code Bifrost. We will present our implementation and a study of the carbon IV 1549 AA line and the iron XII 195 AA line, which is an important line in the Hinode EIS wavelength band, focusing on differences between statistical equilibrium and non-equilibrium ionization results.

Active region plasma outflows and their contribution to the solar wind

Abstract Author(s): Culhane, J. L. (1), van Driel-Gesztelyi, L. (1, 2, 3), Baker, D. (1) Rouillard, A. (4), Démoulin, P. (2), Mandrini, C.H. (5), Opitz, A. (6)
Institution(s): (1) MSSL/UCL, UK. (2) Paris Observatory, LESIA, France. (3) Konkoly Observatory, Hungary. (4) NRL, Washington, USA. (5) IAFE, University of Buenos Aires, Argentina. (6) CNRS, CESR, Toulouse, France.
Email: jlc@mssl.ucl.ac.uk
Session: Energy transport and dissipation through the solar atmosphere and into the heliosphere
Presentation: CT-24

Abstract:
When active regions are adjacent to coronal holes, interchange reconnection often leads to significant evolution of coronal hole boundaries. Reconnection can also take place in regions with a large magnetic connectivity gradient – Quasi-Separatrix Layers (QSLs). Outcomes may include variability of active region-associated hot plasma outflows and the modulation of the solar wind flows on open field lines. In the interval 2 18 January, 2008, we studied a pair of opposite-polarity coronal holes at mid-latitudes on the Sun with two active regions located between them. The active regions are separated by the Heliospheric Plasma Sheet (HPS). We used the Hinode EIS instrument to locate active region-related outflows and measure their velocities. SOHO/EIT imaging was used to follow the evolution of the coronal hole boundaries. STEREO imaging and in-situ data were also employed as were ACE in-situ observations, to assess the resulting impacts on the interplanetary solar wind structure and composition. Results from the work so far will be reported.

Self-consistent reconstruction of the solar corona and the solar wind under the Alfvén wave scenario

Abstract Author(s): Matsumoto, T., Suzuki, T. K.
Institution(s): Nagoya University
Email: takuma.matsumoto@nagoya-u.jp
Session: Energy transport and dissipation through the solar atmosphere and into the heliosphere
Presentation: CT-25

Abstract:
The solar corona is the outermost portion of the solar atmosphere that has extremely higher temperature compared with the cool surface (the photosphere). Above the corona, the supersonic solar winds blow into the interplanetary space. A key ingredient of the coronal heating and the solar wind acceleration is Alfvén wave; transversal wave propagating along magnetic field lines. The energy of Alfvén wave can be converted into thermal energy both through compressible or incompressible processes. In addition to gas pressure, the pressure of Alfvén wave can accelerate the ambient plasma. However, which energy conversion processes can work effectively in the sun has not been elucidated yet. Here we present results of 2D magnetohydrodynamic simulations of Alfvén wave propagation to reproduce both the solar corona and the solar wind above the coronal holes simultaneously. We found that shock heating is effective in the coronal bottom where the solar wind flow is subsonic. This implies that the mass loss rate from the sun is controlled by the shock heating process. In the solar wind acceleration region, both the shock waves and the Alfvén turbulence are turned out to be important for the heating and the acceleration.

Excitation of Low Frequency Electromagnetic Waves in Magnetic Reconnection Laboratory Experiment

Abstract Author(s): Inomoto, M., Kuwahata, A., Ito, S., Tanabe, H., Hayashi, Y., Copinger, P., Ii, T., Gao, B., Ito, T., Yamada, T., Ono, Y.
Institution(s): The University of Tokyo
Email: inomoto@k.u-tokyo.ac.jp
Session: Instabilities, Transients and Eruptions
Presentation: CT-26

Abstract:

Magnetic reconnection plays important roles in rapid eruption and structure formation events in magnetized plasmas. Fast magnetic reconnection is provided by large magnetic dissipation, or the anomalous resistivity in the diffusion region, which is induced by microscopic instabilities in the current sheet. One of the primary candidates of the microinstabilities is the lowerhybrid drift instability (LHDI), which is often observed in space and laboratory experiments. Recent three-dimensional particle simulation studies have pointed out that the drift kink instability (DKI) is triggered after the nonlinear saturation of the LHDI mode when the half-width of the current sheet decreases below the ion gyroradius, resulting in the reconnection enhancement and anomalous ion heating.

Local current sheet behaviors have been experimentally investigated by using toroidal plasma merging devices, in which self-organized magnetic reconnection events develops with small constraint from boundary conditions. Recently, excitation of low frequency electromagnetic waves was observed associated with the magnetic reconnection with a moderate guide field (about half of the reconnecting field). The waves have frequency in the range of ion cyclotron frequency and parallel wavelength in the order of several ion gyroradius. Enhancement of the effective resistivity in the current sheet was observed around the same time when the maximal wave amplitude up to 10 % of the reconnecting field was detected. These experimental results suggest that the DKI like current sheet modulation develops and enhances the reconnection rate.

Simulations of the magnetic Rayeigh-Taylor instability in the Kippenhahn-Schluter pominence model

Abstract Author(s): Hillier, A. (1), Berger, T. (2), Shibata, K. (1) Isobe, H. (3)
Institution(s): (1) Kwasan and Hida Observatories, Kyoto University, Japan (2) Lockheed Martin Advanced Technology Center, Palo Alto, California, USA (3) Unit of Synergetic Studies for Space, Kyoto University, Japan
Email: andrew@kwasan.kyoto-u.ac.jp
Session: Instabilities, Transients and Eruptions
Presentation: CT-27

Abstract:

Observations of quiescent prominences by the Solar Optical Telescope (SOT) on board the Hinode satellite show plumes of hot, underdense material rising through the prominence. These plumes form at the boundary between the prominence and low density bubbles, approximately 10 Mm in size, that appear beneath the prominence, and then rise through the prominence material at speeds of approximately 20 km/s and widths of approximately 1.5 Mm. The plume profile ranges from highly turbulent to smooth, suggesting that the prominence conditions, as well as those of the bubble, are important in determining the dynamics. To investigate this phenomenon, we perform simulations of the magnetic Rayleigh-Taylor instability in a local prominence model. The instability creates rising plumes of hot, underdense material that propagate through the prominence material at a velocity of approximately 6-7 km/s and widths of approximately 1.5 Mm, in rough agreement with the Hinode observations. Nonlinear effects, in which the interaction between plumes drives an inverse cascade process creating large plumes from smaller plumes, are found to be important. Increasing the magnetic field strength creates smoother plume structures. The addition of a strong guide field, which is suggested in some prominence models, does not hinder plume formation but does change the dynamic scaling. The Rayleigh-Taylor instability drives an upward flow of magnetic energy and a downward flow of mass. The results from the simulations well match the characteristics of the observed plumes, suggesting that the magnetic Rayleigh-Taylor instability could be important in determining prominence structure as well as changing the magnetic energy distribution in overlying coronal cavities which ultimately erupt as coronal mass ejections.

Forecasting a CME by Spectroscopic Precursor

Abstract Author(s): Baker, D. (1), van Driel-Gesztelyi, L. (1, 2, 3), Green, L.M. (1)
Institution(s): (1) Mullard Space Science Laboratory, University College London, UK, (2) Observatoire de Paris, Meudon, France, (3) Konkoly Observatory, Budapest, Hungary
Email: db2@mssl.ucl.ac.uk
Session: Instabilities, Transients and Eruptions
Presentation: CT-28

Abstract:
Multi-temperature plasma flows resulting from the interaction between a mature active region (AR) inside an equatorial coronal hole (CH) are investigated. Outflow velocities observed by Hinode EIS ranged from a few to 13 km/s for three days at the AR's eastern and western edges. However, on the fourth day, velocities intensified up to 20 km/s at the AR's western footpoint about six hours prior to a CME. 3D MHD numerical simulations of the observed magnetic configuration of the AR-CH complex showed that the expansion of the mature AR's loops drives persistent outflows along the neighboring CH field. Based on these simulations, intensification of outflows observed pre-eruption on the AR's western side where same-polarity AR and CH field interface, is interpreted to be the result of the expansion of a sigmoidal AR, in particular, a flux rope containing a filament that provides stronger compression of the neighboring CH field on this side of the AR. Intensification of outflows in the AR is proposed as a new type of CME precursor.

Observations and Magnetic Field Modeling of the Flare/CME Event on 2010 April 8

Abstract Author(s): Su, Y. (1), Kliem, B. (2), van Ballegooijen, A. (1), Surges, V. (1), Deluca, E. (1)
Institution(s): (1) Harvard-Smithsonian Center for Astrophysics, Cambridge, MA, USA (2) Institute for Physics and Astronomy, Unversity Potsdam, Potsdam, Germany
Email: ynsu@head.cfa.harvard.edu
Session: Instabilities, Transients and Eruptions
Presentation: CT-29

Abstract:
We present two studies on the flare/CME event that occurred in Active Region 11060 on 2010 April 8. This flare is well observed at multiple EUV and UV channels by SDO/AIA. The CME is observed by STEREO and SOHO/LASCO. We create a series of static magnetic field models, using the flux-rope insertion method developed by van Ballegooijen (2004). The boundary conditions for the magnetic fields are provided by line-of-sight magnetograms taken by SDO/HMI. The best-fit NLFFF model is constrained by the coronal loops observed by SDO/AIA and Hinode/XRT. We find that the axial flux in the best-fit pre-flare NLFFF model (Axi=4e20 Mx) is close to the threshold of instability (Axi=5e20 Mx). The unstable model (Axi=6e20 Mx) matches the flare footpoints and coronal dimmings as observed at the early phase of the event. We also produce scaled versions of these three models in Cartesian geometry, and use these models as realistic initial conditions for three-dimensional zero-beta MHD simulations (Torok & Kliem 2003, Kliem et al. 2004). These MHD simulations confirm that the model with axial flux of 4e20 Mx is stable, while the model with axial flux of 6e20 Mx erupts as a real CME. Detailed comparisons of the CME model with observations (e.g, dynamics, morphology, erupting direction of the CME) will be presented.

Spectral diagnostics of flare and active region plasma based on EUV spectra from SPIRIT spectroheliograph aboard CORONAS-F

Abstract Author(s): Shestov, S. V., Kuzin, S. V., Bogachev, S. A., Reva, A. A.
Institution(s): Lebedev Physical Institute
Email: sshestov@gmail.com
Session: Instabilities, Transients and Eruptions
Presentation: CT-30

Abstract:

EUV spectroheliograph SPIRIT aboard CORONAS-F satellite operated in orbit from 2001 till 2005. The spectroheliograph was built on slitless optical scheme with grazing incidence diffraction grating. Such a scheme provides full-Sun field of view with comparatively high spectral and spatial resolution. Spectral bands of the spectroheliograph 176-207 A and 280-330 A include lines corresponding to a broad range of temperatures: from cold Si VIII and Mg VIII (Tmax - 0.8 MK) to hot Ca XVII and Fe XXIV (Tmax - 10-15 MK). During the satellite operation several thousands of spectoheliograms were registered, including dozens of spectroheliogram with intense solar flares of M- and X-classes. The obtained spectra were used for temperature (DEM) and density plasma diagnostics in flares and active regions. We have found considerable amount of hot plasma in several active regions; for solar flares DEM has been obtained; since for some flares several spectra were registered during decay phase, DEM evolution has been obtained. EUV spectroscopic data from SPIRIT can be used for active region and flare plasma diagnostics, verification of atomic data, verification and evaluation of response functions of EUV telescopes.

Spectroscopic observations of a coronal Moreton wave

Abstract Author(s): Harra, L. (1), Sterling, A. (2), Gomory (3), Veronig, A. (4)
Institution(s): (1) UCL-MSSL, UK, (2) Space Science Office, VP62, NASA Marshall Space Flight Center, Huntsville, AL 35812, USA, (3) Astronomical Institute, Slovak Academy of Sciences, SK-05960 Tatranská Lomnica, Slovakia, (4) Institute of Physics, University of Graz, Universitätsplatz 5, A-8010 Graz, Austria
Email: lkh@mssl.ucl.ac.uk
Session: Instabilities, Transients and Eruptions
Presentation: CT-31

Abstract:
We observe a coronal wave ('EIT wave') on 2011 February~16, using EUV imaging data from SDO/AIA and EUV spectral data from Hinode/EIS. The wave accompanied an M1.6 flare that produced a surge and ejected a Coronal Mass Ejection (CME). EIS data of the wave show a prominent red-shifted signature indicating line-of-sight velocities of ~20 km/s or greater. Following the main red-shifted wave front, there is a low-velocity period (and perhaps slightly blue-shifted), followed by a second redshift somewhat-weaker than the first; this progression may be due to oscillations of the EUV atmosphere set in motion by the initial wave front, although alternative explanations may be possible. Along the direction of the EIS slit the wave front's velocity was ~500 km/s, consistent with its apparent propagation velocity projected against the solar disk as measured in the AIA images, and the second red-shifted feature had propagation velocities between ~200-500 km/s. These findings are consistent with the observed wave being generated by the outgoing CME, as in the scenario for the classic Moreton wave. This type of detailed spectral study of coronal waves has hitherto been a challenge, but is now possible due to the availability of concurrent AIA and EIS data.

A New Look at a Classic Flare Structure

Abstract Author(s): Guidoni, S. E., McKenzie, D. E., Longcope, D. W.
Institution(s): Montana State University – Bozeman
Email: guidoni@physics.montana.edu
Session: Instabilities, Transients and Eruptions
Presentation: CT-32

Abstract:
The M1.4 flare of Jan 28, 2011 has a remarkable resemblance to the famous Tsuneta flare of 1992. It was observed with Hinode/XRT, SDO/AIA, and STEREO (A)/EUVI, giving us higher resolution, more temperature coverage, and stereoscopic views of this iconic structure. We interpret these observations in terms of a newly developed model of retracting reconnected flux tubes. In this model, the retraction drives gas-dynamics shocks that heat and compress the plasma.

The high temperature images reveal a brightening that grows in size to form a tower-like structure above a post-flare arcade. We combine the images with a potential field source surface (PFSS) extrapolation to develop a complete picture of the magnetic field structure and the coronal plasma state variables. XRT provides accurate high temperature measurements of the plasma while the simultaneous high resolution and high-cadence observations from AIA allow us to map the evolution of the plasma. In addition, EUVI data is used to estimate the line of sight depth of the bright tower.

Observed Features of Magnetic Reconnection in 2007 May 19 Flare

Abstract Author(s): Hara, H. (1), Watanabe, T. (1), Harra, L. K. (2), Culhane, J. L. (2), Young, P. R. (3)
Institution(s): (1) National Astronomical Observatory of Japan, (2) UCL-Mullard Space Science Lab., UK, and (3) George Mason University, USA
Email: hirohisa.hara@nao.ac.jp
Session: Instabilities, Transients and Eruptions
Presentation: CT-33

Abstract:
We report observed features that occurred near the loop-top region of a 2007 May 19 flare. We have found a loop-top hot source, a fast jet nearby, and an inflow structure to the hot source in the impulsive phase of the flare from the Hinode EUV Imaging Spectrometer. From the geometrical relationships and observed parameters of these phenomena, we conclude that they provide evidence for magnetic reconnection that occurs near the loop-top region. The reconnection rate estimated from the observed parameters is 0.05-0.1, which supports the Petschek-type magnetic reconnection. The presence of slow-mode and fast-mode MHD shocks is discussed with supporting evidence based on the observed quantities.

Comparative Study of Solar Flare Onset Based on MHD Simulations and Hinode Observations

Abstract Author(s): Kusano, K. (1,2), Bamba, Y. (1), Yamamoto, T. T. (1)
Institution(s): (1) Solar-Terrestrial Environment Laboratory, Nagoya University, Furo-cho, Chikusa-ku, Nagoya, Aichi, 4648601, Japan, (2) Japan Agency for Marine-Earth Science and Technology, Kanazawa-ku, Yokohama, Kanagawa, 2360001, Japan
Email: kusano@nagoya-u.jp
Session: Instabilities, Transients and Eruptions
Presentation: CT-34

Abstract:

Although solar flares are now widely believed to be driven by magnetic energy stored around sunspots, what triggers the onset of them is not well understood yet. Hypotheses for the flare onset mechanism includes the emerging flux model, in which magnetic reconnection caused by the emergence of magnetic flux from below the solar surface to the corona leads to solar flares. However, the condition for this process is still unclear. Here, we study what kind of emerging flux can cause the onset of solar flares based on the comparison between three-dimensional MHD simulations and the Hinode/SOT observation of pre-flare activities. First, in terms of simulations, we found that the small magnetic flux emerged into a sheared magnetic arcade is capable to trigger flare eruption, if and only if the azimuthal orientation as well as the amount of emerging flux meet some condition. In particular, the simulations indicate that there are two different parametric windows for the azimuth of emerging flux to trigger flares. Second, we analyzed the flux emerging activity of AR NOAA 10930 by comparing the Ca II H images and the longitudinal magnetogram taken by Narrowband Filter Imager of Hinode/SOT. As consequence of it, it was shown that some pre-flare brightening events coincide with the rapid emergence of small magnetic bi-polar system. Finally, we will show the geometrical structure of each flux emergence to examine the simulation results for the preferential azimuth of emerging flux to trigger flare.

Imaging Spectroscopic Observation of Filament Eruptions by Hinode/EIS Flare Hunting Study

Abstract Author(s): Imada S., Hara H., Watanabe T., Shimizu T., Harra L.K.
Institution(s): ISAS/JAXA
Email: imada.shinsuke@jaxa.jp
Session: Instabilities, Transients and Eruptions
Presentation: CT-35

Abstract:

So far, Hinode/EIS observed several flares, and revealed the dynamical features associated with flows during the flare. On the other hand, the temporal resolution in most EIS flare observations is not enough to reveal the dynamical features associated with flare. Therefore, we have proposed the fast cadence Flare Hunting Study (~6 min) to concentrate observing the dynamical feature. From 2009 December to 2011 April, Flare Hunting Study produced more than 5000 raster images. We have processed 5000 raster scan data and checked the processed images (intensity, velocity, line width). We have identified the flare not by GOES class but the enhancement of FeXXIII or FeXXIV line intensity. After all, more than 30 individual flare associated events are found. We can observe many downflow signatures during the flares in the coronal emission lines (Te ~ 1MK). For example, redshifted post flare loop, strong redshift near the footpoint of flaring loops during impulsive phase, and redshifted plasma associated with filament eruption.

In this talk, we concentrate the flow characteristics of erupting filament. We found a few filament eruption events associated with flare. We can clearly identify in OVI line. Actually, it seems that those filaments are once erupting and they fall back. EIS clearly observed the velocity signals of the filaments with 6 min cadence. At the beginning of the eruption, some part of the filaments shows the blueshift (a few 10 km/s) in FeXII and FeX. After 6 minutes, FeXII and FeX show the clear redshifts in the leg of filaments, although the filaments seem to be still erupting. The downflow velocities are roughly 100 km/sec (almost sound speed) estimated by double Gaussian fitting. This result may suggest that the filaments lose their mass along the loop during the erupting phase. Further, the mass loss process may work as a positive feedback to the filament eruption (like Parker-Instability).

Current Sheet and Reconnection Inflow-Outflow Observations During Solar Eruptions

Abstract Author(s): Savage, S. (1), Holman, G. (1, 2) Reeves, K. K. (2) Seaton, D. B. (3), McKenzie, D. E. (4), Su, Y. (1)
Institution(s): (1) NASA/GSFC, Greenbelt, MD; (2) Harvard-Smithsonian Center for Astrophysics, Cambridge, MA; (3) Royal Observatory of Belgium, Brussels, Belgium; (4) Montana State University, Bozeman, MT
Email: sabrina.savage@nasa.gov
Session: Instabilities, Transients and Eruptions
Presentation: CT-36

Abstract:
Magnetic reconnection is widely accepted as a dominant source of energy during solar flares; however, observations of it have been indirect and/or incomplete. Using the suite of instruments available spanning wavelength space, we will provide observations and measurements of both the inputs and outputs predicted from reconnection in the form of inflows preceding outflows (i.e. supra-arcade downflows, supra-arcade downflowing loops, upflows, and disconnection events). We will also present evidence for current sheets through which reconnection is expected to occur and discuss current sheet motion during flare progression.

The Hanle Effect from Space for Measuring the Magnetic Fields of the Upper Chromosphere

Abstract Author(s): Bueno, J. T., Stepan, J., Belluzzi, L., et al.
Institution(s): Instituto de Astrofisica de Canarias
Email: jtb@iac.es
Session: Future Needs - Observational, Theoretical and Computational
Presentation: CT-37

Abstract:
We present some theoretical predictions concerning the amplitudes and magnetic sensitivities of the linear polarization signals produced by scattering processes in some UV and FUV spectral lines of the upper chromosphere and transition region, such as Ly-alpha and Mg II k. To this end, we have calculated the atomic level polarization (population imbalances and quantum coherences) induced by anisotropic radiation pumping in semi-empirical and hydrodynamic models of the solar atmosphere, taking into account radiative transfer and the Hanle effect caused by the presence of organized and random magnetic fields. The amplitudes of the emergent linear polarization signals are found to vary typically between a fraction of a percent and a few percent, depending on the scattering geometry and the strength and orientation of the magnetic field. The results shown here encourage the development of UV polarimeters for sounding rockets and space telescopes with the aim of opening up a true diagnostic window for magnetic field measurements in the upper chromosphere and transition region of the Sun.

The Chromospheric Lyman-Alpha SpectroPolarimeter (CLASP)

Abstract Author(s): Kobayashi, K. (1), Tsuneta, S. (2), Trujillo Bueno, J. (3), Bando, T. (2), Belluzzi, L. (3), Casini, R. (4), Carlsson, M. (5), Cirtain, J. (6), De Pontieu, B. (7), Hara, H. (2), Ichimoto, K. (8), Ishikawa, R. (2), Kano, R. (2), Katsukawa, Y. (2), Kubo, M. (2), Kim, T. (6), Manso Sainz, R. (3), Narukage, N. (2), Asensio Ramos, A. (3), Robinson, B. (1), Sakao, T. (9), Shimizu, T. (8), Stepan, J. (3), Suematsu, Y. (2), Watanabe, H. (8), West, E. (6), Winebarger, A. (6)
Institution(s): (1) University of Alabama in Huntsville, Huntsville, AL, USA, (2) National Astronomical Observatory of Japan, Tokyo, Japan, (3) Instituto de Astrofisica de Canarias, Tenerife, Spain, (4) High Altitude Observatory (HAO), Boulder, CO, USA, (5) Institute of Theoretical Astrophysics, University of Oslo, Oslo, Norway, (6) NASA/Marshall Space Flight Center/NSSTC, Huntsville, AL, USA, (7) Lockheed Martin Solar and Astrophysics Laboratory, Palo Alto, CA, USA, (8) Kyoto University, Kyoto, Japan, (9) Institute of Space and Astronautical Science, Japan Aerospace Exploration Agency, Kanagawa, Japan
Email: kk0003@uah.edu
Session: Future Needs - Observational, Theoretical and Computational
Presentation: CT-38

Abstract:
We present an overview of the Chromospheric Lyman-Alpha SpectroPolarimeter (CLASP), a proposed sounding rocket experiment currently under development as collaboration between Japan, USA and Spain. CLASP aims to measure the magnetic field in the upper chromosphere and transition region of the Sun through the detection and measurement of Hanle effect polarization of the Lyman alpha line. The Hanle effect (i.e. the magnetic field induced modification of the linear polarization due to scattering processes in spectral lines) is believed to be a powerful tool for measuring the magnetic field in the upper chromosphere, as it is more sensitive to weaker magnetic fields than the Zeeman effect, and also sensitive to magnetic fields tangled at spatial scales too small to be resolved. The Lyman-alpha (121.567 nm) line has been chosen because it is a chromospheric/transition-region line, and because the Hanle effect polarization of the Lyman-alpha line is predicted to be sensitive to 10-250 Gauss, encompassing the range of interest. Hanle effect is predicted to be observable as linear polarization or depolarization on the order of 0.1% to 1%. The experiment is proposed for flight in 2014.

Poster Abstracts

Network boundary study in coronal hole and quiet Sun regions with HINODE/EIS data

Abstract Author(s): Abbo, L. (1), Gabriel, A. (2)
Institution(s): (1) INAF-Osservatorio Astronomico di Torino, Pino Torinese (TO), 10025 - Italy, (2) Institut d'Astrophysique Spatiale, Université Paris-Sud 11, 91405 Orsay - France
Email: abbo@oato.inaf.it
Session: Magnetic structuring of the Sun from beneath the photosphere through the corona
Presentation: P-1

Abstract:

Images in spectral lines formed through the transition region show the boundaries of the supergranular cells in enhanced brightness, up to coronal temperatures, at which point the cell visibility disappears. This was interpreted as due to the magnetic field lines, concentrated at the cell boundaries, spreading out at the higher level and lower pressure of the corona, leading to near horizontal fields ('canopy' model, e.g. Gabriel 1976). Theory cannot predict the precise temperature of this spreading, which must depend on observations.

Using observations from EIS spectrometer on Hinode and CDS spectrometer on board SOHO, we analyze intensity maps over a range of temperatures through the upper solar atmosphere, from transition region up to coronal layers. Our purpose is to study the network boundary width of supergranular cells through the analysis of spectral lines formed at different temperatures in order to explore the expansion rate with height of the magnetic funnels. The method consists in analyzing the autocorrelation function of monochromatic images over a range of temperatures up to the solar corona. The study concerns coronal hole and quiet Sun regions in order to investigate a possible variation in the temperature and magnetic structure of the flux tubes.

Bayesian model comparison in spectropolarimetry

Abstract Author(s): Asensio Ramos, A.
Institution(s): Instituto de Astrofisica de Canarias
Email: aasensio@iac.es
Session: Magnetic structuring of the Sun from beneath the photosphere through the corona
Presentation: P-2

Abstract:
The selection of a model for the inversion of Stokes profiles is typically done based on subjective reasons. In this talk I present the application of Bayesian model comparison techniques for deciding which is the model best suited to the observations. The Bayesian approach correctly balances the complexity of the model with the amount of information present on the observations.

Pervasive linear polarization signals in the quiet Sun internetwork

Abstract Author(s): Bellot Rubio, L. (1), Orozco Suarez, D. (2)
Institution(s): (1) Instituto de Astrofisica de Andalucia (CSIC), Granada, Spain; (2) National Astronomical Observatory, Mitaka, Japan
Email: lbellot@iaa.es
Session: Magnetic structuring of the Sun from beneath the photosphere through the corona
Presentation: P-3

Abstract:

Using Hinode data, we demonstrate that linear polarization signals occur nearly everywhere in the quiet Sun internetwork. As the noise level is reduced, up to 75% of the area covered by the observations show clear Stokes Q or U signals. The mere presence of linear polarization implies that internetwork fields are very inclined, as suggested by other studies. We determine the distributions of field strength, inclination and azimuth by inverting pixels with Stokes Q or U amplitudes of at least 0.58% of the continuum intensity, i.e., 4.5times the noise level. These signals, which account for more than 50% of the field of view, allow a very precise determination of the magnetic field vector to be made. At the highest angular resolution to date, our results confirm that internetwork fields are weak and highly inclined, but not completely horizontal nor isotropically distributed. We suggest that these fields are the ones traced by Hanle measurements.

Proto-sunspots at the beginning of Solar Cycle 24 observed by THEMIS/MTR and Hinode/SOT

Abstract Author(s): Schmieder, B. (1), Guo, Y. (2), Bommier, V. (1)
Institution(s): (1) Observatoire de Paris, (2) University of Nanjing
Email: brigitte.schmieder@obspm.fr
Session: Magnetic structuring of the Sun from beneath the photosphere through the corona
Presentation: P-4

Abstract:
Coordinated campaigns with THEMIS, Hinode and other instruments have allowed us to study the starting of the new solar cycle in 2009. Ephemeral bipolar regions appear at high latitudes. We performed a comparative study between THEMIS/MTR and Hinode/SOT polarimetry analysis using UNNOFIT or MELANIE inversion codes. SOT allows to detect fine vertical bunches of flux tubes. These bunches of flux tubes never succeed in creating a sunspot and even a pore. MTR allows us to have magnetic information at different levels in the atmosphere through the flux tubes.

MHD waves in magnetic bright points: The construction of magnetic waveguides using solar magneto-seismology

Abstract Author(s): Erdelyi, R. et al.
Institution(s): SP2RC, University of Sheffield
Email: robertus@sheffield.ac.uk
Session: Magnetic structuring of the Sun from beneath the photosphere through the corona
Presentation: P-5

Abstract:

Here we demonstrate how the observation of broadband frequency propagating MHD waves in magnetic flux tubes between the photosphere and TR can provide valuable insight into their magnetic field structure. In a case study, by implementing a full nonlinear 3D MHD simulation with realistic photospheric drivers, we demonstrate how the plasma structure of lower atmospheric magnetic flux tubes can act as a spatially dependent waveguide for a range of MHD waves (kink, sausage, Alfvén etc.). In particular, for the torsional Alfvén waves the frequency filtering of the flux tube is exploited. Importantly, for solar magnetoseismology applications, this frequency filtering is found to be strongly dependent on magnetic field structure. With reference to an observational case study of propagating torsional Alfvén waves using spectroscopic data from the Swedish Solar Telescope (SST), we demonstrate how the observed 2D spatial distribution of maximum power Fourier frequency shows a strong correlation with the presented forward model. This opens the possibility of beginning an era of lower atmospheric (chromospheric) magnetoseismology, to complement the more traditional methods of mapping the magnetic field structure of the solar chromosphere.

Net Circular Polarization as a tool to measure the gradient with height of the penumbral magnetic field

Abstract Author(s): Franz, M., Borrero, J. M., Schlichenmaier, R.
Institution(s): Kiepeneheuer Institut fuer Sonnenphysik
Email: morten@kis.uni-freiburg.de
Session: Magnetic structuring of the Sun from beneath the photosphere through the corona
Presentation: P-6

Abstract:
We investigate the influence of the gradients with height of various atmospheric parameters on the total net circular polarization (N). In our contribution, we demonstrate that at disk center, the correlation between N and Doppler velocity is larger in down-flow channels than it is in up-flow channels. This is due to a) the larger value of the average zenith angle of the magnetic field in down-flow channels and b) the larger difference between the zenith angles of the magnetic field of the individual atmospheric components (Franz 2011). Furthermore, we argue that only a decrease of the magnetic field strength with optical depth can account for the negative N in the center-side penumbra of sunspots at large heliocentric angles. By means of spectral inversion of Stokes profiles, we show that a simple model atmosphere with linear gradients in Doppler velocity and magnetic field strength is sufficient to account not only for the distribution of N, but also for its amplitude. Our results yield a scenario in which the velocity always increases with optical depth, while the gradient of the magnetic field strength with optical depth is either positive or negative, thereby accounting for the pattern of positive and negative N in the center-side penumbra (Franz et al. 2011).

Franz, M.: 2011, PhD Thesis, Kiepenheuer Institute fuer Sonnenphysik
Franz, M., Borrero, J. M., and Schlichenmaier, R.: 2011, A&A, (in preparation)

Visibility of solar prominences in SDO/AIA channels

Abstract Author(s): Heinzel, P., Schmieder, B., Parenti, S., Gunar, S., Golub, L.
Institution(s): Astronomical Institute, Academy of Sciences
Email: pheinzel@asu.cas.cz
Session: Magnetic structuring of the Sun from beneath the photosphere through the corona
Presentation: P-7

Abstract:

SDO/AIA channels cover an extended range of temperatures and can thus be used to diagnose the transition-region plasmas up to coronal ones. In coronal lines one can see central cool parts of prominences as dark structures, which is due to absorption and emissivity blocking. In the range of AIA wavelengths, the main contribution to absorption is the photoionization of HeI and HeII by the coronal line radiation. This allows to determine the column masses of prominences and the ionization degree of helium. An interesting exception is the channel around 171 A, where the prominences surprisingly appear in emission, like in 304 channel. In this contribution we first briefly review our previous work on absorption and blocking and then study the behavior of the 171 emission. We use recently obtained DEM for quiescent prominences and compute the synthetic spectra in selected AIA channels. We then compare 171 and 195 channels and derive conclusions concerning the prominence emissivity, as well as the absorption and blocking. The emission seen in the 171 channel can be used to better constrain prominence DEM curves.

Flux Dependence of cancellation occurrence in Quiet Sun

Abstract Author(s): Iida, Y. (1), Hagenaar, H. (2), Yokoyama, T. (1)
Institution(s): (1) University of Tokyo, Tokyo, Japan, (2) LMSAL, CA, USA
Email: yusukeiid@gmail.com
Session: Magnetic structuring of the Sun from beneath the photosphere through the corona
Presentation: P-8

Abstract:

The frequency of magnetic flux cancellation depends on the flux content of the considered flux elements. This is investigated by using long-term (~140 hours) magnetograms obtained by SOT/FG. Parnell et al. (2009) reported a power-law distribution of flux content with an index of -1.85, which covers a flux range from small patches in quiet Sun to large active regions. This distribution is considered to be achieved and sustained by four magnetic activities, namely emergence, merging, splitting, and cancellation. Though it is important to determine the flux dependence of these activities for the understanding of flux maintenance of the photosphere, there are few reports because of their complexity. Flux dependence of emergence on flux content is reported by Thornton & Parnell (2011). The authors in the Hinode-4th meeting report the flux dependence of merging and splitting. We investigate the flux dependence of cancellation in this study.

The magnetograms obtained by SOT/FG from December 30th in 2008 to January 5th in 2009, whose duration is long enough for a statistical investigation of cancellation, are used. The time interval between magnetograms is five minutes and full field of view is 84"x100". 5973 Cancellations are detected in this data set. Cancellation occurrence rate depends on decreased flux content during cancellation with a power-law index of -2.52. The slope steeper than -2 indicates that tiny cancellations take more important roles in the maintenance of flux distribution. Our findings are combined with the results of previous studies in order to discuss the flux maintenance in quiet Sun.

Vortex tubes as a source of acoustic emission in quiet Sun

Abstract Author(s): Kitiashvili, I. N. (1), Kosovichev, A. G. (1), Lele, S. K. (1), Mansour, N. N. (2), Wray, A. A., (2)
Institution(s): (1) Stanford University, (2) NASA Ames Research Center
Email: irinasun@stanford.edu
Session: Magnetic structuring of the Sun from beneath the photosphere through the corona
Presentation: P-9

Abstract:

Observations of the oscillatory behavior of the solar surface provide information about the photospheric and internal dynamics. Combination of observations and realistic radiative hydrodynamic numerical simulations is an excellent tool for a better understanding of the complicated turbulent phenomena on the Sun. Realistic simulations of quiet-Sun convection show a very important role of swirling motions (vortex tubes), which are ubiquitous on the surface and in near-surface layers. Strong vortex events occur often and are better visible in density and pressure variations. Interaction between the vortex tubes is associated with excitation of acoustic waves in a subsurface layer 150-300km deep. In the talk we will discuss various aspects of the vortex tubes dynamics: the mechanism of formation, the thermodynamic and flow structure, dynamical properties, and the vortex annihilation process as a source of acoustic waves. We will compare the theoretical results with high-resolution observations.

Formation of multi-scale structures in solar magnetoconvection and their dynamics

Abstract Author(s): Kitiashvili, I. N. (1), Kosovichev, A. G. (1), Mansour, N. N. (2), Stenflo, J. O. (3), Wray, A. A. (2)
Institution(s): (1) Stanford University, (2) NASA Ames Research Center, (3) Institute of Astronomy ETH Zurich
Email: irinasun@stanford.edu
Session: Magnetic structuring of the Sun from beneath the photosphere through the corona
Presentation: P-10

Abstract:
Dynamical self-organization phenomena are observed in supergranulation, plage regions, pores and sunspots. Recent progress in computational capabilities allows us to consider various regimes of the solar dynamics based on first physical principles. Realistic radiative MHD simulations help to answer important questions about the physical characteristics of solar magnetoconvection that support processes of magnetic structure formation of various scale. We will discuss results of our numerical simulations from the point of view of spontaneous formation of magnetic structures and self-organization processes on different spatial scales, as well as the role of turbulent vortex tubes in these processes. For comparison with observations we calculate Stokes profiles for the Hinode SP lines and investigate effects of unresolved small-scale turbulent properties.

Photospheric Signature of Granular-scale Flux Emergence and Cancellation

Abstract Author(s): Lim, E.-K., Yurchyshyn, V., Abramenko, V., Ahn, K., Cao, W., Goode, P.
Institution(s): Big Bear Solar Observatory, New Jersey Institute of Technology
Email: eklim@bbso.njit.edu
Session: Magnetic structuring of the Sun from beneath the photosphere through the corona
Presentation: P-11

Abstract:

We studied small-scale flux emergence on granular scales in an active region. New Solar Telescope (NST) of Big Bear Solar Observatory made it possible to clearly observe the photospheric signature of flux emergence with very high spatial (0".0375/pix) and temporal (15 s) resolution. From TiO observations, we found several elongated features stretching from the penumbral filaments at a relatively high speed (> 4 km/s). After an arched darkening appeared at a tip of a penumbral filament, a bright point (BP) developed and quickly moved away forming and stretching an elongated feature. Its size was approximately 3" by 0".5. The moving BP encountered nearby structures and a well-defined elongated shape faded away. Magnetograms from SDO/HMI and NST/IRIM showed that those features are associated with small-scale emerging and moving magnetic features, and their disappearance with magnetic cancellation. With two events, we describe detailed morphological developments, and their different cancellation processes.

Multi-wavelength observation of EUV jet in AR 10960

Abstract Author(s): Matsui, Y. (1), Yokoyama, T. (1), Imada, S. (2)
Institution(s): (1) Univ. of Tokyo, Japan, (2) Institute of Space and Astronautical Science, Japan Aerospace Exploration Agency
Email: yuki.m0921@gmail.com
Session: Magnetic structuring of the Sun from beneath the photosphere through the corona
Presentation: P-12

Abstract:
We report the relationship between the velocity and the temperature of a solar EUV jet. This jet occurred in the active region NOAA 10960 on 2007 June 5. Multi-wavelength spectral observations with EIS/Hinode allow us to know Doppler velocities at the wide temperature range. We analyzed the inclination angle of this jet from the stereoscopic analysis with STEREO. Using this inclination angle and Doppler velocity, we derived the real velocity of the jet. We found: (1) The jet consists of multi-temperature plasmas in a few 10^4 K to a few MK range. (2) The dependence of velocity upon the plasma temperature shows that the jet has two major components. (3) One component is a hot jet whose velocity is close to the sound speed at temperatures above 1 MK. (4) The other is a cool jet (< 1MK) which has approximately 250 km/s speed and has no dependence on plasma temperature. We interpret that the hot jet is driven by the chromospheric evaporation mechanism because of its temperature dependence and that the cool one is driven by the magnetic Lorentz force because of its supersonic speed and non-dependence on temperature. A morphological interpretation of this event is given based on the reconnection model by utilizing the multi-instrumental observations. Discussion of such double driving mechanisms for a jet event is also given along with our recent MHD simulations.

A Case for Polar Magnetic Field Diagnostics from the Perspective of the Solar Dynamo

Abstract Author(s): Dibyendu, N.
Institution(s): Indian Institute of Science Education and Research, Kolkata, India
Email: dnandi@iiserkol.ac.in
Session: Magnetic structuring of the Sun from beneath the photosphere through the corona
Presentation: P-13

Abstract:

The solar cycle involves the recycling of the toroidal and poloidal components of the Sun's magnetic field mediated via various flux transport processes. The toroidal field is produced in the interior of the Sun through stretching of the poloidal component by differential rotation. While there is no consensus on the mechanisms involved in poloidal field creation, recent evidence strongly supports the ideas of Babcock and Leighton — who envisaged that the decay and dispersal of tilted bipolar active regions is the main contributor to the poloidal field. This process, which plausibly constitutes one-half of the dynamo mechanism, occurs at photospheric and near-surface layers and can therefore be observationally constrained. Moreover, recent solar dynamo simulations aimed at exploring the physics of solar cycle predictability point out that the polar field of the preceding cycle is the primary determinant of the strength of the following cycle. Based on these ideas, I will present a case for accurate quantitative diagnostics of the Sun's polar magnetic field.

CME-related changes in line-of-sight magnetic field strength in dimming regions observed by Hinode on 14 December 2006

Abstract Author(s): Pedram, E. (1), Matthews, S. (1), van Driel-Gesztelyi, L. (1, 2, 3)
Institution(s): (1) University College London - Mullard Space Science Laboratory, (2) Observatoire de Paris, LESIA, (3) Konkoly Observatory of Hungarian Academy of Sciences
Email: epe2@mssl.ucl.ac.uk
Session: Magnetic structuring of the Sun from beneath the photosphere through the corona
Presentation: P-14

Abstract:

Following many coronal mass ejections (CMEs), dark areas referred to as coronal dimming regions have been observed to form within and around the erupting active region. We probe the nature of coronal dimmings in relation with the expanding CME though the analysis of their photospheric magnetic field in the flare and CME event of 14 December 2006 using data from Hinode's SOT. We have systematically analysed the variation of the magnetic field strength in a large region surrounding AR 10930 using Hinode SOT stokes V data. Our analysis shows that at the site of the dimmings there is a decrease in the magnetic field strength at the onset of the dimming in the dominant polarity of the plage regions surrounding the AR, persisting during the dimming without recovering to pre-CME values. This finding indicates a permanent reconfiguration and opening of the magnetic field lines as a result of a change in their inclination angle in the dominant polarity of the plage regions surrounding the erupting active region leading to a decrease in the plasma density observed as coronal dimming.

Magnetic field topology of pores and naked sunspot

Abstract Author(s): Sainz Dalda, A. (1), Tarbell, T. (2), Title, A. (2)
Institution(s): (1) Stanford-Lockheed Institute for Space Research, Palo Alto , CA, USA, (2) Lockheed Martin Solar and Astrophysics Laboratory, Palo Alto, CA, USA.
Email: asainz@lmsal.com
Session: Magnetic structuring of the Sun from beneath the photosphere through the corona
Presentation: P-15

Abstract:

Pores and naked sunspot are well-known solar features for long time ago. However, their magnetic topology and evolution are still unrevealed. Spectropolarimetric data with a high cadence, sensitivity, spatial and spectral resolution taken with the instrument SOT/SP on-board of the satellite Hinode have helped to shed light on them. We present the evolution of the magnetic field vector and thermodynamic magnitudes of a large-sized pore. Numerical simulations use to reproduce naked sunspot and pores as a sunspot without penumbra during either its evolution (naked sunspot) or its full life (pore). Our results offer the values that the model and numerical simulation must explain and reproduce respectively. In addition, paradoxically, the lack of penumbrae in these structures may give us a better understanding of its originating mechanism.

Convective flows in a sunspot penumbra

Abstract Author(s): Scharmer, G. B., Henriques, V. M. J.
Institution(s): Institute for Solar Physics of the R. Swedish Academy of Sciences
Email: scharmer@astro.su.se
Session: Magnetic structuring of the Sun from beneath the photosphere through the corona
Presentation: P-16

Abstract:

We discuss small-scale flows in the interior part of a sunspot penumbra, observed with SST/CRISP at 0.15 arcsec spatial resolution in the CI 5380 and Fe I 6301 lines. Both lines show clear correlation between intensity and vertical velocity, demonstrating the presence of overturning convection. The measured RMS velocities are sufficient to compensate penumbral radiative losses. The relation between the convective flows and the magnetic field topology are discussed.

Diagnosing the Prominence-Cavity Connection

Abstract Author(s): Schmit, D., Gibson, S.
Institution(s): University of Colorado-Boulder, High Altitude Observatory
Email: schmitd@colorado.edu
Session: Magnetic structuring of the Sun from beneath the photosphere through the corona
Presentation: P-17

Abstract:

The magnetic field is thought to play a central role in both the support of the prominence as well as the thermodynamic isolation of the surrounding cavity. We use the Hinode/EIS and SDO/AIA datasets to probe for the first time the dynamical link between these related structures. These observations are compared to the 3D magnetic geometries predicted by MHD models. The dynamic features are explained within the context of 1D field-aligned momentum and energy imbalance.

Statistics of mass loading of quiescent prominences

Abstract Author(s): Schwartz, P. (1, 2), Heinzel, P. (1), Kotrc, P. (1), Anzer, U. (3), Kupryakov, Yu. A. (4)
Institution(s): (1) Astronomical Institute, Academy of Sciences of the Czech Republic, Ondrejov, Czech Republic, (2) Astronomical Institute, Slovak Academy of Sciences, Tatranska Lomnica, Slovak Republic, (3) Max-Planck-Institut fuer Astrophysic, Garching, Germany, (4) Sternberg Astronomical Institute, Moscow, Russia
Email: schwartz@asu.cas.cz
Session: Magnetic structuring of the Sun from beneath the photosphere through the corona
Presentation: P-18

Abstract:

From May through June 2011, a multi-spectral observing campaign of quiescent prominences took place. Observations were carried out in EUV by AIA/SDO, in soft X-rays by XRT on Hinode (HOP) and in H_alpha by horizontal spectrographs of the Ondrejov observatory. Our aim was to observe a large number of quiescent prominences, in order to make statistics of their total masses. The total mass of each prominence is obtained by integration of the column density of the hydrogen and helium plasma over the whole prominence area. The column density is obtained using semi-automatic code based on the method of Heinzel et al. (2008) and the code is capable of analyzing a large amount of prominence observations. Moreover, we improved the method by taking into account non-symmetrical distributions of the coronal X-ray and EUV emissivity in front and behind the prominence. H_alpha intensities are used to estimate the hydrogen ionization degree, a very important parameter for the mass-loading determination.

Understanding chromospheric swirls in the solar corona

Abstract Author(s): Scullion, E. (1), Wedemeyer, S. (1), Rouppe van der Voort, L. (1), Fedun, V. (2), Erdelyi, R. (2)
Institution(s): (1) Institute of Theoretical Astrophysics, University of Oslo, Norway; (2) SP2RC, University of Sheffield, Applied Mathematics Department, UK
Email: eamonms@astro.uio.no
Session: Magnetic structuring of the Sun from beneath the photosphere through the corona
Presentation: P-19 (**Digital Poster Display**)

Abstract:
Recently discovered, and frequently occurring, chromospheric swirls may play an important role in channeling magnetic energy and plasma from the solar photosphere through to the hot outer solar corona. Spatially confined swirl events where first detected (2009) in the chromospheric Ca-II 854.2nm spectral line with the 1-m Swedish Solar Telescope (SST). Their characteristic vortex motions are believed to be driven by the build up of magnetic tension in the intergranular lanes and forced through photospheric convective buffeting. But, until now, it was unknown (both observationally and numerically) whether there was a coronal counterpart to these swirls. Also, more importantly, is there sufficient energy flux in the swirls to heat the outer atmosphere and contribute to the coronal heating? Here we present unique co-observations of chromospheric swirls, as observed with the SST / CRISP, SDO (Solar Dynamics Observatory) and Hinode (XRT/SOT/EIS) from May 2011. We successfully co-align these observations and reveal the coronal counterpart of swirls. Furthermore, we present a supporting 3D numerical model of swirl formation using a fully non-linear MHD (Magneto-HydroDynamic) code called SAC (Sheffield Advanced Code). We investigate wave propagation (driven by photospheric convection) and subsequent wave transmission through the chromosphere and into the corona. With this study we address an important piece of the puzzle regarding solar swirls with respect to their signature in the solar corona and, henceforth, further our understanding of how small-scale processes (which dominate the solar chromosphere) become coupled into the magnetized corona.

Spontaneous Pore Formation in Magneto-Convection Simulations

Abstract Author(s): Stein, R. (1), Nordlund, A. (2)
Institution(s): (1) Michigan State University/Niels Bohr Institute, (2) Copenhagen University
Email: stein@pa.msu.edu
Session: Magnetic structuring of the Sun from beneath the photosphere through the corona
Presentation: P-20 (**Digital Poster Display**)

Abstract:
Pores form spontaneously in simulations of emerging, minimally structured (uniform, untwisted, horizontal) magnetic field from a depth of 20 Mm in a domain 48 Mm wide. The inflow field strength was slowly increased from 200 G to 1 or 5 kG with an e-folding time of 5 hours. The field emerges first in a mixed polarity "pepper and salt pattern", but then due to the underlying large scale magnetic field structure collects into separate, unipolar concentrations. In the 5 kG case a pore formed spontaneously after 19 hours and in the 1 kG case after 44 hours. The pores have both accumulated a magnetic flux of about 2x1020 Mx. The magnetic concentration in the pore first forms near the surface at the edge of a large rising magnetic loop. As time goes in they accumulate more magnetic flux and extend downward, as high magnetic flux, low temperature and low density concentrations, reaching all the way to the bottom of the 20 Mm computational domain. They have a filamentary structure near the surface, but appear more coherent deeper in the interior. The minimum intensity in the pore is 20% of the average intensity and they are edge brightened in parts of their circumference. The magnetic field is vertical in the pore interior and inclined to the vertical at angles greater than 45 deg near their edges. The pores have lasted for over 10 hours so far. Stokes spectra of the Fe I 630.15 and 630.25 nm lines have been calculated and degraded by the Hinode annular psf, the slit diffraction and frequency smoothing for both quiet Sun and plage regions of the simulation. This work has been supported by NASA grants NNX07AO71G, NNX07AH79G and NNX08AH44G and NSF grant AST0605738. The simulations where performed on the pleiades cluster of the NASA Advanced Supercomputing Division at the Ames Research Center.

Structure and Dynamics of the Quiescent Prominence Eruption on 2010 December 6

Abstract Author(s): Su, Y., van Ballegooijen, A.
Institution(s): Harvard-Smithsonian Center for Astrophysics, Cambridge, MA, USA
Email: ynsu@head.cfa.harvard.edu
Session: Magnetic structuring of the Sun from beneath the photosphere through the corona
Presentation: P-21 (**Digital Poster Display**)

Abstract:
We present observations of the quiescent prominence that erupted on 2010 December 6. This prominence contains two parts: one part located in the active region remnants contains mainly horizontal threads, and another part located in the quiet Sun contains mainly vertical threads. Combination of SDO/AIA and STEREO/SECCHI/EUVI allows us to see the fine structures of this prominence both at the limb and on the disk. H-alpha observations from KSO are also included. We focus on the fine structures and dynamics of this prominence before, during, and after the eruption. Prior to the eruption, STEREO shows that filament material frequently ejects from the active region part to the quiet Sun part. This ejection results in the formation of a tree-like structure (concentration of dark vertical threads) near the border between the active region remnants and the quiet Sun. Around 14:18 UT, brightenings appeared around the filament in the active region remnants, which is followed by the lifting off of the filament starting from the center of the active region remnants. Most parts of the filament are erupted except a small fraction near the quiet Sun end. The filament left behind shows vertical threads in SDO/AIA at the east limb, but a thin dark filament on the disk is observed by STEREO/EUVI.

Hemispheric Helicity Trend for Solar Cycle 24

Abstract Author(s): Hao, J., Zhang, M.
Institution(s): National Astronomical Observatory of China
Email: zhangmei@bao.ac.cn
Session: Magnetic structuring of the Sun from beneath the photosphere through the corona
Presentation: P-22

Abstract:
Using vector magnetograms obtained with the Spectro-polarimeter (SP) aboard Hinode satellite, we studied two helicity parameters (local twist and current helicity) of 64 active regions occurred in the descending phase of solar cycle 23 and the ascending phase of solar cycle 24. Our analysis gives the following results. (1) The 34 active regions of the solar cycle 24 follow the so-called hemispheric helicity rule, whereas the 30 active regions of the solar cycle 23 do not. (2) When combining all 64 active regions as one sample, they follow the hemispheric helicity sign rule as in most other observations. (3) Despite with the so-far most accurate measurement of vector magnetic field given by SP/Hinode, the rule is still weak with large scatters. (4) The data show evidence of different helicity signs between strong and weak fields, confirming previous result from a large sample of ground-based observations. (5) With two example sunspots we show that the helicity parameters change sign from the inner umbra to the outer penumbra, where the sign of penumbra agrees with the sign of the active region as a whole. From these results, we speculate that both the Sigma-effect (turbulent convection) and the dynamo have contributed in the generation of helicity, whereas in both cases turbulence in the convection zone has played a significant role.

Coronal structure and outflow velocities overlaying network and coronal holes

Abstract Author(s): Abbo, L. (1), Gabriel, A. (2)
Institution(s): (1) INAF-Osservatorio Astronomico di Torino, Pino Torinese (TO), 10025 - Italy, (2) Institut d'Astrophysique Spatiale, Université Paris-Sud 11, 91405 Orsay – France
Email: abbo@oato.inaf.it
Session: Magnetic structuring of the Sun from beneath the photosphere through the corona
Presentation: P-23

Abstract:
Outflow velocity maps in quiet Sun and coronal hole regions from EIS/Hinode data have been derived over a range of coronal and transition region temperatures. These are used in order to study effects due to the underlying supergranule network and of coronal holes. To identify clearly the supergranular network and its associated magnetic structure, we have used data from SDO: specifically 1600 Å images from AIA and magnetic fields from HMI. Our observations, together with others published previously (e.g. Hassler et al. 1999), are interpreted in terms of the magnetic field of the network in the transition region, involving the release of energy and leading to the solar wind outflow.

Partial Frequency Redistribution Effects on the Scattering Polarization Pattern of Ly-alpha

Abstract Author(s): Belluzzi, L. (1), Trujillo Bueno, J. (2), Manso Sainz, R. (3)
Institution(s): (1) Instituto de Astrofisica de Canarias
Email: belluzzi@iac.es
Session: Magnetic structuring of the Sun from beneath the photosphere through the corona
Presentation: P-24

Abstract:

A very promising diagnostic tool for investigating the magnetic fields of the upper chromosphere and transition region of the Sun is the Hanle effect (i.e. the modification of the linear polarization produced by scattering processes due to the presence of a magnetic field), in the hydrogen Lyman-alpha line.

A deep understanding of the physics of scattering polarization in Lyman-alpha represents the first step in the development of such a diagnostic tool. In particular, it is important to carefully investigate the impact on the linear polarization pattern of this line of partial frequency redistribution effects.

In this contribution, we show some interesting results concerning the expected scattering polarization pattern in the Lyman-alpha line, as obtained taking into account partial frequency redistribution and radiative transfer effects in semi-empirical models of the solar atmosphere.

Time damping of non-adiabatic magnetohydrodynamic waves in a partially ionised prominence medium: Effect of a background flow

Abstract Author(s): Barcelo, S., Ballester, J. L.
Institution(s): Dept. Matematiques. Universitat Illes Balears
Email: s.barcelo@uib.es, marc.carbonell@uib.es
Session: Magnetic structuring of the Sun from beneath the photosphere through the corona
Presentation: P-25

Abstract:

The simultaneous occurrence of flows and time damped small-amplitude oscillations in solar prominences is a common phenomenon. These oscillations are mostly interpreted in terms of magnetohydrodynamic (MHD) waves. We study the time damping of linear non-adiabatic MHD waves in a flowing partially ionised plasma with prominence-like physical conditions. While in the case without flow there is a critical wavenumber at which the period of Alfvén and fast waves goes to infinite, when a flow is present two different critical wavenumbers appear. When the second critical wavenumber is attained the period of both branches become equal. In general, the time damping of Alfvén and fast waves is dominated by resistive effects, and its damping ratio is very inefficient when compared to observations. The damping of slow and thermal waves is basically dominated by non-adiabatic effects, and for slow waves it is possible to obtain a damping ratio close to observations, although it would correspond to long period oscillations with large damping times not often observed. The consideration of a structured medium produces new features such as the apparition of four critical wavenumbers for Alfvén waves, and one critical wavenumber for slow waves. For fast waves, constrained propagation substantially improves, within the range of observed wavelengths, the ratio of the damping time to period. In general, the results point out that ion-neutral collisions are an inefficient mechanism to explain the observed time damping of prominence oscillations if they are produced by Alfvén and fast waves. If the oscillations are produced by slow waves, only long period oscillations with large damping times produce damping ratios in agreement with observations.

A high-resolution study of Ca II H time-series as observed with Hinode

Abstract Author(s): de Wijn, A. G.
Institution(s): NCAR
Email: dwijn@ucar.edu
Session: Magnetic structuring of the Sun from beneath the photosphere through the corona
Presentation: P-26 (**Digital Poster Display**)

Abstract:
I present a study of time series of Ca II H images taken with Hinode/SOT. I identify small bright points that we associate with strong, mostly vertical magnetic field through comparison with G-band imaging and inversions of spectropolarimetric observations. I show that not all magnetic bright points are associated with kiloGauss field. These fields appear bright as a result of optical-depth effects resulting from the Wilson depression, and the emission seen in our observations likely results mostly from the wings of the Ca II H line. There is excellent correspondence between the Ca II H and Fe I 630.15 nm line core intensity, except tenous emission around the network field concentrations in the former that is absent in the latter. Comparison with limb observations shows that this "network haze" most likely corresponds to spicules.

Flux cancellation events in high-temporal, high-spatial resolution Hinode SOT quiet sun data

Abstract Author(s): Fischer, C. E. (1), de Wijn, A. G. (2), Keller, C.U. (3), Lites, B. W. (2)
Institution(s): (1) European Space Research and Technology Centre, ESA, Noordwijk, The Netherlands, (2) High Altitude Observatory, NCAR, Boulder, USA, (3) Astronomical Institute Utrecht, UU , Utrecht, The Netherlands
Email: cfischer@rssd.esa.int
Session: Magnetic structuring of the Sun from beneath the photosphere through the corona
Presentation: P-27 (**Digital Poster Display**)

Abstract:
We analyze a quiet-sun high-temporal, high-spatial resolution spectropolarimetric data set in combination with chromospheric filtergrams and high photosphere magnetograms recorded by the Hinode Solar Optical Telescope (SOT). The data set consists of a 4-hour time series with a field of view of 41 arcsec by 4.8 arcsec and scanned by the SP with a cadence of 1 minute. In addition we retrieve co-temporal and co-spatial Mg I b2 magnetograms and Ca II H filtergrams. We search for signatures of flux cancellation events and characterize their temporal evolution at different atmospheric heights. We find 33 flux cancellation events, with 25 showing a horizontal magnetic flux component located between the opposite polarity patches during the cancellation process.

Comparisons of observed and simulated umbral dots

Abstract Author(s): Hansteen, V., Ortiz, A.
Institution(s): Institute of theoretical astrophysics, University of Oslo
Email: viggoh@astro.uio.no
Session: Magnetic structuring of the Sun from beneath the photosphere through the corona
Presentation: P-28

Abstract:
We study and compare the properties of observed and simulated umbral dots (UDs). The observations were made at a spatial resolution of 0.14 arcsec and contain full Stokes measurements of a pore taken with the Crisp Imaging Spectro-Polarimeter at the Swedish 1 m Solar Telescope (Ortiz et al., 2010). We determine the general appearance, temporal evolution and flow velocity at different heights in the photosphere from a bisector analysis of the Fe I 630 nm lines. In addition, we use Stokes Q, U, and V profiles to characterize the magnetic properties of these structures. We find that most UDs are associated with strong upflows in deep photospheric layers. Some of them also show concentrated patches of downflows at their edges, with sizes of about 0.25 arcsec, velocities of up to 1000 m/s, and enhanced net circular polarization signals. These results are compared to Bifrost numerical models of magnetoconvection in the presence of strong magnetic fields, where we also can describe the general structure and evolution of the simulated UDs both in the convection zone below the photosphere and into the chromosphere above the photospheric UDs.

A comparison of flow patterns around coronal structures as observed by Hinode and SDO

Abstract Author(s): Hurlburt, N.
Institution(s): Lockheed Martin/ATC
Email: hurlburt@lmsal.com
Session: Magnetic structuring of the Sun from beneath the photosphere through the corona
Presentation: P-29 (**Digital Poster Display**)

Abstract:
Large scale flows in the vicinity of filaments, coronal holes and active regions are investigated. We identify sets of each over the year of past year using the Heliophysics Events Knowledgebase (HEK). Surface velocities are extracted from SOT and HMI data cubes using a spectral optical flow method and there properties are compared, both to assess the relative accuracy of the derived flows and to compare with coronal observations of AIA and XRT.

Structure of the inverse-Evershed flow in sunspots observed by SOT

Abstract Author(s): Ichimoto, K.
Institution(s): Kyoto University
Email: ichimoto@kwasan.kyoto-u.ac.jp
Session: Magnetic structuring of the Sun from beneath the photosphere through the corona
Presentation: P-30

Abstract:

The Solar Optical Telescope (SOT) aboard Hinode revealed the nature of the fine scale structure and dynamics of sunspot penumbra with the unprecedentedly stable high resolution imaging and high precision spectropolarimetry. The radial filamentary structure of penumbra and the conspicuous photospheric outflow known as the Evershed effect are understood as a natural consequence of thermal convection under the influence of strong sunspot magnetic fields. The interlocking structure of penumbral magnetic field, in which the elevation angle of magnetic field vector changes alternatively along the azimuthal direction with the spatial scale of the filament width, are demonstrated, where the Evershed outflow takes place along nearly horizontal field channels. Higher in the atmosphere, there is a reversed flow toward the umbra known as the inverse Evershed flow, while the nature nor the origin of which is still unknown. The SOT/NFI Dopplergram in the core of NaD1 line shows filamentary structures of oppositely directed Doppler signals over the penumbra. In this paper, we present the spatial structure of the inverse Evershed effect in relation to the penumbral interlocking field structure and its temporal behavior. A possible mechanism that drives the inverse Evershed flow will also be discussed.

Overturning Convection in Sunspot Penumbra: Observation in Deep Photospheric Spectral Line C I 5380

Abstract Author(s): Joshi, J.
Institution(s): Max-Planck Institute for solar system research, Katlenberg-Lindau, Germany
Email: joshi@mps.mpg.de
Session: Magnetic structuring of the Sun from beneath the photosphere through the corona
Presentation: P-31

Abstract:
We observed a sunspot in active region NOAA 11113 with the 1-meter Swedish Solar Telescope (SST) on 2010, October 17. Sunspot was located at heliocentric angle of 28 and spectropolarimetric observation was made in Deep photospheric C I 5380 and mid photospheric Fe I 5250 spectral lines. We study overturning convection in the sunspot penumbra. Recent high resolution observations in Deep photospheric C I 5380 line has found direct evidence of overturning convection in penumbra(Joshi et al., 2011; Scharmer et al., 2011) and support that heat transport in sunspot penumbra is accomplished by overturning convection. Three-Dimensional radiative MHD simulations suggest that convective structure in penumbrae restricted at surface and sub-surface layers. Results from comparison of velocity structure of the sunspot penumbra in mid and deep photosphere will be presented. Properties of convective motion along the axis penumbral filaments will be studied and compared with twist-ing motion of penumbral filaments to establish relation between twisting motion and overturning convection.

Power spectra of the solar surface convection and implication to local dynamo

Abstract Author(s): Katsukawa, Y., Orozco Suarez, D.
Institution(s): National Astrnomoical Observatory of Japan
Email: yukio.katsukawa@nao.ac.jp
Session: Magnetic structuring of the Sun from beneath the photosphere through the corona
Presentation: P-32

Abstract:

On the solar surface, interaction between magnetic fields and surface convection produces varieties of structures over the broad spatial scale from ~100 km, such as thin flux tubes, to 10^5 km, such as sunspots and active regions. Spatial power spectra of velocity and magnetic fields on the solar surface provide a clue to understand in which scale kinetic and magnetic energies are generated, transferred, and dissipated in the solar atmosphere. The HINODE Solar Optical Telescope (SOT) is the most suitable instrument to study it observationally owing to stable image quality, especially at the scale smaller than granulation. We made the power spectra using spectro-polarimeter (SP) data separately in internetwork and network regions as a function of mean unsigned magnetic flux. When the unsigned flux is very weak (<10 G), i.e. in the internetwork regions, the power spectra of magnetic energies have a peak at ~700 km which is comparable with the granular scale. At the scale smaller than granulation, the power spectrum exhibits power-law distribution with an index of ~ -1.3. Numerical simulations of granular convection indicated that magnetic fields were created by local dynamo action at the spatial scale smaller than the observational resolution limit, and magnetic energies at the scale dominated the overall magnetic energies. But the power spectrum derived in our study is inconsistent with them, because the magnetic energies tend to be suppressed at the scale smaller than 500 km. When the unsigned flux is large (>100 G), on the other hand, the power spectra of kinetic and magnetic energies tend to exhibit less clear peak at the granulation scale, but have a single power-law distribution, which implies that kinetic and magnetic energies strongly interact each other at every spatial scale.

Comparing Photospheric Magnetic Fields and Subsurface Flows in the Quiet Sun

Abstract Author(s): Kubo, M. (1), Sekii, T. (1), Gizon, L. (2, 3)
Institution(s): (1) National Astronomical Observatory of Japan, Tokyo, Japan, (2) Max Planck Institute for Solar System Research, Katlenburg-Lindau, Germany, (3) Institute for Astrophysics, University of Gottingen, Germany
Email: masahito.kubo@nao.ac.jp
Session: Magnetic structuring of the Sun from beneath the photosphere through the corona
Presentation: P-33 (**Digital Poster Display**)

Abstract:

Magnetic fields are dominated by the fluid immediately below the quiet-Sun photosphere. Therefore, it is expected that the magnetic field distribution is controlled by the convective motions. Magnetic concentrations that have vertical and strong fields are observed along the boundaries of the convective cells. A most prominent feature in the quiet Sun is the network magnetic field that partially outlines supergranular cells. It is believed that the network magnetic field is formed by the advection of intranetwork fields via the supergranular flows. On the other hand, spectropolarimetric observations using the Solar Optical Telescope (SOT) reveal that the quiet intranetwork regions are pervaded by horizontal magnetic fields. Information about subsurface convective flows would be helpful for understanding the organization of magnetic fields on the solar surface. We compare the photospheric magnetic field vector with the subsurface supergranular flows. The magnetic field vector is derived from the spectropolarimetric measurements with the Hinode/SOT. Our target is a quiet region around disk center. The field-of-view of 160"x160" includes several supergranular cells. The subsurface flow patterns are inferred using (time-distance) helioseismology and a time series of Dopplergrams. The Dopplergrams are observed at a 45-second cadence by the Helioseismic and Magnetic Imager onboard Solar Dynamics Observatory. Larger magnetic concentrations with vertical and stronger fields are observed in the region where the subsurface converging flows at supergranular scale are dominant. This confirms that the network magnetic fields are advected by the supergranular flows. Some stronger horizontal fields in the converging regions coincide with the stronger vertical fields. Such horizontal fields are presumably associated with the magnetic canopy above supergranules. However, stronger horizontal magnetic fields are observed not only in the region of subsurface converging flows but also in the region of diverging flows, an observation for which we have no explanation.

Temperature Structure of a Coronal Cavity

Abstract Author(s): Kucera, T. A. (1), Gibson, S. E. (2), Schmit, D.J. (3, 2)
Institution(s): (1) NASA/GSFC, (2) NCAR/HAO, (3) U. Colorado
Email: Therese.A.Kucera@nasa.gov
Session: Magnetic structuring of the Sun from beneath the photosphere through the corona
Presentation: P-34

Abstract:

We analyze the temperature structure of a coronal cavity observed in Aug. 2007. Coronal cavities are long, low-density structures located over filament neutral lines and are often seen as dark elliptical features at the solar limb in white light, EUV and X-rays. When these structures erupt they form the cavity portions of CMEs. It is important to establish the temperature structure of cavities in order to understand the thermodynamics of cavities in relation to their three-dimensional magnetic structure.

To analyze the temperature we compare temperature ratios of a series of iron lines observed by the Hinode/EUV Imaging Spectrometer (EIS). We use those lines to constrain a forward model of the emission from the cavity and streamer. The model assumes a coronal streamer with a tunnel-like cavity with elliptical cross-section and a Gaussian variation of height along the tunnel length. Temperature and density can be varied as a function of altitude both in the cavity and streamer. The general cavity morphology and the cavity and streamer density have already been modeled using data from STEREO's SECCHI/EUVI and Hinode/EIS (Gibson et al. 2010 and Schmit & Gibson 2011).

The AZAM Disambiguity Utility for the Hinode Spectro-Polarimeter

Abstract Author(s): Lites, B. W.
Institution(s): HAO/NCAR
Email: lites@ucar.edu
Session: Magnetic structuring of the Sun from beneath the photosphere through the corona
Presentation: P-35

Abstract:

The AZAM utility is a software package for interactive resolution of the 180 ambiguity of the transverse component of the magnetic field vector. In addition to this capability, AZAM also provides the user with a platform that performs many other useful tasks involving examination and display of the results of inversion of solar Stokes profile measurements. Developed initially during the mid- 1990s for use on data from the HAO/NSO Advanced Stokes Polarimeter (SP) and written entirely in IDL, AZAM has been extensively modified to work with data from the Hinode Spectro-Polarimeter. It is implemented in SolarSoft, and will soon be available for use by the community. The interactive ambiguity resolution procedure of AZAM is based on attaining continuity of the field vector over the observed field of view. The present version of AZAM for Hinode SP accepts as an input the routine inversion results from the MERLIN implementation of the Unno-Rachkovsky solution to the equations of polarized radiative transfer for a Milne-Eddington model atmosphere — inversion results produced routinely for all SP data.

Emergence and disappearance of magnetic field in the quiet Sun at the photosphere

Abstract Author(s): Martinez-Sykora, J. (1)
Institution(s): (1) Lockheed Martin Solar & Astrophysics Lab, Palo Alto, CA, USA, (2) Institute of Theoretical Astrophysics, University of Oslo, Norway, (3) Instituto Astrofisico de Andalucia, Granada, Spain
Email: juanms@lmsal.com
Session: Magnetic structuring of the Sun from beneath the photosphere through the corona
Presentation: P-36

Abstract:

We studied characteristics and statistics of strong asymmetric profiles in Stokes V in quiet sun, using Hinode/SOT, and compare with synthetic observations; i.e., single lobe profiles in Stokes V. These profiles require the existence of a velocity gradient along the line of sight, possibly associated with gradients of magnetic field strength, inclination and/or azimuth. However, these asymmetric profiles do not depend on the velocity or/and sign of the velocity. In the quiet sun, magnetic field is continuously emerging and disappearing at small scales due to the convective motions and the input of new flux from deeper layers. From the realistic simulations, using Bifrost code, we note that most of these small scale processes have stratifications with gradients of magnetic field strength, inclination and velocities. As a consequence, these stratifications are associated with the existence of single-lobe Stokes V profiles in the solar photosphere. We show that most of these profiles come from magnetic flux emergence and disappearance in small scales in the simulations. Most of the stratifications show jumps in the magnetic field configuration. Finally, we emphasize the importance of statistic analysis in these single-lobe Stokes V profiles using Hinode/SOT and the comparison with the synthetic profiles from the simulations. This comparison will ultimately improve the realism of the simulations and quantify the flux emergence and disappearance in the quiet sun.

Time-distance helioseismology analyses of multi-wavelength datasets obtained with Hinode/SOT and SDO/HMI

Abstract Author(s): Nagashima, K. (1), Zhao, J. (1), Duvall, Jr., T. (2), Kosovichev, A. G. (1), Parchevsky, K. (1), Sekii, T. (3)
Institution(s): (1) Stanford University, (2) NASA Goddard Space Flight Center, (3) NAOJ
Email: kaorin@stanford.edu
Session: Magnetic structuring of the Sun from beneath the photosphere through the corona
Presentation: P-37

Abstract:

Helioseismology analysis is useful for probing the interior structure and dynamics of the Sun. Its usefulness, however, is not limited to sub-surface diagnostics. When we use multi-layer observation datasets, it provides us with an opportunity to examine the wave propagation between the layers (Nagashima et al. 2009), and also the oscillation physics of the solar atmosphere. We use multi-wavelength observations from Hinode/SOT and SDO/HMI to carry out the time-distance helioseismology analysis: we calculate the cross-correlation function of the wavefields, measure the travel times of acoustic waves, and investigate the wave-field properties. Our preliminary results reveal differences in the cross-correlation functions and travel times between different observation layers (wavelengths). Investigation of the differences is particularly important for helioseismology analyses of the solar polar regions, because for the polar observation datasets the line formation height may depend on the distance from the disk center even for the case of the single-wavelength observation, and may cause systematic uncertainties in meridional flow measurements by local helioseismology. For a better understanding of the observational results, we use numerical simulations of solar oscillations.

High-resolution observations of type II spicules

Abstract Author(s): Rouppe van der Voort, L.
Institution(s): University of Oslo
Email: rouppe@astro.uio.no
Session: Magnetic structuring of the Sun from beneath the photosphere through the corona
Presentation: P-38 (**Digital Poster Display**)

Abstract:
Type II spicules are a class of spicules that are characterized by short lifetimes and high apparent velocities. Combined with their narrow spatial widths, type II spicules are challenging to observe. We use the CRISP imaging spectropolarimeter at the Swedish 1-m Solar Telescope on La Palma to observe type II spicules at the limb and their counterparts on the solar disk, the so-called "RapidBlue-shifted Excursions" (RBEs). The combination of adaptive optics and image post-processing allows CRISP to attain high resolution simultaneously in the spatial, temporal and spectral domains. Here we present results from the analysis of several high-quality data sets which allow to constrain the physical properties of type IIspicules.

On the nature of prominence bubbles and plumes

Abstract Author(s): Schmieder, B., Heinzel, P., Zapior, M., Gunar, S.
Institution(s): Observatoire de Paris-Meudon
Email: brigitte.schmieder@obspm.fr
Session: Magnetic structuring of the Sun from beneath the photosphere through the corona
Presentation: P-39 (**Digital Poster Display**)

Abstract:
A hot topic recently discussed is the nature of large prominence bubbles seen in various spectral lines, including H-alpha and CaII where they appear as dark features (Berger et al.). However, in selected SDO/AIA coronal channels they usually appear brighter relative to surrounding dark structures. The latter are due to absorption and emissivity blocking of the respective coronal-line radiation. The question is whether the bubbles in these AIA channels are hotter and/or denser compared to surrounding corona or coronal cavity. In this contribution we investigate some examples of bubbles and related plumes, using the time series in selected SDO/AIA channels and co-temporal MSDP observations in the H-alpha line obtained at Wroclaw-Bialkow observatory.

An abrupt magnetization in the upper chromosphere of the quiet Sun

Abstract Author(s): Stepan, J. (1), Trujillo Bueno, J. (1), Ramelli, R. (2), Bianda, M. (2)
Institution(s): (1) Instituto de Astrofisica de Canarias, Spain, (2) Istituto Ricerche Solari Locarno, Switzerland
Email: stepan@iac.es
Session: Magnetic structuring of the Sun from beneath the photosphere through the corona
Presentation: P-40

Abstract:

The only way to obtain quantitative empirical information on the strength and orientation of the magnetic field of the solar atmosphere is through the measurement and interpretation of the polarization signals that some physical mechanisms introduce in spectral lines. Unfortunately, the Zeeman effect as a diagnostic tool is of limited practical interest for the "measurement" of the magnetic fields of the quiet solar chromosphere. Here we show that the Hanle effect in strong spectral lines is the physical mechanism that should be increasingly exploited for quantitative explorations of the magnetism of the quiet solar chromosphere. To this end, we show how scattering polarization observations of the H-alpha line can be modelled by means of multilevel radiative transfer simulations in magnetized atmospheric models. Of particular interest is that the amplitude and shape of the scattering polarization profiles of the H-alpha line are very sensitive to the strength and structure of the chromospheric magnetic field. We show that the interpretation of the available observations in terms of one-dimensional radiative transfer modeling suggests that there is an abrupt and significant magnetization in the upper chromosphere of the quiet Sun.

Calculating Magnetic Free Energy Using the Minimum Current Corona Model in Evolving Active Regions: NOAA AR11158

Abstract Author(s): Tarr, L., Longcope, D.
Institution(s): Montana State University
Email: ltarr@physics.montana.edu
Session: Magnetic structuring of the Sun from beneath the photosphere through the corona
Presentation: P-41 (**Digital Poster Display**)

Abstract:

The Minimum Current Corona (MCC) model provides a way to estimate stored coronal energy using the number of field lines connecting regions of positive and negative photospheric flux. MCC assumes that the amount of flux connecting pairs of regions is fixed, even as the photospheric field evolves. As the fixed flux in each domain becomes increasingly different from a potential field configuration the system builds up magnetic free energy. We have developed a method for quantifying the field evolution by tracking photospheric magnetic sources measured with SDO/HMI, and therefore energy storage. In particular, we present an algorithm quantifying the flux evolution of each pair of regions due to emergence through the photosphere. We have applied this method to calculate the increase in magnetic free energy in NOAA Active Region 11158, which underwent a GOES X2.2 class flare around 02:00 on Feb. 15th, 2011.This work was supported NASA LWS.

Some dynamic analysis of the photosphere with HINODE/SOT and SDO

Abstract Author(s): Roudier, T. (1), Malherbe, J. M. (2), Rieutord, M. (1), Berger, T. (3), Frank, Z. (3), Prat, V. (1), Renon, N. (4), Gizon, L. (5), Svanda, M. (5)
Institution(s): (1) IRAP Univ. de Toulouse, CNRS, 14 avenue E. Belin, 31400 Toulouse, France, (2) LESIA, Observatoire de Paris, Section de Meudon, 92195 Meudon, France, (3) Lockheed Martin Advance Technology Center, Palo Alto, CA, USA, (4) CALMIP, DTSI Université Paul Sabatier, Université de Toulouse 31062 Toulouse, France, (5) Max-Planck-Institut für Sonnensystemforschung Max-Planck-Strasse 2, 37191 Katlenburg-Lindau, Germany
Email: roudier@ast.obs-mip.fr
Session: Magnetic structuring of the Sun from beneath the photosphere through the corona
Presentation: P-42 (**Digital Poster Display**)

Abstract:

The dynamics of the solar surface and its interaction with the magnetic structures control in great part the outer atmosphere of the Sun. We study the interactions of velocity scales on the Sun's surface, from granulation to supergranulation and their interaction with magnetic fields. We analyse a 48 h time sequence of the quiet Sun photosphere obtained with the Solar Optical Telescope onboard HINODE. This analysis allows us to better characterize Trees of Fragmenting Granules issued from repeated fragmentation of granules. We show their crucial role in the advection of the magnetic field and in the build up of the network. These results demonstrate that the long living families contribute to the formation of the magnetic network and suggest that supergranulation could be an emergent length scale building up as small magnetic elements are advected and concentrated by TFG flows. Observations have been obtained on September 4, 2010, by SOT on board of the satellite HINODE, in magnetically insensitive FeI 557.6 nm line. Acoustic events (AE, defined as spatially concentrated propagating waves) have been derived from amplitudes and phases of vertical Doppler with outstanding spatial resolution (0.3) and field of view. AE partly contribute (10%) to energy transport involved in the chromospheric heating and could be the drivers of the solar oscillations. Very recent observations of HINODE/SOT and SDO/HMI have allowed us, with the HMI-continuum data, to measure the horizontal (vx,vy) all over (almost) the solar surface. These velocity fields are calculated every 30 minutes with spatial window of 2.5 Mm.

Comparison of multi-height observations with a 3D MHD sunspot model

Abstract Author(s): Jaeggli, S. A. (1), Lin, H. (1), Rempel, M. (2), Uitenbroek, H. (3)
Institution(s): (1) Institute for Astronomy - University of Hawaii, (2) High Altitude Observatory, National Center for Atmospheric Research, (3) National Solar Observatory/Sacramento Peak
Email: jaeggli@ifa.hawaii.edu
Session: Magnetic structuring of the Sun from beneath the photosphere through the corona
Presentation: P-43

Abstract:

In sunspots the contribution to the horizontal pressure support from the curvature force and the geometrical height of formation which magnetic field measurements sample are poorly constrained observationally due to the effect of radiative transfer. In cool atmospheres, observations of the sunspot photosphere probes geometrically deeper layers, information on the magnetic field gradients cannot be easily derived even using multi-wavelength, multi-height observations. Recent MHD atmosphere models of sunspots analyzed with the Rybiki-Hummer radiative transfer code allow for direct comparison with simultaneous multi-height observations of the Fe I magnetic field diagnostics at 1565 and 630.2 nm in sunspots observed using the Facility Infrared Spectropolarimeter at the Dunn Solar Telescope.

Inversion of physical parameters in coronal magnetic structures

Abstract Author(s): Arregui, I. (1), Ballester, J. L. (1), Goossens, M. (2), Oliver, R. (1), Asensio Ramos, A. (3)
Institution(s): (1) Universitat de les Illes Balears, Spain, (2) Katholieke Universiteit Leuven, Belgium, (3) Instituto de Astrofisica de Canarias, Spain
Email: inigo.arregui@uib.es
Session: Energy transport and dissipation through the solar atmosphere and into the heliosphere
Presentation: P-44 (**Digital Poster Display**)

Abstract:
Magnetohydrodynamic seismology aims to determine difficult to measure physical parameters in the solar corona by a combination of observed and theoretical properties of waves and oscillations. We first describe relevant examples of the application of seismology techniques to transversely oscillating coronal loops, observed by TRACE, and prominence fine structures, observed by Hinode. We next show how the use of statistical techniques based on Bayesian inference, in combination with Markov chain Montecarlo simulations, can constrain difficult to measure physical parameters. An example is provided in which a bayesian inference technique is applied to transverse coronal loop oscillations. The bayesian approach enable us to infer the most probable values of the relevant parameters, for given observed periods and damping times, and to extract their confidence levels incorporating observed uncertainties in a consistent manner. We believe the development of this kind of technique will be of high value for the future of solar atmospheric seismology, when the inversion of physical parameters will be based on the combination of large scale numerical parametric results and the analysis of data sets obtained from, e.g., SOLAR-C.

Differential Emission Measure Analysis of a Polar Coronal Hole During the Recent Solar Minimum

Abstract Author(s): Hahn, M., Landi, E., Savin, D. W.
Institution(s): Columbia University
Email: mhahn@astro.columbia.edu
Session: Energy transport and dissipation through the solar atmosphere and into the heliosphere
Presentation: P-45

Abstract:

We have performed a differential emission measure (DEM) analysis for a polar coronal hole observed during the solar minimum in 2007. The analysis was performed for the above-limb portions of five observations from the EUV Imaging Spectrometer on Hinode. The slit pointings also included quiet Sun corona near the boundary with the coronal hole. The analysis shows that the plasma is not strictly isothermal anywhere, but rather has a high-temperature component that extends up to log T(K) = 6.2 - 6.3. The size and importance of this component depend on location and its evolving magnitude marks the boundary between the coronal hole and the quiet corona, where it becomes dominant. Our results highlight the potential limitations of isothermal analyses. Such methods actually measure a DEM-weighted average temperature and as a result can infer artificial temperature gradients. The isothermal analyses also do not detect different structures along the line-of-sight, which can affect the interpretation of density diagnostic line ratios.

EVE non-detection of Doppler-shifted He II 304 Å

Abstract Author(s): Hudson, H., Fletcher, L., MacKinnon, A., Woods, T.
Institution(s): SSL, UC Berkeley
Email: hhudson@ssl.berkeley.edu
Session: Energy transport and dissipation through the solar atmosphere and into the heliosphere
Presentation: P-46

Abstract:

The Extreme-ultraviolet Variability Experiment (SDO) gives a new perspective on the EUV spectroscopy of solar flares, with several new insights. The spectra have 10-s cadence, excellent dynamic range, and spectral resolution adequate to measure Doppler motions subject to Sun-as-a-star limitations. In this presentation we describe the search for broad wings in the He II 304 Å line, in which the Orrall & Zirker (1976) mechanism suggests broad Doppler-shifted wings resulting from charge exchange. The EVE data provide excellent limits on the intensity of such line wings and thereby suggest that alpha particles do not significantly penetrate to un-ionized atmospheric regions. The data thus far analyzed include two gamma-ray events and two X-class flares.

Power-law index of nanoflares in a coronal loop modified by observational conditions

Abstract Author(s): Kitagawa, N., Yokoyama, T.
Institution(s): The University of Tokyo
Email: kitagawa@eps.s.u-tokyo.ac.jp
Session: Energy transport and dissipation through the solar atmosphere and into the heliosphere
Presentation: P-47

Abstract:

One-dimensional numerical simulation of an impulsively heated coronal loop was conducted. Since Parker (1983) had suggested topological dissipation of coronal magnetic fields braided by photospheric convection, a number of studies has been investigated the validity of coronal heating by that mechanism called ``nanoflare'' (Parker 1988). From observations, it was indicated that the occurrence frequency distribution of solar flares, including major flare (E~1033 erg) down to nanoflare (E~1024 erg), obeys to power-law with an index of around -1.6 (see review by Aschwanden & Parnell 2002). However, in consideration of the result shown by Shimizu (1995) that the power-law distribution becomes flat when spatial resolution is reduced, a value of the index from previous observations may not be conclusive. In addition, temporal cadence, the angle between our line of sight (LOS) and loop plane, and the detection algorithm of heating signatures are likely to influence on the derived power-law index of observations. We have tackled to this issue by using one-dimensional simulation of a coronal loop heated by impulsive energy input representing nanoflare. The energy input obeys to a power-law distribution with the index of 1.6, 2.0, 2.4. Synthesized data observed with TRACE were made through reduced temporal cadence (10s-120s) and spatial resolution (0.5"-4"). Our findings indicate that the derived thermal energy distribution is influenced by spatial resolution rather than temporal cadence, and the methodological difference produces different type of the derived distribution, and LOS angle against loop plane also influences the shape of the derived distribution.

Properties in the North and South Polar Coronal Holes in the Ascending Phase of Solar Cycle 24, and Comparison with the Associated Solar Wind

Abstract Author(s): Ko, Y.-K. (1), Young, P. R. (1, 2), Wang, Y.-M. (1), Warren, H. P. (1)
Institution(s): (1) Naval Research Laboratory, Washington, DC, USA, (2) George Mason University, Fairfax, VA, USA
Email: yko@ssd5.nrl.navy.mil
Session: Energy transport and dissipation through the solar atmosphere and into the heliosphere
Presentation: P-48

Abstract:

Polar coronal holes (CHs) are the most prominent open-field regions on the Sun during the years around solar minimum when solar wind emanating from the high-latitude polar CHs can often reach the ecliptic and measured in-situ by solar wind instruments at 1 AU. In addition, the off-ecliptic trajectory of Ulysses has offered a unique opportunity for measuring the solar wind from deep within the polar CH. It has been found from the Ulysses 1st pole-to-pole fast scan, which was during the descending phase of Cycle 22, that the fast wind ion composition from the north polar CH is "cooler" than that from the south polar CH. On the other hand, recent work on the solar wind with polar CH source regions shows that during the descending phase of Cycle 23, it is the south polar CH that is "cooler". Such intriguing differences should be closely related to the properties intrinsic in these CHs that can be investigated by magnetic and spectroscopic observations. This motivated a series of Hinode observations on polar CHs (HOP146) that intend to look for clues for such differences. We present the physical properties in the north and south polar CHs, as well as their boundary region, derived from Hinode/EIS observations from Dec.2009 to Aug.2010. We discuss the differences between the two CHs and the variations with time. The properties of the solar wind that can be traced back to either polar coronal hole during this period are also presented and compared with these EIS observations.

Statistical Analysis of EIS spectra in Active Regions

Abstract Author(s): Lee, E., Williams, D. R., Lapenta, G.
Institution(s): Katholieke Universiteit Leuven
Email: edwin.lee@wis.kuleuven.be
Session: Energy transport and dissipation through the solar atmosphere and into the heliosphere
Presentation: P-49

Abstract:

In our study, we apply statistical and functional methods to assess the underlying motions in coronal active regions that give rise to the different shapes of emission line profiles seen in spectroscopic images observed by Hinode/EIS. We observe the evolution of 1" slit raster data at multiple coronal temperatures, in different subregions, and during different events, including flux emergence. Assuming the emission line profiles to be a credible proxy for the statistical ensemble of the coronal plasma, we employ a set of tools on the profiles to derive conclusions about its motion along the line of sight. Our tools include both "objective" and "biased" ways of improving the availability of information inferable from EIS observations, without over-constraining the data with ad-hoc assumptions. We compare several methods for improving to the signal-to-noise ratio in our statistics and show the effect of each on data selection. Spectroscopic simulations (akin to synthetic spectra) are also performed to better assess the motion of the plasma and the effects of flux emergence and magnetic reconnection.

Heating of Flare Foops During a Two-ribbon Flare on 2011 March 07

Abstract Author(s): Liu, W-J (1); O'Hara, J. (1, 2); Peck, C. (1); Qiu, J (1); Longcope, D. W. (1)
Institution(s): (1) Montana State University, Bozeman, (2) St Andrews University
Email: wliu@physics.montana.edu
Session: Energy transport and dissipation through the solar atmosphere and into the heliosphere
Presentation: P-50

Abstract:

Many eruptive flares exhibit two extended ribbons in the lower-atmosphere outlining the feet of the post-flare coronal arcade. High-cadence and high-resolution UV observations by TRACE reveal that the flare ribbon consists of small patches sequentially brightened along the ribbon, suggesting that reconnection takes place sequentially forming individual post-flare loops along the arcade, as often seen in coronal observations in the EUV wavelengths. These reconnection events and formation of new loops continue well into the decay phase. Our recent study (Qiu et al. 2010) further shows that the spatially resolved UV brightness at the foot-points of individual loops grows rapidly on timescales of a few minutes, followed by a long decay on timescales of more than 10 minutes. The rapid rise of UV radiation is correlated with the hard X-ray light curve during the impulsive phase, hence is most likely a direct response of instantaneous heating in the reconnection formed flux tubes. In this study, we utilize the spatially resolved UV brightness time profiles to reconstruct instantaneous heating functions of individual flux tubes, and compute evolution of each flux tube using the EBTEL model (Klimchuk et al. 2008). The temperature and density of these flux tubes are then used to calculate light curves in other energy bands and compare favorably with observations by RHESSI, GOES and AIA. This study presents the first effort to constrain heating functions of flare loops directly using all available observables, and provides a powerful way to examine physics of heating discrete flux tubes formed by reconnection events throughout the flare.

Propagation of Polar Coronal Jets in the Fast Solar Wind

Abstract Author(s): Miralles, M. P. (1), Cranmer, S. R. (1), Raymond, J. C. (1), Savcheva, A. S. (1), Stenborg, G. (2), Deluca, E. E. (1)
Institution(s): (1) Harvard-Smithsonian Center for Astrophysics, Cambridge, MA, USA, (2) Interferometrics Inc., Herndon, VA, USA
Email: mmiralles@cfa.harvard.edu
Session: Energy transport and dissipation through the solar atmosphere and into the heliosphere
Presentation: P-51

Abstract:
We present results of an ongoing observational study of the physical properties and kinematics of polar coronal jets. While magnetic reconnection is considered the prime driving mechanism of the ejected plasma, the processes at work during reconnection are not yet completely understood. We use a combination of X-ray, UV, and visible-light imaging to probe the jet plasma, and we trace polar jets from their reconnection sites into the fast solar wind. Multi-instrument measurements of polar jets will put firm constraints on the mechanisms driving the jets and on the relative contribution of jets to the overall fast solar wind.

This work is supported by NASA grant NNX09AH22G to the Smithsonian Astrophysical Observatory.

What Powers Coronal Heating and the Solar Wind According to Hinode

Abstract Author(s): Moore, R., Sterling, A., Cirtain, J., Falconer, D.
Institution(s): NASA/Marshall Space Flight Center/NSSTC
Email: ron.moore@nasa.gov
Session: Energy transport and dissipation through the solar atmosphere and into the heliosphere
Presentation: P-52

Abstract:

From Hinode's ground-breaking high-resolution observations of solar X-ray jets, Type-II spicules, and granule-size emerging bipolar magnetic fields in quiet regions and coronal holes, we advocate a scenario for powering coronal heating and the solar wind. In this scenario, Type-II spicules and Alfvén waves are generated by granule-size emerging bipolar magnetic fields in the manner of the generation of X-ray jets and accompanying Alfvén waves by larger magnetic bipoles. From observations and this scenario, we estimate that Type-II spicules and their co-generated Alfvén waves carry into the corona an area-average flux of mechanical energy of about 7×10^5 erg cm^{-2} s^{-1}. This is enough to power the corona and solar wind in quiet regions and coronal holes. Therefore, the discoveries by Hinode of Alfvén waves in X-ray jets, Type-II spicules, and granule-size emerging bipoles, together indicate that the granule-size emerging bipoles, by making Type-II spicules, are the main power source of coronal heating, the solar wind, and hence the entire heliosphere. Thus, provided that coordinated high-resolution observations confirm that Type-II spicules come from the granule-size emerging bipoles, Hinode has discovered the specific magnetic activity that powers the global corona and solar wind.

This work was funded by NASA's Science Mission Directorate through the Heliophysics Guest Investigator's Program, the Hinode Project, and the Living With a Star Targeted Research and Technology Program.

Diagnostics of coronal temperature based on the calibration result of X-Ray Telescope and further calibration

Abstract Author(s): Narukage, N. (1), Sakao, T. (1), Kano, R. (2), Shimojo, M. (2)
Institution(s): (1) Institute of Space and Astronautical Science, Japan Aerospace Exploration Agency (ISAS/JAXA), Sagamihara, Kanagawa, JAPAN, (2) National Astronomical Observatory of Japan (NAOJ), Mitaka, Tokyo, JAPAN
Email: narukage@solar.isas.jaxa.jp
Session: Energy transport and dissipation through the solar atmosphere and into the heliosphere
Presentation: P-53

Abstract:

The X-Ray Telescope (XRT) onboard the Hinode satellite is an X-ray imager that observes the solar corona with nine X-ray analysis filters which have different temperature responses. One of the most significant scientific features of this telescope is its capability of diagnosing coronal temperatures from less than 1 MK to more than 10 MK. To make full use of this capability, Narukage et al. (2011) calibrated the coronal temperature response of XRT including the effect of on-orbit contamination. They showed that, for some filter pairs, there is a discrepancy between the filter-ratio temperatures with the calibrated result and with the instrumental parameters before calibration. In this paper, we investigate whether the results of coronal temperature diagnostics before the calibration are appropriate, i.e., are comparable to the filter ratio temperature based on the calibration result. For example, though Reale et al. (2009) showed the presence of plasma around 10 MK in a non-flaring coronal active region with the filter ratio of med-Be and med-Al filters, we find that its temperature should be around 2 MK. Meanwhile, the filter ratio temperature in flares derived with calibrated thick filters (thick-Al and thick-Be) is around 3 or 4 MK, which is cooler than the expected temperature. As described in Narukage et al. (2011), the calibration of thick-Al and thick-Be filters is not enough, since only one characteristic X-ray line was available in the ground-based calibration because of little transmission of low-energy X-rays for the thick filters. In this paper, we calibrate these thick filters with the data sets of active regions.

DEMs for EIS and AIA

Abstract Author(s): Plowman, J. (1), Martens, P. (1), Ritchie, M. (2), Scott, J. (1), Sharma, R. (3)
Institution(s): (1) Montana State University, Bozeman, MT, USA, (2) University of St Andrews, Scotland, UK, (3) Mohanlal Sukhadia University, Rajasthan, India
Email: plowman@physics.montana.edu
Session: Energy transport and dissipation through the solar atmosphere and into the heliosphere
Presentation: P-54

Abstract:
We present a method for constructing Differential Emission Measures (DEMs) using data from solar imagers such as EIS and AIA, and apply it to a coronal loop observed on April 19, 2011. The performance of our DEM inversion is compared to other methods, and the ability of such inversions in general to faithfully reproduce a set of test temperature distributions is analyzed. We also compare the observed loop temperature distributions to an analytic strand heating model developed by Martens (2010).

Hot plasma detected in active regions by Hinode/XRT and SDO/AIA

Abstract Author(s): Reale, F., Testa, P., Guarrasi, M., De Luca, E. E., Peres, G., Golub, L.
Institution(s): University of Palermo
Email: reale@astropa.unipa.it
Session: Energy transport and dissipation through the solar atmosphere and into the heliosphere
Presentation: P-55

Abstract:
Multiple ratios of Hinode/XRT filters showed evidence of a minor very hot emission measure component in active regions. Recently also SDO/AIA detected hot plasma in the core of an active region. Here we provide estimations that the amount of emission measure of the hot component detected with SDO is consistent with that detected with Hinode/XRT.

Simultaneous observation of high temperature plasma of solar corona by TESIS/CORONAS-PHOTON and XRT/Hinode.

Abstract Author(s): Reva A. A, Kuzin S. V., Bogachev S. A., Shestov S. V.
Institution(s): Lebedev Physical Institute of the Russian Academy of Sciences
Email: reva_anton@mail.ru
Session: Energy transport and dissipation through the solar atmosphere and into the heliosphere
Presentation: P-56 (**Digital Poster Display**)

Abstract:

TESIS is a space-borne complex of instrumentation created for investigation of the solar corona. TESIS was launched aboard CORONAS-PHOTON satellite, which was operating in near-Earth orbit from March 2009 to November 2009. Two TESIS channels—monochromatic MgXII 8.42 Å and narrow-band FeXX 132 Å – were detecting high temperature plasma with T > 5 MK, which is close to temperature bands of some Hinode channels. At the same time, TESIS Mg XII channel is monochromatic and does not register emission of plasma with temperature less than 5 MK. That is why Mg XII channel is an excellent marker for the region where hot plasma really exists. Different temperature response of TESIS and XRT telescopes allows to perform more precise plasma temperature diagnostics. In 2009 CORONAS-PHOTON and Hinode both operated on near-Earth orbit. In present work we analyze an active region, which was observed simultaneously by XRT and TESIS. This active region was observed from May 29 till June 10, 2009. We build temperature maps of the active region with XRT data, and compare them with Mg XII data about high temperature plasma. Surprisingly, we found no hot plasma (T>5 MK) on XRT temperature maps, but there was strong signal in Mg XII channel. That means that additional combined XRT-TESIS analysis is required for more accurate high temperature diagnostics.

Elemental abundances, as a new source of uncertainty of the Hinode/XRT filter-ratio temperatures and emission measures of coronal structures.

Abstract Author(s): Takeda, A., Kobelski, A., McKenzie, D., Yoshimura, K.
Institution(s): Montana State University
Email: takeda@mithra.physics.montana.edu
Session: Energy transport and dissipation through the solar atmosphere and into the heliosphere
Presentation: P-57

Abstract:

In the current standard Hinode/XRT analysis software, the filter-ratio temperatures and emission measures are calculated from the XRT temperature response that assumes the 'coronal' abundances proposed by Feldman et al. (1992). These elemental abundances are characterized by an enhancement of the elements with low first ionization potential (FIP) by a factor of ~4 relative to their photospheric values. However, their study was based on the XUV spectrum formed less than 1 MK and thus our knowledge of coronal abundances over 1 MK is still insufficient. In view of these uncertainties, we calculated the XRT temperature response assuming two alternative sets of abundances, i.e., photospheric abundances (Grevesse and Sauval, 1998) and the 'hybrid' abundances (Fludra and Schmelz, 1999) with use of CHIANTI atomic database version 6.01. We found two fundamental effects: Firstly, that the new response functions with photospheric and hybrid abundances have lower peak counts (~30% and ~60%, respectively) according to the reduced abundances of the low FIP elements, compared with the original response with the 'coronal' abundances. Secondly, the filter ratios with the photospheric and hybrid abundances tend to yield lower temperatures (~30% and ~15%, respectively in significant cases) than the coronal abundances. The emission measures derived for a given filter ratio are generally higher with the photospheric (~300%) and hybrid (~170%) abundances than with the coronal abundances, reflecting the reduced amplitude of the response functions with the former two abundances. We evaluated the significance of these differences, by comparing them with the uncertainty of the temperatures and emission measures derived from the observational data of active region (AR10923). The results obtained from the careful estimate of the uncertainty due to photon noise (statistical error) and the photometric (systematic) errors are presented.

Transverse kink oscillations in threads observed with Hinode

Abstract Author(s): Terradas, J.
Institution(s): Universitat de les Illes Balears, E-07122 Palma de Mallorca, Spain
Email: jaume.terradas@uib.es
Session: Energy transport and dissipation through the solar atmosphere and into the heliosphere
Presentation: P-58

Abstract:

Hinode observations show ubiquitous transverse oscillations in flowing threads. The combination of waves and flow leads to a rich variety of effects that can help to have a better understanding of the nature of threads. In this work we use the magnetohydrodynamic (MHD) equations to analyze the effects of flow on transverse kink waves in the linear and nonlinear regime. We discuss how the periods and damping rates of kink waves are modified by the presence of flows. We also show that for large amplitude MHD kink oscillations nonlinearities might induce instabilities of Kelvin-Helmholtz type at the thread boundaries. We discuss the implications of the results respect to Hinode observations of transverse kink oscillations.

Temperature Diagnostics of a solar active region using a Single-filter observation of Hinode/XRT

Abstract Author(s): Terzo S., Reale, F.
Institution(s): INAF - Astronomical Observatory of Palermo
Email: terzo@astropa.inaf.it
Session: Energy transport and dissipation through the solar atmosphere and into the heliosphere
Presentation: P-59

Abstract:
Spectroscopic observations are best suited to obtain temperature information in the solar corona. Broadband X-ray observations can provide limited temperature diagnostics through filter ratios. A high cadence observation of an active region made with a single Hinode/XRT filter allows us to use an alternative approach: we measure the time fluctuations of the pixel count rate and use the variance as a temperature proxy. We show preliminary results and discuss limitations.

A new model of TSI based on solar surface magnetic energy

Abstract Author(s): Tian, Z.
Institution(s): Beijing Normal University
Email: tianzhijia@gmail.com
Session: Energy transport and dissipation through the solar atmosphere and into the heliosphere
Presentation: P-60 (**Digital Poster Display**)

Abstract:
Several models of TSI have been made based on some solar parameters, such as sunspot area, sunspot number, and magnetic fields. Here we present a new method of reconstructing TSI based on solar surface magnetic energy. In the view of energy, we will analyse TSI.

Explaining observed red and blue-shifts using multi-stranded coronal loops

Abstract Author(s): Walsh, R. W., Regnier, S., Pearson, J.
Institution(s): University of Central Lancashire
Email: rwwalsh@uclan.ac.uk
Session: Energy transport and dissipation through the solar atmosphere and into the heliosphere
Presentation: P-61 (**Digital Poster Display**)

Abstract:
Magnetic plasma loops have been termed the building blocks of the solar atmosphere. However, it must be recognized that if the range of loop structures we can observe do consist of many "sub-resolution" elements, then current one-dimensional hydrodynamic models are really only applicable to an individual plasma element or strand. Thus a loop should be viewed as an amalgamation of these strands. They could operate in thermal isolation from one another with a wide range of temperatures occurring across the structural elements. This scenario could occur when the energy release mechanism consists of localized, discrete bursts of energy that are due to small-scale reconnection sites within the coronal magnetic field – the nanoflare coronal heating mechanism. These energy bursts occur in a time-dependent manner, distributed along the loop/strand length, giving a heating function that depends on space and time. An important observational discovery with the Hinode/EIS spectrometer is the existence of red and blue-shifts in coronal loops depending on the location of the footpoints (inner or outer parts of the active region), and the temperature of the emission line in which the Doppler shifts are measured. Based on the multi-stranded model developed by Sarkar and Walsh (2008, ApJ, 683, 516), we show that red and blue-shifts exist in different simulated Hinode/EIS passbands: cooler lines (Si VII) being dominated by red-shifts, whilst hotter lines (FeXV) are a combination of both. Characteristic Doppler shifts generated fit well with observed values.

Plasma flows in active region fan loops

Abstract Author(s): Young, P. R. (1), O'Dwyer, B. (2), Mason, H. E. (2)
Institution(s): (1) George Mason University, (2) University of Cambridge, UK
Email: pyoung9@gmu.edu
Session: Energy transport and dissipation through the solar atmosphere and into the heliosphere
Presentation: P-62

Abstract:
EIS is the first coronal spectrometer to allow plasma flows in coronal loops to be tracked from the transition region into the corona. Results for an isolated fan loop structure will be presented showing that redshifts (downflows) of 15-20 km/s are found for temperatures up to 0.8 MK, but an abrupt change to a rest velocity is found for temperatures of 1.0 MK and above. As the 0.8 MK and 1.0 MK plasmas spatially co-exist in the same locations in the loop, the results are interpreted in terms of two sets of loop strands, one of which is cool and downflowing, the other is hotter and at rest. The implications for models of fan loops are discussed.

Signature of Alfvén waves energy deposition above polar coronal holes with Hinode/EIS

Abstract Author(s): Bemporad, A., Abbo, L.
Institution(s): INAF-Osservatorio Astronomico di Torino, Pino Torinese (TO), 10025 – Italy
Email: abbo@oato.inaf.it
Session: Energy transport and dissipation through the solar atmosphere and into the heliosphere
Presentation: P-63

Abstract:
Between February 24-25, 2009, the EIS/Hinode spectrometer performed special 'sit & stare' observations above the South polar coronal hole continuously over more than 22 hours. Spectra were acquired with the 1" slit placed off-limb, covering altitudes up to 0.48 solar radii (1.74e2 Mm), in order to study the non-thermal spectral line broadenings. We have analyzed spectral lines such as FeXII 186.88, FeXII 195.12, FeXIII 202.04, HeII 256.32, and CaXVII 192.81, observed with good statistics up to higher altitudes. Results show that the FWHM of Fe XII 195.12 line increases up to about 0.16 solar radii, then decreases higher up. EIS stray light has been estimated and removed and from the observed line intensities and line profile widths we have derived electron density and non-thermal velocity profiles. The analysis suggests significant energy deposition by Alfvén waves in a polar coronal hole above 0.16 solar radii, by assuming conservation of the wave energy flux along magnetic flux tubes. We also present first preliminary results from a further EIS off-limb study recently performed in coordination with SOHO/UVCS, including more EIS spectral lines.

X-ray and EUV filter responses and AR emission model for the non-thermal kappa-distributions

Abstract Author(s): Dzifcakova, E. (1), Dudik, J. (2, 1), Karlicky, M. (1)
Institution(s): (1) Astronomical Institute of the Academy of Sciences of the Czech Republic, Fricova 298, 251 65 Ondrejov, Czech Republic, (2) DAPEM, Faculty of Mathematics, Physics and Informatics, Comenius University, Mlynska Dolina F2, 842 48 Bratislava, Slovak Republic
Email: elena@asu.cas.cz
Session: Energy transport and dissipation through the solar atmosphere and into the heliosphere
Presentation: P-64 (**Digital Poster Display**)

Abstract:
The XRT and AIA filter responses to emission for the non-thermal electron with enhanced number of the particles in the high-energy tail (kappa-distributions) were calculated. Generally, the filter responses for the kappa-distributions are wider and shifted to higher temperatures. This behavior can affect temperature diagnostic. The effect of the non-thermal kappa-distributions on the resulting forward models of active region emission was analyzed. We have shown that their influence is small except for the extreme non-thermal cases.

Temperature diagnostic of an Active Region brightening observed by XRT

Abstract Author(s): Dudik, J. (1, 2), Reeves, K. (3), Schmieder, B. (4), Dzifcakova, E. (2), Golub, L. (3)
Institution(s): (1) DAPEM, Faculty of Mathematics, Physics and Informatics, Comenius University, Mlynska Dolina F2, 842 48 Bratislava, Slovak Republic, (2) Astronomical Institute of the Academy of Sciences of the Czech Republic, Fricova 298, 251 65 Ondrejov, Czech Republic, (3) Harvard-Smithsonian Center for Astrophysics, 60 Garden St. MS 58, Cambridge, MA 02138, USA, (4) LESIA, Observatoire de Paris, 5 Place Jules Janssen, 921 90 Meudon, France
Email: elena@asu.cas.cz
Session: Energy transport and dissipation through the solar atmosphere and into the heliosphere
Presentation: P-65 (**Digital Poster Display**)

Abstract:
We analyze the temperature distribution of the active region observed by HINODE/XRT. The active region shows several loop brightenings in the active region core. The temperature structure is derived using three different methods: a single filter-ratio, Combined Improved Filter Ratio (CIFR) and a hardness-to-softness ratio utilizing five filters. Although the temperature distributions are similar, there can be rather large errors in individual pixels. The last method offers best option for minimalizing the S/N ratio and constrains the higher temperatures in brightening to less than 5 MK. The diagnosed temperatures are compared to the results of DEM analysis, which also shows relative absence of plasma with higher T.

Thermal Evolution of a Coronal Bright Point

Abstract Author(s): Farid, S. (1), Mulu-Moore, F. (2), Winebarger, A. (2), Cirtian, J. (2), Saar, S. (1)
Institution(s): (1) Harvard-Smithsonian Center for Astrophysics, Cambridge, MA (2) NASA-Marshall Space Flight Center Hunstville, AL
Email: sfarid@cfa.harvard.edu
Session: Energy transport and dissipation through the solar atmosphere and into the heliosphere
Presentation: P-66

Abstract:
Coronal bright points (BPs) appear as small, compact, and relatively cool groups of short loops visible in X-ray and EUV images. They are usually accompanied by magnetic bipoles and are often associated with jets, particularly when in coronal holes. BPs have been observed since Skylab, however many questions about their origin, evolution, and variation remain. We have recently demonstrated that joint observations from HINODE/XRT and SDO/AIA can constrain the differential emission measure (DEM) of BPs. Now we examine the thermal and morphological evolution of a long-lived bright point located near the boundary of an on-disk coronal hole. We compute the DEM over the lifetime of the BP and examine changes in the associated magnetic bipole. We explore its thermal evolution from emergence, core brightening, the discharge of a small jet, decay and re-emergence.

High-frequency Acoustic Waves in the Solar Atmosphere: Comparing Hinode/SP Observations with Numerical Simulations

Abstract Author(s): Fleck, B. (1), Straus, T. (2), Severino, G. (2)
Institution(s): (1) ESA, (2) INAF/OAC
Email: bfleck@esa.nascom.nasa.gov
Session: Energy transport and dissipation through the solar atmosphere and into the heliosphere
Presentation: P-67

Abstract:
Even 60 years after the pioneering papers by Schwarzschild and Biermann, the role of high-frequency acoustic waves for the energy balance of the solar atmosphere is still intensely debated. Here we investigate the signatures of high-frequency acoustic waves in Hinode/SP observations and compare them to those found in line spectra synthesized from high-resolution 3D radiation-hydrodynamics simulations. The Hinode/SP time series extends over 4 hours, with a cadence of 16 s and a spatial resolution of 0.16 arcsec/pixel. The numerical simulation of the Sun's surface layers was computed with the radiation hydrodynamics code CO5BOLD. The simulated domain is defined by a fixed 3D Cartesian grid with 400 x 400 x 300 cells, each of size 14 km x 14 km x 7.5 km. The simulation thus covers a horizontal area of 5.6 x 5.6 Mm. Periodic lateral boundaries are used. The transmitting upper boundary is located at a height of approximately 900 km above the visible solar surface, while the open lower boundary lies 1.4 Mm below the surface. The part of the simulation that we used has completely relaxed and covers approximately two hours of solar time with snapshots saved every 10 s. A line-synthesis code, based on the assumption of local thermodynamic equilibrium (LTE), was then fed with the physical parameters of the simulation to produce synthetic, two-dimensional spectra of the photospheric lines of Fe 6301/6302 (Hinode/SP), Fe 6173 (SDO/ HMI), and Ni 6768 (SOHO/MDI). The resulting Doppler velocity time series are analyzed using Fourier techniques and compared to the observed Hinode/SP spectra.

The mass balance between the chromsphere and corona

Abstract Author(s): Hansteen, V, Guerreiro, N., Gudiksen, B.
Institution(s): Institute of Theoretical Astrophysics, University of Oslo
Email: viggoh@astro.uio.no
Session: Energy transport and dissipation through the solar atmosphere and into the heliosphere
Presentation: P-68

Abstract:
In general and on average, observations of transition region emission lines reveal the presence of redshifts in lines formed from the top of the chromosphere up to temperatures of about 250000 K and blueshifts for temperatures greater than that. However, it is doubtful that the apparent large downward flows in the lower transition region represent a net flow emptying of the corona, so some mechanism must be responsible for maintaining the mass balance between the lower atmospheric layers and the corona. We use a 3D-MHD code, Bifrost, which includes non-grey, non-LTE radiative transfer in the photosphere and lower chromosphere, optically and effectively thin radiation in the upper chromosphere, transition region and corona, conduction along the magnetic field lines and heating through the ohmic dissipation of tangled magnetic field lines to simulate the solar atmosphere. The motion of material originally in the transition region is tracked both as a minority fluid and in the form of corks. We report on the coronal mass balance and the mass flow mechanism for conditions perhaps typical of the quiet sun.

Simulated vs observed emission measures of the solar corona

Abstract Author(s): Hansteen, V. (1), Testa, P. (2), De Pontieu, B. (3), Martinez, J. (1,3), Carlsson, M. (1), Gudiksen, B. (1)
Institution(s): (1) Institute of theoretical astrophysics, University of Oslo, (2) Harvard Smithsonian Center for Astrophysics, Cambridge MA (3) Lockheed Martin Solar and Astrophysics Laboratory, Palo Alto CA
Email: viggoh@astro.uio.no
Session: Energy transport and dissipation through the solar atmosphere and into the heliosphere
Presentation: P-69

Abstract:

The Extreme ultraviolet Imaging Spectrograph (EIS) onboard Hinode and the Atmospheric Imaging Assembly (AIA) onboard the Solar Dynamics Observatory (SDO) provide a wealth of information on the physical conditions in the solar corona. These observational constraints are used to help determine the heating mechanisms driving the dynamics and energetics of coronal loops. In this poster we carry out detailed comparisons between differential emission measures, densities and temperatures of observed coronal plasma with those produced by numerical models of coronal loops. The simulations are made using a 3d-MHD code, Bifrost, and span a numerical domain from the convection zone into the corona, include radiative losses from optically thick and thin lines in the chromosphere and corona, as well as thermal conduction. These simulations self-consistently produce a hot corona through the ohmic dissipation of tangled magnetic field lines. We will explore the limitations of the diagnostics and their implications, as a function of the plasma parameters.

Propagation of Slow-Modes through the Transition Region in Network Magnetic Elements

Abstract Author(s): Kato, Y. (1), Carlsson, M. (2), Hansteen, V. (2), Steiner, O. (3)
Institution(s): (1) NAOJ, Tokyo, Japan, (2) ITA, University of Oslo, Oslo, Norway, (3) KIS, Freiburg, Germany
Email: kato.yoshiaki@nao.ac.jp
Session: Energy transport and dissipation through the solar atmosphere and into the heliosphere
Presentation: P-70 (**Digital Poster Display**)

Abstract:
We investigate the propagation of longitudinal slow modes, which are excited within magnetic flux concentrations by convective downdrafts in the immediate surroundings of the magnetic element, using radiation magnetohydrodynamic (RMHD) simulations of the solar atmosphere comprising the layers from the upper convection zone to the lower corona. We name this the "magnetic pumping process". We find that the generated slow modes travel along the magnetic flux concentration in the upward direction, develop into a shock wave in chromospheric heights, and propagate further through the transition region. In the course of propagation through the transition region, a small fraction of the longitudinal slow mode is converted into a transverse wave mode. We report on how much energy is deposited by propagating shock waves through the transition region and we discuss on the dissipation process above the photosphere within the magnetic flux concentration.

Observation of Magnetic Fluctuations with Ion Cyclotron Frequency Range during Reconnection in Plasma Merging Experiment

Abstract Author(s): Kuwahata, A., Boxin, G., Ito, T., Oka, H., Tanabe, H., Ito, S., Inomoto, M., Ono, Y.
Institution(s): The University of Tokyo
Email: kuwahata@ts.t.u-tokyo.ac.jp
Session: Energy transport and dissipation through the solar atmosphere and into the heliosphere
Presentation: P-71

Abstract:

Magnetic reconnection has the deep relationship to solar activities, such as solar flares, solar winds and CMEs. Recent laboratory experiments have demonstrated that plasmoid ejection, waves and current sheet instabilities are important for the fast reconnection and resulting plasma heating and/or particle acceleration. In this paper, low frequency magnetic fluctuations generated by driven magnetic reconnection have been investigated in the TS-3 torus plasma merging device. Large amplitude magnetic fluctuations with ion cyclotron frequency range were observed inside the current sheet during magnetic reconnection in plasma merging experiment with a guide field: the guide field at the X-point Bx of 65mT is comparable to the reconnecting magnetic field B// in this experiment. The frequency spectrum of the magnetic fluctuation has clear peak at 2MHz, which is about twice as high as the local ion cyclotron frequency at the X point. The magnetic field variation due to the fluctuation is larger than 20% of the reconnecting magnetic field. In the initial phase of reconnection, the fluctuation brought a magnetic field modification like an island structure. Then the fluctuation was observed to travel radially to the downstream when the current sheet half width was compressed to ion gyroradius or inertia length. The magnetic fluctuation was observed to propagate radially across the reconnected magnetic field with velocity of about 70km/s, which is comparable to the local Alfvén velocity, and strongly damped at the downstream region. Large electric field fluctuations and the enhancement of reconnection rate were also observed. These results suggest that the fast magnetic reconnection is provided by non-steady current sheet modification.

Heating of Flare Loops During a Two-ribbon Flare on 2005 May 13

Abstract Author(s): Liu, W. J., Qiu, J., Longcope, D. W.
Institution(s): Montana State University, Bozeman
Email: wliu@physics.montana.edu
Session: Energy transport and dissipation through the solar atmosphere and into the heliosphere
Presentation: P-72 (**Digital Poster Display**)

Abstract:

Many eruptive flares exhibit two extended ribbons in the lower-atmosphere outlining the feet of the post-flare coronal arcade. High-cadence and high-resolution UV observations by TRACE reveal that the flare ribbon consists of small patches sequentially brightened along the ribbon, suggesting that reconnection takes place sequentially forming individual post-flare loops along the arcade, as often seen in coronal observations in the EUV wavelengths. These reconnection events and formation of new loops continue well into the decay phase. Our recent study (Qiu et al. 2010) further shows that the spatially resolved UV brightness at the foot-points of individual loops grows rapidly on timescales of a few minutes, followed by a long decay on timescales of more than 10 minutes. The rapid rise of UV radiation is correlated with the hard X-ray light curve during the impulsive phase, hence is most likely a direct response of instantaneous heating in the reconnection formed flux tubes. In this study, we utilize the spatially resolved UV brightness time profiles to reconstruct instantaneous heating functions of individual flux tubes, and compute evolution of each flux tube using the EBTEL model (Klimchuk et al. 2008). The temperature and density of these flux tubes are then used to calculate light curves in other energy bands and compare favorably with observations by RHESSI and GOES. This study presents the first effort to constrain heating functions of flare loops directly using all available observables, and provides a powerful way to examine physics of heating discrete flux tubes formed by reconnection events throughout the flare.

Coronal Heating and Magnetic Properties of Solar Active Regions: Confronting the Relationship with High Resolution Observations from Hinode SOT and XRT

Abstract Author(s): Nandy, D. (1), Hazra, S. (1), Ravindra, B. (2)
Institution(s): (1) Indian Institute of Science Education and Research, Kolkata, India, (2) Indian Institute of Astrophysics, Bangalore, India
Email: dnandi@iiserkol.ac.in
Session: Energy transport and dissipation through the solar atmosphere and into the heliosphere
Presentation: P-73

Abstract:

The brightest regions of the Sun's corona are associated with active regions indicating that the magnetic properties of active regions play a crucial role in coronal heating. Exploring the relationship between coronal X-ray flux and active region properties can therefore illuminate the mechanisms responsible for the heating of stellar coronae. While it is thought that active region non-potentiality and currents should influence coronal heating, studies from the Yohkoh era have not found any evidence in support of this. We revisit this relationship between active region magnetic properties and coronal heating by comparing co-spatiotemporal coronal X-ray and photospheric vector magnetic field observations from the XRT and SOT instruments, respectively, onboard the Hinode satellite. Here, we present a summary of our main findings.

Thermal properties and evolution of a coronal cavity as observed by the X-Ray Telescope on Hinode

Abstract Author(s): Reeves, K. K. (1), Gibson, S. E. (2), Kucera, T. A. (3), Hudson, H. S. (4), Kano, R. (5)
Institution(s): (1) Harvard-Smithsonian Center for Astrophysics (2) HAO/NCAR (3) NASA GSFC (4) SSL, U. C. Berkeley, (5) National Astronomical Observatory of Japan
Email: kreeves@cfa.harvard.edu
Session: Energy transport and dissipation through the solar atmosphere and into the heliosphere
Presentation: P-74

Abstract:
Coronal cavities are voids in coronal emission often observed above high latitude filament channels. Sometimes, these cavities have areas of bright X-ray emission in their centers (i.e. Hudson et al. 1999). In this study, we use data from the X-ray Telescope (XRT) on Hinode to examine the thermal emission properties of a cavity observed during July 2008 that contains bright X-ray emission in its center. Using ratios of XRT filters, we find evidence for elevated temperatures in the cavity center. The area of elevated temperature evolves from a ring-shaped structure at the beginning of the observation, to an elongated structure two days later, finally appearing as a compact round source four days after the initial observation. We use a morphological model to fit the cavity emission, and find that a uniform structure running through the cavity does not fit the observations well. Instead, the observations are reproduced by modeling several short cavity "cores" with different parameters on different days. These changing core parameters may be due to some observed activity heating different parts of the cavity core at different times. We also find that core temperatures of 1.75 MK, 1.7 MK and 2.25 MK (for 19 July, 21 July and 23 July, respectively) in the model lead to structures that are consistent with the data, and that line-of-sight effects serve to lower the effective temperature derived from the filter ratio.

Study of Small-Scale Chromospheric Plasmoid Ejections with Improved Hinode Ca II H Filtergrams

Abstract Author(s): Suematsu, Y.
Institution(s): National Astronomical Observatory of Japan
Email: suematsu@solar.mtk.nao.ac.jp
Session: Energy transport and dissipation through the solar atmosphere and into the heliosphere
Presentation: P-75 (**Digital Poster Display**)

Abstract:

We present observations of intermittent ejections of small-scale blob-like chromospheric structures which may indicate magnetic reconnection process between cool chromosphere and hot coronal magnetized layers. The observations were taken with Hinode SOT/BFI Ca II H filtergrams at an active region when a large sunspot region was just on the west limb. The activity of the blob ejections was seen near an apex of low-lying chromospheric loop systems which are likely to connect the sunspot and its outer opposite polarity regions. The blob ejections were dominantly directed to the sunspot like the motion of inverse Evershed flows but also directed away from the sunspot, sometimes showing bi-directional flows. The size of blobs ranges from 0.2 to 1 arcsec and their apparent velocities exceed 50 km/sec. To derive detailed structures and motion of the blob ejections, we improved the filtergrams by applying a kind of phase diversity image restoration method. We discuss the observational results with a context of magnetic reconnection models.

Laboratory Experiment on Plasma Heating During Magnetic Reconnection in Torus Plasma Merging Device TS-3 and TS-4

Abstract Author(s): Tanabe, H. (1), Kuwahata, A. (1), Oka, H. (1), Annoura, M. (1), You, S. (2), Inomoto, M. (1), Ono, Y. (1)
Institution(s): (1) University of Tokyo, (2) University Washington
Email: tanabe@ts.t.u-tokyo.ac.jp
Session: Energy transport and dissipation through the solar atmosphere and into the heliosphere
Presentation: P-76

Abstract:

We have investigated the energy dissipation mechanism of magnetic reconnection, a key physics of violent plasma acceleration and heating in solar flare, by use of torus plasma merging experiment on TS-3 and TS-4. Making use of the accessibility to the diffusion region in this laboratory experiment, we studied the heating mechanism of the magnetic self-organization process by probe measurements and ion Doppler optical diagnostics. The line-integrated effect for the passive ion Doppler measurement is removed by tomographic reconstruction technique [1]; we can discuss local heating mechanism for ion and electron both. The measured results clearly show that ions are heated at the down stream area of outflow jet and the electron temperature profile has a peak at the current sheet region, indicating that the ions are mainly heated by the damping energy of outflow jet by viscosity and shock, while the electrons are heated by resistive current sheet dissipation. The ion heating efficiency depend on the varied guide toroidal field Bt. The maximum ion temperature T_i~140eV is obtained in the counter helicity merging spheromaks with no guide field B_t, T_i~100eV in the co-helicity merging spheromaks with B_t~B_p (reconnection field) and T_i~50eV in the tokamak merging with B_t>B_p. The tokamak merging experiment with varied guide field Bt revealed that the ion temperature increment ΔT_i after reconnection decreases inversely with the guide field B_t but that ΔT_i tends to be saturated in high guide field regime.

[1] H. Tanabe., et al., Rev. Sci. Instrum., submitted (2011)

The role of the magnetic field in the formation of chromospheric spicules

Abstract Author(s): Tarbell, T. (1), de la Cruz Rodriguez, J. (2), De Pontieu, B. (1), Rouppe van der Voort, L. (2), Sekse, D. (2), Pereira, T. (4), Martinez-Sykora, J. (1, 2), Hansteen, V. (2), McIntosh, S. (3), Carlsson, M. (2), Sainz-Dalda, A. (5)
Institution(s): (1) LMSAL, (2) UiO, (3) HAO, (4) NASA Ames, (5) Stanford
Email: tarbell@lmsal.com
Session: Energy transport and dissipation through the solar atmosphere and into the heliosphere
Presentation: P-77 (**Digital Poster Display**)

Abstract:

Fast moving, so-called "type II spicules" have recently been implicated in providing the corona with hot plasma. However, we do not understand how they form, and what role the magnetic field plays in driving these supersonic jets into the corona. The recent discovery of so-called rapid blue shifted events (RBEs), the disk counterpart of type II spicules, allows us to study in detail the magnetic field configuration at the root of these jets. We use a one hour long timeseries of H-alpha 6563Å and Ca II 8542Å images obtained with the CRISP instrument at the Swedish Solar Telescope (SST) in La Palma, Spain to identify the rapid chromospheric upflows. To determine whether the photospheric field configuration at the roots of spicules can provide insight into the formation mechanism of spicules, we analyze the vector magnetic field at the spicule roots using data from the Helioseismic and Magnetic Imager (HMI) onboard the Solar Dynamics Observatory (SDO), as well as fast raster scans from the SpectroPolarimeter (SP) onboard Hinode. We also use spectropolarimetric observations in Ca II 8542Å to investigate how the chromospheric magnetic field is related to the formation of spicules, and more generally heating in the upper chromosphere. We compare our observations with synthetic observations from 3D radiative MHD simulations using the Bifrost code.

High-speed Outflows on Plume-like Structures of the Quiet Sun and Coronal Holes

Abstract Author(s): Tian, H., McIntosh, S. W., Habbal, S. R., He, J.
Institution(s): High Altitude Observatory, National Center for Atmospheric Research
Email: htian@ucar.edu
Session: Energy transport and dissipation through the solar atmosphere and into the heliosphere
Presentation: P-78 (**Digital Poster Display**)

Abstract:

Observations from the Atmospheric Imaging Assembly (AIA) onboard the Solar Dynamics Observatory (SDO) reveal ubiquitous episodic outflows (jets) with an average speed around 120 km s^{-1} at temperatures often exceeding a million degree in plume-like structures, rooted in magnetized regions of the quiet solar atmosphere. These outflows are not restricted to the well-known plumes visible in polar coronal holes, but are also present in plume-like structures originating from equatorial coronal holes and quiet-Sun regions. Outflows are also visible in the "inter-plume" regions throughout the atmosphere. Furthermore, the structures traced out by these flows in both plume and inter-plume regions continually exhibit transverse (Alfvénic) motion. Our finding suggests that high- speed outflows originate mainly from the magnetic network of the quiet Sun and coronal holes, and that the plume flows observed are highlighted by the denser plasma contained therein. These outflows might be an efficient means to provide heated mass into the corona and serve as an important source of mass supply to the solar wind. We demonstrate that the quiet-Sun plume flows can sometimes significantly contaminate the spectroscopic observations of the adjacent coronal holes - greatly affecting the Doppler shifts observed, thus potentially impacting significant investigations of such regions.

Evidence of magnetic heating of chromosphere

Abstract Author(s): Tsuneta, S. (1), Ueda, K. (1), Reardon, K. (1), Cauzzi, G. (2), Ishikawa, R. (1)
Institution(s): (1) NAOJ, (2) Arcetri
Email: saku.tsuneta@nao.ac.jp
Session: Energy transport and dissipation through the solar atmosphere and into the heliosphere
Presentation: P-79 (**Digital Poster Display**)

Abstract:

Cauzzi et al. (2009) demonstrated with IBIS that the width of the H-alpha line may be a very good measure of chromospheric temperature. Following this paper, we performed high-cadence, high-resolution limb (and disk-center) observations at two wavelengths (blue and red) of the H-alpha line with Hinode. The limb observations allow us to better see the vertical structure of the chromospheres, but are difficult to obtain with ground-based telescopes due to the limitations of adaptive optics.

The temperature maps thus obtained appear quite different from usual high-resolution H-alpha maps (Cauzzi et al.). We present remarkable movies of the near-limb (and disk center) chromospheric temperature structures. While the inter-network regions are filled with acoustic-shock signatures with approximately 3 min period, the network regions have a different appearance than that shown by Cauzzi et al.

Instead, we see heated, canopy-like inclined fine-threads around the network magnetic concentrations. This suggests the existence of a heating mechanism such as magnetic reconnection in the ubiquitous emerging magnetic fields in and around the chromospheric network regions. It is quite interesting to evaluate this phenomena in terms of the viewpoint recently proposed by De Pontieu et al. (2009, 2011).

Slow-mode oscillations of hot coronal loops excited at flaring footpoints

Abstract Author(s): Wang, T. (1, 2), Liu, W. (3), Ofman, L. (1, 2), Davila, J. M. (2)
Institution(s): (1) Catholic University of America, Washington, DC, USA, (2) NASA's Goddard Space Flight Center, Greenbelt, MD, USA, (3) Lockheed Martin Solar and Astrophysics Laboratory, CA, USA.
Email: tongjiang.wang@nasa.gov
Session: Energy transport and dissipation through the solar atmosphere and into the heliosphere
Presentation: P-80 (**Digital Poster Display**)

Abstract:
A large number of strongly damped oscillations in hot coronal loops have been observed by SOHO/SUMER in the past decade in Doppler shifts of flaring (>6 MK) lines (Fe XIX and Fe XXI). These oscillations with periods on the order of 10-30 minutes were interpreted as fundamental standing slow modes. They often manifest features such as recurrence and association with a flow (100-300 km/s) pulse preceding to the oscillation, which suggests that they are likely driven by microflares at the footpoints. With coordinated RHESSI observations, we have found a dozen such events supporting this conjecture. A typical event is presented here. By analyzing RHESSI hard X-ray and GOES/SXI soft X-ray emissions as well as SUMER Doppler shifts, we identify the flare that triggers the loop oscillations.

From RHESSI spectra, we measure physical parameters such as temperature, emission measure, and thermal/non-thermal energy contents as functions of time. We discuss the wave excitation mechanism based on these observations. Our results provide important observational constraints that can be used for improving theoretical models of magnetosonic wave excitation, and for coronal seismology.

Modeling Slow Speed Solar Wind Streams

Abstract Author(s): Warren, H., Mariska, J.
Institution(s): NRL
Email: harry.warren@nrl.navy.mil
Session: Energy transport and dissipation through the solar atmosphere and into the heliosphere
Presentation: P-81 (**Digital Poster Display**)

Abstract:

One of the most significant discoveries with the EIS instrument on Hinode is the detection of persistent, high-speed outflows from large areas at the periphery of many active regions. Recent work has determined the properties of these outflows and provided strong evidence that they connect to the heliosphere and contribute to the slow speed solar wind. One curious property of the active region outflows is that they are easily measured in emission lines from Fe XII and Fe XIII, indicating temperatures well above 1 MK. The outflowing plasma in polar coronal holes, in contrast, is characterized by much lower temperatures. Previous work on the hydrodynamics of open flux tubes has emphasized the importance of the energy deposition at low heights for determining the asymptotic properties of the solar wind. Strong heating near the base leads to slower wind speeds and higher temperatures and densities. Here we discuss the application of 1D hydrodynamic models to EIS observations of the active region outflows and the implication of these results to the properties of the slow speed solar wind.

Time series of synthetic spectra from prominence oscillations

Abstract Author(s): Heinzel, P., Ballester, J. L., Zapior, M., Oliver, R.
Institution(s): Astronomical Institute, Academy of Sciences
Email: pheinzel@asu.cas.cz
Session: Instabilities, Transients and Eruptions
Presentation: P-82

Abstract:
MHD models of prominence oscillations have been constructed in the past for various modes of oscillations. However, in order to constrain these models against existing observations, one needs time series of synthetic spectra of the oscillating prominence. Here we perform, for the first time, a full non-LTE radiative-transfer synthesis of time-dependent hydrogen and calcium spectra emergent from model prominences with oscillations. For this exploratory work we use a rather simple 1D slab model with various modes of oscillations, illuminated by the incident solar radiation. We solve coupled equations of radiative transfer and statistical equilibrium, in the presence of internal velocity fields, and obtain theoretical temporal variations of the line intensities, widths and Doppler shifts or line asymmetries. These can be directly compared with observations having high spectral resolution. Finally we discuss limitations of our approach and future prospects.

Interactions and Eruptions of Two Filaments Observed by Hinode, SOHO, and STEREO

Abstract Author(s): Li, Y., Ding, M. D.
Institution(s): Montana State University
Email: yingli@nju.edu.cn
Session: Instabilities, Transients and Eruptions
Presentation: P-83

Abstract:
We investigate the interactions between two filaments and the following eruptions from different angles of view, observed by Hinode, the Solar and Heliospheric Observatory (SOHO), and the Solar Terrestrial Relations Observatory (STEREO). In the event, the two filaments rose high, interacted with each other, and finally produced ejections along two different paths. We measure the bulk-flow velocity using spectroscopic data. There appeared significant outflows with a speed of hundreds of km/s during the ejections, and also some downflows of about tens of km/s at the edge of the eruption region during the last stage. The erupting material contained plasmas with a wide temperature range of 10^4-10^6 K.

Distribution of the Sizes and Fluxes Produced in Patchy Reconnection

Abstract Author(s): McKenzie, D. E. (1), Savage, S. L. (2)
Institution(s): (1) MSU, (2) NASA-GSFC
Email: mckenzie@solar.physics.montana.edu
Session: Instabilities, Transients and Eruptions
Presentation: P-84

Abstract:
Supra-arcade downflows (SADs) are downward-moving features observed in the hot, low-density region above posteruption flare arcades. They are believed to be created by patchy reconnection in the post-CME current sheet, and so their characteristics provide information about the process of their creation. For example, the "fractal current sheet" scenario proposed in the literature may be expected to yield a power-law distribution of sizes and/or fluxes. We examine 120 cross-sectional areas and magnetic flux estimates from low-resolution observations of SADs, and find that (1) the areas are consistent with a log-normal distribution, and (2) the fluxes are consistent with both a log-normal and an exponential distribution. Neither set of measurements is compatible with a power-law distribution, and so the data do not appear to support a fractal process for SAD creation. Because these measurements are derived from low-resolution (pre-Hinode) observations, we anticipate that improved flare images with higher resolution will provide a better probe of the sizes and fluxes that are characteristic of patchy reconnection. We will show that with the recently increasing solar activity, Hinode/XRT and SDO/AIA are optimally positioned for advancing this type of study.

Asymmetric Magnetic Reconnection in Coronal Mass Ejection Current Sheets

Abstract Author(s): Murphy, N. A. (1), Miralles, M. P. (1), Pope, C. L. (1, 2), Raymond, J. C. (1), Reeves, K. K. (1), Seaton, D. B. (3), Webb, D. F. (4)
Institution(s): (1) Harvard-Smithsonian Center for Astrophysics, Cambridge, MA, USA, (2) Elmhurst College, Elmhurst, IL, USA, (3) Royal Observatory of Belgium, Brussels, Belgium, (4) Boston College, Boston, MA, USA
Email: namurphy@cfa.harvard.edu
Session: Instabilities, Transients and Eruptions
Presentation: P-85

Abstract:

Flux rope models of coronal mass ejections (CMEs) predict the formation of an elongated current sheet in the wake behind the rising plasmoid. Features identified as current sheets have been seen during a number of eruptions observed by instruments such as XRT, EIS, LASCO, and AIA. These current sheets frequently drift or tilt with time at rates of up to 20 degrees/day, much faster than could be accounted for by solar rotation. This drift could be caused by different parts of the current sheet actively reconnecting at different times, the rising plasmoid propagating at an angle and pulling the current sheet along with it, or asymmetry from the reconnection process itself. We investigate the effects of line-tied asymmetric reconnection in CME current sheets using resistive magnetohydrodynamic simulations. The X-line drifts away from the Sun and toward the upstream region with the stronger magnetic field. Because the X-line is located near the low-altitude base of the current sheet, most of the energy is directed upward toward the rising plasmoid rather than toward the lower boundary representing the photosphere. The rate of drift predicted from the simulations is comparable to the observed rate of current sheet tilting during the Cartwheel CME. The post-flare loops show a characteristic skewing that is observable by XRT.

X-ray jets and Bright Points: evidence for sympathetic activity

Abstract Author(s): Pucci, S. (1), Poletto, G. (2), Sterling, A.C. (3), Romoli, M. (4)
Institution(s): (1)Department of Physics and Astronomy, University of Firenze, Firenze, Italy, (2) NAF - Arcetri Astrophysical Observatory, Firenze, Italy, (3) Space Science office, VP 62, Marshall Space Flight Center, Huntsville, AL 35812, USA, (4) Department of Physics and Astronomy, University of Firenze, Firenze, Italy
Email: stpucci@arcetri.astro.it
Session: Instabilities, Transients and Eruptions
Presentation: P-86 (**Digital Poster Display**)

Abstract:
We present in this work an analysis of X-ray Bright Points (BPs) and X-ray jets that occurred within the northern polar coronal hole, as observed by the Hinode X-Ray Telescope (XRT) over two time intervals, each of about 20 hours during the period 2-4 Nov 2007. We performed a photometric analysis of the BPs observed within two selected subregions of the coronal hole and examined whether there is any correlation between the BPs intensity fluctuations and the occurrence of jets originating within the same area. Our results show: 1) The most important BP brightness fluctuations occur nearly simultaneously for different BPs, and 2) Jets are observed in close temporal association with these multiple-brightening events. We interpret these jet events in terms of magnetic connectivity changes that concurrently produce the BPs brightness fluctuations, surmising that magnetic interactions that produce both the BPs and jets in polar coronal holes are small-scale versions of active-region-scale phenomena whereby interacting bipoles trigger flares and eruptions.

Hinode and SDO Observations of the Onset of a CME-Producing Eruption

Abstract Author(s): Sterling, A., Moore, R.
Institution(s): NASA Marshall Space Flight Center
Email: alphonse.sterling@nasa.gov
Session: Instabilities, Transients and Eruptions
Presentation: P-87

Abstract:

We observe the onset dynamics and characteristics of a GOES mid-C-level, CME-producing eruption of 2011 June 1, using data from both SDO and Hinode. Hinode experienced satellite night prior to the peak of the event, but it observed well the start of the eruption. The eruption itself was a complex affair, with at least three peaks in the GOES soft X-ray intensity profile. Hinode/XRT and SDO/HMI data show that, near the time of the event's initiation, a strong "pre-flare" soft X-ray brightening occurred at the site of a strong island of positive magnetic flux isolated in a sea of surrounding negative flux. This positive flux island steadily declines by about a factor of two in strength over the eight hours prior to eruption, consistent with that flux island undergoing cancelation with surrounding field. Combined AIA and HMI data show that following the initial preflare episode, a two-stage cascade of eruptions subsequently occurs along the main polarity inversion line of the erupting region, with this cascade contributing to the complexity of the GOES light curve. A filament in one of the eruptions becomes intertwined with brightly-emitting filament strands during the eruption, similar to characteristics we have seen in other events. In AIA 304 images we measure steady pre-eruption flows at locations near the eruption of ~20-60 km/s, while flows along the filament structures during eruption onset reach up to ~200km/s. Our observations suggest that flux cancelation near the isolated positive island triggered release of magnetic energy, leading to successive destabilizations and eruptions of larger-scale magnetic structures.

A new view of the structure, evolution and eruption of a polar crown cavity

Abstract Author(s): Walsh, R. W., Regnier, S., Alexander, C. E.
Institution(s): University of Central Lancashire
Email: rwwalsh@uclan.ac.uk
Session: Instabilities, Transients and Eruptions
Presentation: P-88

Abstract:
We report on the evolution of a negative curvature (U-shaped) polar crown cavity observed on 13th June 2010. Concentrating primarily on SDO/AIA data, we define the polar crown cavity as a density depletion sitting above denser polar crown filament plasma that is draining down the cavity by gravity. As part of the filament, plasma at different temperatures (ranging from 50,000 K to 0.6 MK) is observed co-located within the cavity dips, sustained by a competition between gravity and magnetic tension of the curved magnetic field. The evolution follows very closely the classical three-part ejection model of filament, cavity and outer shock front. In fact, the eruption of the cavity can be decomposed into two distinct phases; a slow rise phase (approximately 0.6 km s^{-1}) followed by an acceleration phase (with mean speed 25 km s^{-1}). Possible trigger mechanisms of the eruption, whether external (e.g. nearby flaring) and/or internal (e.g. kink instability, mass loading) will be presented to give a fuller three-dimensional view of the entire event. Note that the preliminary analysis of the cavity has been accepted for publication (Regnier, Walsh & Alexander, 2011, A & A, 533, L1).

High-Temperature & High-Speed Downflows in an Impulsive Flare of 2011 March 12

Abstract Author(s): Watanabe, T. (1), Hara, H. (1), Imada, S. (2), Watanabe, K. (2), Shimizu, T. (2)
Institution(s): (1) NAOJ, (2) ISAS/JAXA
Email: watanabe@uvlab.mtk.nao.ac.jp
Session: Instabilities, Transients and Eruptions
Presentation: P-89

Abstract:

A new EIS study for flares (#390: HH_Flare_180x160_v2) enables a high-cadence raster scanning observation for an area of 180 arcsec x 160 arcsec, with 2 arcsec slit shifting E-W 5 arcsecs per exposure. The exposure time is set to 10 seconds, and the time cadence of raster scan is about 360 seconds. This study have caught an initial phase of a C9.6 flare occurred on March 12, 2011.

This flare was very impulsive, started at 17:19UT, and ended at 17:34UT in GOES soft X-ray light curves. RHESSI spectra and images drawn in the energy range of E < 25 keV showed thermal nature of the source, while a few small bursts in the 25 - 50 keV energy range revealed the precipitation sites of non-thermal electrons.

Fast downflows reaching + 200 km/sec at these footpoints were observed in the iron emission lines formed in lower temperatures than that of FeXVI, namely, log Te < 6.4. The line profile of the OVI line of the transition-region origin even showed downward moving plasma with a speed of + 150 km/sec.

The observing spectral windows for FeXIV density-sensitive line pairs did not cover their entirely redshifted line profiles, but the electron density of these fast-moving plasmas has been estimated to be ne ~ 10^{10} cm^{-3}.

Comparing AIA and RHESSI images with EIS raster images, these high-speed downflows are considered to have close relationship with a saturated conduction front generated by thermal heating at the apices of the flaring loops reaching their foot-points.

Statistical Analyses of White-Light Flares observed by Hinode/SOT

Abstract Author(s): Watanabe, K. (1), Shimizu, T. (1), Masuda, S. (2), Ichimoto, K. (3)
Institution(s): (1) ISAS/JAXA, 3-1-1 Yoshinodai, Chuo-ku, Sagamihara, Kanagawa, Japan (2) STE Laboratory, Nagoya University, Furo-cho, Chikusa-ku, Nagoya, Japan (3) Kwasan/Hida Observatories, Kyoto University, Yamashina, Kyoto, Japan
Email: watanabe.kyoko@isas.jaxa.jp
Session: Instabilities, Transients and Eruptions
Presentation: P-90

Abstract:

We have used Hinode flare catalog (http://st4a.stelab.nagoya-u.ac.jp/gemsis/hinode_flare/) to perform a statistical study of white-light flares. We found 11 white-light events by using G-band and continuum data of Hinode/SOT until now.

White-light flares are flares that show an enhancement in the visible continuum. White-light emissions are well correlated with HXR and radio emissions in time profile and emission location. So, there is some consensus that the origin of white-light emission is accelerated particles, in particular non-thermal elections.

Previously we analyzed one of the 11 white-light events on December 14th, 2006 in detail. In this event, a significant enhancement of white-light (G-band) emission was observed, and white-light and hard X-ray emissions were seen at almost the same location. We assume that the thick target model to calculate the power of the accelerated electrons from the X-ray spectra, and we also assume a blackbody model to calculate the power of white-light emission. The power of the white-light emission is well correlated with hard X-ray power, which has a cutoff energy of 40keV (Watanabe et al., 2010).

Recent white-light events (e.g. X2.2 flare on 15 February 2011) were observed by using three continuum bands (Red, Green and Blue). From these data, we can determine precisely the temperature of the region where the white-light emissions were enhanced. Moreover, hard X-ray emissions were also observed by RHESSI.

In this talk, we present analysis results of recent white-light flares in detail and a statistical analysis of the SOT white-light events. We also discuss the flare parameters and review models to explain the observations in terms of particle acceleration.

A High-Velocity Motion of Active Region Loops Triggered by a 2011 Feb 18 Flare

Abstract Author(s): Aoki, K. (1), Hara, H. (2)
Institution(s): (1) University of Tokyo, Tokyo, Japan, (2) National Astronomical Observatory of Japan, Tokyo, Japan
Email: kunichika.aoki@nao.ac.jp
Session: Instabilities, Transients and Eruptions
Presentation: P-91

Abstract:

We report a high-velocity plasma motion near the lop-top region of large-scale active-region loops after the occurrence of the M-class flare at the active region NOAA11158 on 2011 Feb 18. The motion was detected during the impulsive phase of the M-class flare by the Doppler-shift measurement in Fe XXIV at 192 Å with the Hinode EUV imaging spectrometer (EIS). In order to identify the high-velocity component from the temporal evolution of the coronal structures, we use high-cadence EUV images at 94 and 131 Å from Atmospheric Imaging Assembly (AIA) on Solar Dynamics Observatory (SDO). We have found that the Doppler velocity near the loop-top region reaches 200-400 km/s and the motion is also identified in the AIA EUV images. Before the appearance of the high-speed plasma, large-scale loops were heated to a flare temperature in association with the occurrence of the M-class flare. One of the loops that rose vertically at ~200 km/s interacted with other loop structures located above it. We discuss the possible mechanisms that are responsible for the high-velocity motion near the loop-top region from the detailed Doppler feature and the 3D coronal structures that are determined by the stereoscopic measurement from AIA 193 Å and STEREO-A 195 Å images.

The Rayleigh-Taylor Instability in Solar Prominences: a review of Hinode and SDO results

Abstract Author(s): Berger, T.
Institution(s): Lockheed Martin Solar and Astrophysics Laboratory
Email: berger@lmsal.com
Session: Instabilities, Transients and Eruptions
Presentation: P-92 (**Digital Poster Display**)

Abstract:
We review the discovery and analysis of the Rayleigh-Taylor (RT) instability in quiescent polar crown prominences. Discovered shortly after the Hinode launch by the SOT instrument, we have since analyzed these instabilities using all three Hinode instruments as well as the Solar Dynamics Observatory AIA instrument. We find that the instability is caused by the emergence of 1 MK plasma "bubbles" from the chromosphere below quiescent prominences. The buoyancy instability sets in at the interface between the hot under-dense bubbles and the cooler dense prominence plasma above. We speculate that these bubbles are caused by emerging twisted magnetic flux which is heated to coronal temperatures low in the atmosphere via reconnection with the surrounding coronal magnetic fields. Quiescent prominences and their associated coronal cavities can thus be seen as large-scale magneto-convection flow systems in which high temperature magnetic flux is buoyantly injected from below while the condensing return flow from the coronal cavity forms the cool downflows typical of quiescent prominences. We discuss the implications of this finding for understanding polar crown CMEs and eruptive events in general.

Differential Emission Measures from the Regularized Inversion of SDO and Hinode data

Abstract Author(s): Hannah, I. G., Kontar, E. P., Fletcher, L.
Institution(s): University of Glasgow
Email: iain.hannah@glasgow.ac.uk
Session: Instabilities, Transients and Eruptions
Presentation: P-93

Abstract:
Observations from SDO and Hinode provide an unprecedented view of plasma in the solar atmosphere. However the inference of how much material is emitting at each temperature - the Differential Emission Measure DEM - from these data sets is an ill-posed inverse problem. We present a model independent regularization algorithm used in RHESSI X-ray software that makes use of general constraints on the form of the DEM. The regularization produces error and temperature resolution estimates on the calculated DEM, thus giving an objective criteria as to whether the underlying plasma distribution is iso- or multi-thermal. We also investigate how the kernel uncertainties influences the DEM and its accuracy. Our algorithm is computationally fast making it ideal for the challenging amounts of SDO data. We demonstrate this technique applied to synthetic data from a range of DEM models and obtain the regularized DEM from a variety of phenomena observed with SDO and Hinode.

Confirmation of prominence oscillations by simultaneous observations from two remote sites

Abstract Author(s): Zapior, M., Kotrc, P., Heinzel, P.
Institution(s): Astronomical Institute, Academy of Sciences
Email: pheinzel@asu.cas.cz
Session: Instabilities, Transients and Eruptions
Presentation: P-94

Abstract:
Prominence oscillations are predicted by currently developed MHD models (e.g. Oliver 2009). There are different oscillation modes classified according to the observed amplitudes in the Doppler signal and periods. We concentrated on small-scale oscillations that may be excited by MHD waves in the prominence body. Their observational confirmation is rather difficult due to predicted low amplitudes (1-2 km/s). The signal may be influenced by non-solar factors. A confirmative method for avoiding these problems is an observation of the same prominence by independent remote telescopes. Such observations were made only once by Balthasar et al. (1993) who found 0.5, 12 and 20 minute periods. Here we present the first results of our Czech-Polish observational campaign of prominence oscillations. Two remote telescopes (Ondrejov Observatory and Wroclaw University Observatory), separated by 220 km, observed the same prominence simultaneously with a high temporal resolution. A strong correlation of Doppler signals was revealed and several periods of small scale oscillation were detected. Three periods (22, 28, 45 min) were present in both data sets and therefore considered as real ones. With high spectral resolution we can study the line shape evolution and compare our results with theoretical models (see contribution by Heinzel et al. at this meeting).

Small Scale Structures inside the Reconnecting Current Sheet: Observations and Theories

Abstract Author(s): Lin, J.
Institution(s): Yunnan Astronomical Observatory, Kunming, China
Email: jlin@ynao.ac.cn
Session: Instabilities, Transients and Eruptions
Presentation: P-95

Abstract:

One of the most significant predictions of the catastrophe model of solar eruptions developed by Lin & Forbes (2000) is a long current sheet that forms following the onset of the eruption. Various modes of plasma turbulence as a result of plasma instabilities are invoked inside the current sheet, yielding fast dissipation of the magnetic field, namely magnetic reconnection, through the sheet. Because the timescale of reconnection is long compared to the timescale of the onset stage, dissipation of the sheet is slow, so the current sheet is able to become fairly long. The evolution in the global feature of the current sheet is significant constrained by the local Alfvén speed, and the internal properties and features of the sheet, on the other hand, are dependent in an apparent way on the development of the turbulence caused by the instabilities. The tearing mode instability among those that may occur in the sheet is the most important one that accounts for the large thickness and high electric resistivity of the current sheet. In the present work, we show a set of events that were observed to develop long and thick current sheets with several apparent features indicating the progress of the turbulence in the sheet, and the results of numerical experiments of magnetic reconnection occurring in a long current sheet. We noticed that apparent features of the tearing usually appear in the environment of high magnetic Reynolds number, and numerical experiment duplicated the scaling of the current sheet deduced on the basis of the tearing mode.

Flare detection in Hinode XRT lightcurves

Abstract Author(s): Posson-Brown, J., Kashyap, V., Grigis, P.
Institution(s): Harvard-Smithsonian Center for Astrophysics
Email: jpossonbrown@cfa.harvard.edu
Session: Instabilities, Transients and Eruptions
Presentation: P-96

Abstract:

One of the greatest challenges in solar coronal physics is to obtain a statistically complete sample of short duration events like coronal bright points. Such samples are necessary to fully characterize the properties of these events and understand the physical basis of such phenomena. Datasets are best acquired automatically, without manual intervention, in order to avoid introducing observer biases. We evaluate several algorithms for detecting flare events in time series data. One algorithm determines where derivatives of the Gaussian-smoothed lightcurves cross certain thresholds. A second algorithm segments the Loess-smoothed lightcurves between consecutive minima, then joins adjacent segments if their extrema are not statistically distinguishable. A third algorithm is a hybrid of the first two. We also investigate the use of a robust Bayesian wavelet-based event detection method. We generate simulated datasets with similar properties to observed Hinode XRT quiet Sun lightcurves and test each algorithm these datasets. The performance of each algorithm on the simulated lightcurves is scored according to the rates of false positive (Type I) and false negative (Type II) errors. We use these results to optimize the parameters values of each algorithm. We compare the performances of the algorithms and evaluate the efficiency with which they are able to detect small events. Such evaluations are relevant to properly interpret the observed steepening of the slope of the solar flare energy distribution at small energies.

Physical parameters of a blowout jet observed by Hinode XRT and Stereo SECCHI

Abstract Author(s): Pucci, S. (1), Poletto, G. (2), Sterling, A.C. (3), Romoli, M. (4)
Institution(s): (1) Department of Physics and Astronomy, University of Firenze, Firenze, Italy, (2) INAF - Arcetri Astrophysical Observatory, Firenze, Italy, (3) Space Science office, VP 62, Marshall Space Flight Center, Huntsville, AL 35812, USA, (4) Department of Physics and Astronomy, University of Firenze, Firenze, Italy
Email: stpucci@arcetri.astro.it
Session: Instabilities, Transients and Eruptions
Presentation: P-97 (**Digital Poster Display**)

Abstract:
This work presents a multi instrument analysis of the strong X-ray jet which occurred in the north polar coronal hole on 3 nov 2007 at 11:50 UT. The jet has characteristics of a ``blowout jet'' (Moore et al. 2010), and was observed by Hinode XRT over its entire duration (40 minutes) with only the Al-poly filter, used in high cadence (80 images per hour). Stereo EUVI A and B observed the jet at wavelengths 171 Å, 195 Å, 284 Å and 304 Å, with, respectively, cadences of 27, 6, 3 and 6 images per hour. An extension of the jet was also observed with cor1. The EUVI observations allow us to derive the temperature of the jet via the double filter ratios color-color technique (Chae et al., 2002). We are able to calculate temperatures and emission measures in the prejet, the maximum, and the fade-out phases, which are all observed even in the low-cadence 284 filter. These EUVI-derived parameters are then used to calculate a predicted Hinode XRT Al-poly intensity, and we compare that prediction with the observed XRT values. Our results are discussed in terms of the geometrical and physical parameters of the event, with the focus on identifying the characteristics of blow-out jets as observed by the different instruments.

Coronal Rotation from XBPs Observed with Hinode/XRT

Abstract Author(s): Kariyappa, R. (1), DeLuca, E. E. (2)
Institution(s): (1) Indian Institute of Astrophysics, (2) Harvard-Smithsonian Center for Astrophysics
Email: rkari@iiap.res.in
Session: Instabilities, Transients and Eruptions
Presentation: P-98

Abstract:

We have selected a large number of XBPs over synoptic soft X-ray full-disk images observed using Al-Mesh with X-Ray Telescope (XRT) onboard the Hinode spacecraft during July-December, 2008. We have analyzed the full-disk images using SSW in IDL. We used the tracer method to identify and trace the passage of XBPs over the solar disc with the help of overlaying grids. We also obtained the position (Latitude and Longitude), size & brightness information for XBPs using tracer method as a function of time and thus calculated sidereal angular rotation rate of corona at different latitudes. We have compared the rotation rate with latitude, size and brightness of XBPs. The important results derived from these analysis are: (i) the rate with which solar corona rotates differentially like the photosphere and chromosphere; (ii) the larger XBPs show a lower sidereal angular rotation rate, the smaller XBPs exhibit higher rotation rate, similar to sunspots; and (iii) it is not clear on brightness of XBPs with coronal rotation rate, needs further investigation.

Structure and Dynamics of Quiescent Prominence Eruptions

Abstract Author(s): Su, Y., Lu, M., van Ballegooijen, A.
Institution(s): Harvard-Smithsonian Center for Astrophysics, Cambridge, MA, USA
Email: ynsu@head.cfa.harvard.edu
Session: Instabilities, Transients and Eruptions
Presentation: P-99 (**Digital Poster Display**)

Abstract:
We present a survey on the fine structure and dynamics of quiescent prominence eruptions both on the disk and at the limb. We have identified 52 quiescent prominence eruptions by looking at AIA daily movies from April to June in 2011. Among these events, there are 26 symmetric eruptions (coherent loop-like eruptions) and 26 asymmetric eruptions (one footpoint lifts off) as shown by AIA and STEREO/EUVI observations. Vertical threads are identified in 14 out of the 52 events, while horizontal threads are observed in almost all eruptions. We find 17 events with obvious twisting motion, and 10 eruptions seem to untwist from a more complicated structure. For 14 selected limb events, we carry out a detailed study of the eruption dynamics using AIA observations at 304 Angstrom. We find that the initial heights of these erupting prominences are located around 50-110 Mm above the limb. The eruptions start from a speed of less than 5 km/s, then increase to several tens km/s in the AIA field of view. The maximum speed of these events is 50 km/s. The acceleration plots show a positive acceleration in the range of 0 to 20 m/s^2. No significant difference is identified in the dynamics of the symmetric and asymmetric eruptions.

EUV spectroscopic observations of CME-related kinematics

Abstract Author(s): Tian, H., McIntosh, S. W., Wang, X.
Institution(s): High Altitude Observatory, National Center for Atmospheric Research
Email: htian@ucar.edu
Session: Instabilities, Transients and Eruptions
Presentation: P-100

Abstract:
CME-related kinematics have rarely been investigated by using EUV spectroscopic observations. We analyzed several data sets obtained by EIS during CMEs and coronal dimmings. CME-related kinematics are clearly revealed in the EIS spectra. Preliminary results are summarized as following: (1) During the eruption phase coronal emission lines often clearly exhibit two components, an almost stationary component accounting for the background emission and a highly blueshifted (~200 km/s) component representing emission from the erupting material. Combining the projected speed of the erupting material derived from imaging observations and the speed of the blueshifted component we can calculate the real speed of the erupting material. (2) A single Gaussian fit of the line profile usually produces large blue shift and greatly enhanced line width, which seems to be the result of the superposition of the two components. (3) The intensity ratio of the blueshifted component and the background component is sometimes larger than 1, and in some cases it decreases with increasing temperature. (3) In one observation we found that the speed of the blueshifted component increases with increasing temperature. (4) Coronal dimming regions are found to be characterized by significant blueshift and enhanced line width by using a single Gaussian fit. While an asymmetry analysis of the line profiles clearly indicates that these are actually caused by the superposition of a strong background component and a relatively weak (~20%) high-speed (~100 km/s) component.

Influence of static and stochastic electric fields on electron beams bombarding the chromosphere

Abstract Author(s): Varady, M. (1, 2), Karlicky, M. (2), Moravec, Z. (1)
Institution(s): (1) Purkinje University, Faculty of Science, Usti nad Labem, Czech Republic, (2) Astronomical Institute, Academy of Sciences, Ondrejov, Czech Republic
Email: mvarady@physics.ujep.cz
Session: Instabilities, Transients and Eruptions
Presentation: P-101

Abstract:

Using a test-particle approach we study the influence of static and stochastic electric fields on propagation of electron beams along the magnetic field lines from the primary acceleration site in the coronal current sheets downwards to the chromosphere. The results are compared with the most common, classical model of electron beam propagation, scattering and thermalisation given by Emslie (1978) and the effects on chromospheric heating and hard X-ray emission are discussed.

RHD Modelling of Solar Flares

Abstract Author(s): Varady, M. (1, 2), Kasparova, J. (2), Moravec, Z. (1), Heinzel, P. (2), Karlicky, M. (2)
Institution(s): (1) Purkinje University, Faculty of Science, Usti nad Labem, Czech Republic, (2) Astronomical Institute, Academy of Sciences, Ondrejov, Czech Republic
Email: mvarady@physics.ujep.cz
Session: Instabilities, Transients and Eruptions
Presentation: P-102

Abstract:
In the context of interpreting the non-thermal hard X-ray emission and gamma lines emanating from the footpoints of flare loops, most contemporary flare models assign a fundamental role during the flare energy release, transport and deposition to the high energy non-thermal particle beams. In our contribution we concentrate on RHD modelling of the spectroscopic properties of chromospheric flare emission in optical hydrogen lines generated due to the bombardment of the chromosphere and photosphere by particle beams with power-law spectra.

The Neupert Effect as a Function of Pitch Angle Distribution and Energy Budget in Simulated Flares

Abstract Author(s): Winter, H. (1), Reeves, K. (1), Egan, A. (2)
Institution(s): (1) Harvard-Smithsonian Center for Astrophysics, Cambridge, MA, USA, (2) Barnard College, NY, NY, USA
Email: hwinter@cfa.harvard.edu
Session: Instabilities, Transients and Eruptions
Presentation: P-103 (**Digital Poster Display**)

Abstract:

The Neupert Effect is the well known empirical result that the hard X-ray emission of about half of large, impulsive flares looks like the derivative of the soft X-ray emission. This relationship between the non-thermal, hard X-ray emission and the thermal, soft X-ray emission supports the theory that the majority of the energy liberated by the flare is in the form of non-thermal, high-energy electrons which then heat the thermal plasma and drive chromospheric evaporation. Observational estimates currently put the energy budget of a flare as ~75% in non-thermal processes and ~25% in thermal processes. However, the observational estimates of the thermal and non-thermal energy in flares are currently uncertain to within an order of magnitude. It is also unclear as to why ~24% of large, impulsive flares have their soft X-ray emission peak well before the end of the hard X-ray emission in direct violation of the Neupert Effect. In this work, we address the question of how non-thermal particle properties affect the observed Neupert Effect by simulating a series solar flares using the HyLoop code. HyLoop simulates non-thermal particles interacting a with thermal plasma and the thermal plasma's response to those interactions. A series of flares are simulated with different non-thermal particle parameters, such as pitch-angle distribution and non-thermal fraction of total flare energy. The hard and soft X-rays emissions are synthesized for each simulation. These simulated emissions are then used to determine what impacts the non-thermal particle parameters have on the observed Neupert Effect.

Study of Solar Flare Energetic Electrons by Using Synthesized Emission Based on Fokker-Planck Simulation Results

Abstract Author(s): Yokoyama, T., Kitagawa, H., Minoshima, T., Kawate, T.
Institution(s): U. Tokyo, JAMSTEC, Kyoto U.
Email: yokoyama.t@eps.s.u-tokyo.ac.jp
Session: Instabilities, Transients and Eruptions
Presentation: P-104

Abstract:
Temporal, spatial and spectral variation of emissions from solar flares are studied by solving the electrons transport in a flare loop and their production of photons. The issue of generation mechanisms of high-energy electrons in flares have been known but have not yet understood for more than decades. In observations, for example, the Nobeyama Radioheliograph has made clear descriptions on the gyro-synchrotron emissions from them, such as, relative brighter loop-tops than footpoints, and steeper (softer) spectra toward footpoints. Hinode SOT also observed optical emission from several flares. These observational results should include information on the phase-space-density of injected electrons and could be used as keys to the acceleration mechanisms. It is, however, not straightforward and is a difficult task since such injection information is strongly modulated through the transport and the emission processes. We study this problem by a "forward" approach: First, we solve the electron transport Fokker-Planck equation along a flare loop. The dependence of phase-space density on time, space, electrons pitch-angle, and their energy is derived. The pitch-angle scattering by the Coulomb collisions throughout the loop and the electrons loss at both footpoints are included. Second, the gyro-synchrotron emission (assumed optically-thin) is derived from non-isotropic distribution of emitting electrons. We found that: (1) The loop top is relatively brighter than the footpoints. (2) Both footpoints have steeper (softer) spectrum than the loop top. (3) The emission is harder than what is expected from the isotropic electrons.

Solar coronal shocks and particle acceleration as deduced from EUV, radio, and in-situ observations

Abstract Author(s): Kozarev, K. A. (1), Korreck, K. E. (2), Lobzin, V. V. (3), Dayeh, M. A. (4), Schwadron, N. A. (5)
Institution(s): (1) Boston University/Center for Astrophysics, (2) Smithsonian Astrophysical Observatory, (3) The University of Sydney, Sydney, Australia, (4) Soutwest Research Institute, San Antonio, TX, (5) University of New Hampshire, Durham, NH
Email: kkozarev@cfa.harvard.edu
Session: Instabilities, Transients and Eruptions
Presentation: P-105

Abstract:

We use remote ultraviolet and radio observations of the Sun to characterize shocks forming in the low solar corona, and to investigate whether they can accelerate charged particles fast enough for the appropriate timescales of such coronal shocks. We utilize observations from SDO/AIA, and the Learmonth radio observatory. We determine dynamical properties of shock waves, and attempt to estimate relative orientation of the shock fronts to the overlying coronal magnetic fields. In the current theoretical framework of shock acceleration a perpendicular orientation of the shock to magnetic fields is favored for the fast acceleration of charged particles. We use a potential field source surface model of the coronal magnetic fields together with the observations to estimate how efficient coronal shock waves may be in accelerating particles. Finally, we test this approach by analyzing in situ observations during shock wave events.

Photometric Uncertainties within XRT

Abstract Author(s): Kobelski, A. R. (1), Saar, S. H. (2), McKenzie, D. E. (1), Weber, M. A. (2), Reeves, K. K. (2), DeLuca E. E. (2)
Institution(s): (1) Montana State University, Bozeman, MT, USA (2) Harvard Smithsonian Center for Astrophysics, Cambridge, MA, USA
Email: akobelski@physics.montana.edu
Session: Future Needs - Observational, Theoretical and Computational
Presentation: P-106 (**Digital Poster Display**)

Abstract:

We have developed estimates of the systematic photometric uncertainties for the X-Ray Telescope on Hinode. These estimates are included as optional returns from the standard XRT data reduction software, xrt_prep.pro. Included in the software estimates are uncertainties from instrument vignetting, dark current subtraction, split bias leveling, fourier filtering and JPEG compression. Sources of uncertainty that rely heavily on models of plasma radiation or assumptions of elemental abundances, such as photon noise, are not included in the software. We will present the results of this study, and discuss their implementation into the xrt data analysis pipeline.

The emergent technology of space-qualified liquid-crystal variable retarders for solar remote sensing

Abstract Author(s): Uribe-Patarroyo, N.
Institution(s): Boston University*
Email: uribepnr@gmail.com
Session: Future Needs - Observational, Theoretical and Computational
Presentation: P-107

Abstract:
New instruments for the study of solar magnetic fields that make use of liquid-crystal modulators have appeared and are being designed recently. Among them, the successful Imaging Magnetrograph eXperiment (ImaX) onboard the SUNRISE mission used two liquid-crystal variable retarders (LCVRs) as polarization modulators, which performed exceptionally well in this ballon-borne mission, with near-space environmental requirements. IMaX served as the seed for the Solar Orbiter Helioseismic Polarimetric Imager (SO/PHI), which is approaching its preliminary design phase, in which LCVRs form the basis of the polarization modulation package. Motivated by the requirements of SO/PHI and Solar Orbiter's coronagraph METIS/COR, our group performed the project "Validation of LCVRs for the Solar Orbiter Polarization Modulation Package", as required by the European Space Agency to increase the LCVR technology readiness level to TRL5 "Component Validation in Relevant Environment". We present the main results of this project: the environmental testing of LCVRs under space conditions, including a campaign to test the effects of gamma and proton radiation, outgassing, vibration and shock, thermo-vacuum and ultraviolet radiation. It can be concluded that LCVRs are insensitive to high-energy radiation, vibration and shock and thermo-vacuum. The degradation induced by ultraviolet radiation is known, and our study established precise effects for different liquid crystals, which consisted in a progressive change in the performance, but not in destruction of the samples up to the tested levels. The results of this validation can be extrapolated into other uses of liquid-crystal variable retarders, such as in tunable Lyot filters, application which is being considered for Solar-C, and provide a significant step towards full space qualification of high-performance LCVRs for space applications.

(*) Currently at Iberoptics Sistemas pticos, C/ Gamonal 16, Of. 4-1, E-28031 Madrid, Spain; and Department of Electrical & Computer Engineering, Boston University, Boston, Massachusetts 02215, USA.

The X-ray Telescope & Spectrograph - Coronal Instrumentation for the Solar-C Mission

Abstract Author(s): DeLuca, E. E. (1), Golub, L. (1), Kobayashi, K. (2), Bookbinder, J. (1), Cheimets, P. (1), Lemen, J.(3), Longcope, D. (4), McKenzie, D. (4), Korreck, K. (1), Reeves, K. (1), Weber, M. (1), Winbarger, A. (5)
Institution(s): (1) CfA, (2) UAH, (3) LMSAL, (4) MSU, (5) MSFC
Email: edeluca@cfa.harvard.edu
Session: Future Needs - Observational, Theoretical and Computational
Presentation: P-108

Abstract:

The Solar-C Plan-B mission described in the Interim Report emphasizes the importance of coronal imaging and spectroscopy for the success of the mission. We describe an instrument suite that combines high resolution imaging (0.5"/pixel) and high resolution spectroscopy (1"/pixel, 5mA/pixel, 70km/s). The X-ray Telescope & Spectrograph (XTS) fits in the baseline volume and mass described in the Interim Report. It consists of a GI imager channel (XTS-I) feeding a low noise rapid read (~700fps) CMOS detector and an X-ray slit spectrograph channel (XTS-S) based on the MaGIXS rocket design.

Instrument for the Chromospheric Lyman-Alpha SpectroPolarimeter (CLASP) program

Abstract Author(s): Kano, R. (1), Narukage, N. (2), Ishikawa, R. (1), Kubo, M. (1), Katsukawa, Y. (1), Suematsu, Y. (1), Hara, H. (1), Bando, T. (1), Tsuneta, S. (1), Watanabe, H. (3), Ichimoto, K. (3), Kubo, M. (4), Song, D. (5), Kobayashi, K. (6), Trujillo Bueno, J. (7)
Institution(s): (1) National Astronomical Observatory of Japan, Tokyo, Japan, (2) Institute of Space and Astronautical Science, Japan Aerospace Exploration Agency, Kanagawa, Japan, (3) Kyoto University, Kyoto, Japan, (4) Meisei University, Tokyo, Japan, (5) Soul National University, Soul, Korea, (6) University of Alabama in Huntsville, Huntsville, AL, USA, (7) Instituto de Astrofisica de Canarias, Tenerife, Spain
Email: ryouhei.kano@nao.ac.jp
Session: Future Needs - Observational, Theoretical and Computational
Presentation: P-109

Abstract:

The "Chromospheric Lyman-Alpha Spectro-Polarimeter (CLASP)" is a sounding rocket experiment to explore magnetic fields in the upper chromosphere and transition region by measuring the linear polarization in the Lyman-alpha line (121.567nm). The Lyman-alpha line from on-disk targets must be linearly polarized by scattering processes, and the linear polarization at the line center is expected to vary between 0.1~1% by the Hanle effect depending on the strength and orientation of magnetic fields. Therefore, the CLASP instrument is designed to measure the linear polarization with a polarimetric sensitivity of 0.1% and a spectral resolution of 0.01nm. The instrument consists of a large aperture (287 mm) Cassegrain telescope, a grating spectrograph, and a polarimeter. Reflective optical elements are essentially used there, because optical materials, with a few exceptions (e.g. Magnesium Fluoride, MgF2), easily absorb the Lyman-alpha light. The primary mirror of the telescope uses a narrowband multilayer coating that reflects the Lyman-alpha but transmits the visible light onto an absorber behind the primary mirror. This minimizes both the heat load and off-band contamination in the spectrograph. A constant-line-spacing spherical grating mounted in an inverse Wadsworth geometry disperses the light from the 1.6"-slit on the Cassegrain focus into two channels: plus and minus 1st-order beams. They are a matched pair of imaging systems consisting of an offset parabolic mirror, a reflective polarization analyzer placed at the Brewster's angle, and a CCD camera for each, and simultaneously measure the orthogonal linear polarizations. A rotating half waveplate made of MgF2 is behind the slit, and allows measurement of both Stokes Q and U with the fixed polarization analyzers.

Observing the Dynamic Sun with SPIES

Abstract Author(s): Lin, H.
Institution(s): Institute for Astronomy - University of Hawaii
Email: lin@ifa.hawaii.edu
Session: Future Needs - Observational, Theoretical and Computational
Presentation: P-110 (**Digital Poster Display**)

Abstract:
The SpectroPolarimetric Imager for the Energetic Sun (SPIES) is a new instrument optimized for the study of the small scale and highly dynamic solar phenomena such as the ubiquitous penumbral micro jets or surface dynamo associated with the solar convective motion. Understanding the physics of these dynamic phenomena requires detailed information of the magnetic, thermal, and dynamic properties of the solar atmosphere at every stage of their evolutionary history. Although these properties can be obtained with existing high performance spectropolarimeters such as the SpectroPolarimeter on board the Hinode space solar observatory, or the Facility IR Spectropolarimeter on the Dunn Solar Telescope, these instruments cannot yet observe with time resolution comparable to the dynamic time scale of these dynamic events over the required field of view. SPIES is a true-imaging spectropolarimeter specifically constructed to address this deficiency in our observing capability. It is based on a fiber optic array integral field unit, and is capable of observing a 64 x 32 pixel field simultaneously with high spatial and spectral resolution. It can obtain the full Stokes spectra of the field with a temporal resolution of a few seconds. This paper presents the design and characteristics of the instrument, as well as preliminary results from a sunspot magnetic field observation using the FeI 1565 nm line pair.

Realistic simulations of the impact of partial ionization on the chromosphere

Abstract Author(s): Martinez-Sykora, J.
Institution(s): (1) Lockheed Martin Solar & Astrophysics Lab, Palo Alto, CA, USA, (2) Institute of Theoretical Astrophysics, University of Oslo, Norway
Email: juanms@lmsal.com
Session: Future Needs - Observational, Theoretical and Computational
Presentation: P-111

Abstract:

We investigate the importance and consequences of introducing neutral particles into the MHD equations in 3D advanced radiative MHD simulations obtained from the Bifrost code. We use a model that spans the upper layer of the convection zone to the low corona. The chromosphere and transition region is partially ionized and the interaction between ionized particles and neutral particles has important consequences on the thermodynamics of these layers. We implemented the effects of the partial ionization using the generalized Ohm's law, i.e., we consider the effects of the Hall and ambipolar diffusion in the induction equation. The different approximations going from 3 particles to the generalized Ohm's law has been tested in 2.5D simulations and we note that the assumptions behind the generalized Ohm's law are not always satisfied in the upper-chromosphere and in the transition region.

Warm Coronal Rain on Young Solar Analog, EK Draconis?

Abstract Author(s): Ayres, T., France, K.
Institution(s): University of Colorado
Email: Thomas.Ayres@Colorado.edu
Session: Solar-Stellar Connections
Presentation: P-112

Abstract:
We have obtained a moderate resolution (R~ 18,000), 129-143 nm spectrum of 50 Myr old solar analog EK Draconis, using the super-sensitive Cosmic Origins Spectrograph on Hubble Space Telescope. The brief twenty-minute "SNAPshot" observation, remarkably, captured two distinct flares-like enhancements in the Si IV 140 nm doublet (T~ 60,000 K); unusually broad profiles of Si IV and the C II 133 nm chromospheric multiplet (T~ 30,000 K); and very prominent Fe XXI 135 nm coronal forbidden line emission (T~ 10 MK). The bright Si IV features are significantly redshifted compared to the milder, although still redshifted, equivalent components of Alpha Centauri A, a close twin of the Sun. The broad, shifted, flaring hot-line profiles of EK Dra reveal not only that the subcoronal plasma of the young sun is highly dynamic, but also that the Si IV-bearing gas must be continually accreting onto the lower atmosphere, perhaps the stellar equivalent of warm "coronal rain." Furthermore, the erratically variable Si IV emission is not matched in the neighboring temperature regimes, traced by chromospheric C II and coronal Fe XXI; so the Si IV outbursts do not correspond to the normal flare process, which impulsively heats coherently through the atmosphere. Instead, the Si IV events more likely represent episodes of catastrophic cooling: cloud-bursts associated with the coronal rain, if you will.

Calibrating the Solar-Stellar Coronal Connection: Using Hinode XRT to Measure Stellar Coronae

Abstract Author(s): Saar, S. H., Testa, P.
Institution(s): Smithsonian Astrophysical Observatory
Email: saar@cfa.harvard.edu
Session: Solar-Stellar Connections
Presentation: P-113

Abstract:

Despite decades of X-ray observations of both solar and stellar coronae with various instruments, the precise position of solar X-ray emission levels in a broader astrophysical context is surprisingly uncertain. This is largely due to cross-calibration problems and the difficulty in observing the same targets with both solar and stellar instruments. Here we report on a new attempt at direct cross-calibration between solar and stellar missions: observations by Hinode XRT of a young, X-ray active F star HD199143. This star has been previously studied by ROSAT and Chandra, and is eclipsed by the Sun every January. We observed the star in the Al-poly filter for a total of ~12 hours on ingress and egress. After careful data processing, we searched for a small excess along the star's apparent path. We discuss the tentatively successful results in the context of the most up-to-date calibrations of Hinode, Chandra and ROSAT count rates for this star, as well asfurther observational and analysis plans.

Mass and Energy Loss Due to CMEs Throughout the Sun's History

Abstract Author(s): Saar, S. H. (1), Korreck, K. (1), Aarnio, A. (2)
Institution(s): (1) Smithsonian Astrophysical Observatory, (2) University of Michigan
Email: saar@cfa.harvard.edu
Session: Solar-Stellar Connections
Presentation: P-114

Abstract:
We combine solar CME statistics, the fraction of flares by energy with associated CMEs, and stellar flare statistics by energy to make estimates of the mass and kinetic energy loss due to CMEs in stars as a function of their mean X-ray luminosity. We then use X-ray - rotation and rotation - age relationships to convert these into estimates of the CME-related mass and energy losses as a function of age. We find that in younger stars, CME-related mass loss can be a significant fraction of the total. In support of this, our estimates match observed mass loss rates in two active stars. We estimate the time history of solar mass loss due to CMEs.

DEM analysis at impulsive phase footpoints

Abstract Author(s): Graham, D. R., Fletcher, L., Hannah. I. G., Kontar, E. P.
Institution(s): School of Physics and Astronomy, University of Glasgow, UK, G12 8QQ
Email: dgraham.glasgow@gmail.com
Session: Instabilities, Transients and Eruptions
Presentation: P-115

Abstract:

The chromospheric footpoints of a solar flare in the impulsive phase have been observed to be locations of high electron density and temperature. The depth in the atmosphere where this emission originates, and how it is formed are still relatively unanswered questions. The differential emission measure (DEM) is a useful tool to study the temperature structure of a plasma, showing the amount of emitting plasma as a function of temperature. We have used the regularised inversion method by I. G. Hannah and E. P. Kontar to calculate the DEM at the footpoints of a solar flare. Spectral data from SDO/EVE and Hinode/EIS provide EUV emission lines in a wide range of temperatures. The combination of high cadence and wavelength coverage from EVE, and high spatial/spectral resolution from EIS are ideal for this task and will hopefully shed light on the character of flare footpoint plasma.

Index

(Click **Bolded** Reference to Jump to Abstract Page)

A. P. Singh, K., CT-16
Aarnio, A., P-114
Abbo, L., **P-1**, **P-23**, P-63
Abramenko, V., P-11
Ahn, K., P-11
Alexander, C. E., P-88
Annoura, M., P-76
Antolin, P., **CT-5**
Anzer, U., P-18
Aoki, K., **P-91**
Arregui, I., **P-44**
Asensio Ramos, A., CT-38, **P-2**, P-44
Ayres, T., **P-112**
Baker, D., CT-24, **CT-28**
Ballester, J. L., P-25, P-44, P-82
Bamba, Y., CT-34
Bando, T., CT-38, P-109
Barcelo, S., **P-25**
Bellot Rubio, L., CT-12, **P-3**
Belluzzi, L., CT-37, CT-38, **P-24**
Bemporad, A., **P-63**
Berger, T., CT-27, P-42, **P-92**
Bianda, M., P-40
Bogachev, S. A., CT-30, P-56
Bommier, V., P-4
Bookbinder, J., P-108
Borrero, J. M., P-6
Boxin, G., P-71
Bueno, J. T., **CT-37**, CT-38, P-24, P-40, P-109
Cameron, R. H., CT-15
Cao, W., P-11
Carlsson, M., **IT-5**, IT-12, CT-14, CT-38, P-69, P-70, P-77
Casini, R., **IT-3**, CT-38
Cauzzi, G., P-79
Cheimets, P., P-108
Cheung, M. C. M., **CT-15**
Cirtain, J., CT-38, P-52, P-66
Copinger, P., CT-26
Cranmer, S. R., P-51
Culhane, J. L., **CT-24**, CT-33
Davila, J. M., CT-17, P-80
Dayeh, M. A., P-105
de la Cruz Rodriguez, J., P-77
DeLuca, E., CT-8, CT-10, CT-29, P-51, P-55, P-98, P-106, **P-108**
Del Zanna, G., CT-21
De Moortel, I., **CT-20**
Démoulin, P., CT-24
De Pontieu, B., **IT-12**, CT-1, CT-13, CT-14, CT-18, CT-38, P-69, P-77
de Wijn, A. G., **P-26**, P-27
Dibyendu, N., **P-13**
Ding, M. D., P-83
Dudik, J., P-64, **P-65**
Duvall Jr., T., P-37
Dzifcakova, E., **P-64**, P-65
Egan, A., P-103
Erdelyi, R., **P-5**, P-19
Falconer, D., P-52
Farid, S., **P-66**
Fedun, V., P-19
Fischer, C. E., **P-27**
Fleck, B., **P-67**
Fletcher, L., **IT-10**, P-46, P-93, P-115
Frank, Z., P-42
Franz, M., **P-6**
France, K., P-112
Gabriel, A., P-1, P-23
Gao, B., CT-26
Gibson, S. E., P-17, P-34, P-74
Gizon, L., P-33, P-42
Golub, L., IT-12, P-7, P-55, P-65, P-108
Gomory, CT-31
Goode, P., P-11
Goossens, M., P-44
Graham, D. R., **P-115**
Green, L.M., CT-28
Grigis, P., P-96
Guarrasi, M., **CT-22**, P-55
Gudiksen, B.V., IT-5, CT-23, P-68, P-69
Guerreiro, N., P-68
Guidoni, S. E., **CT-32**
Gunar, S., P-7, P-39
Guo, Y., P-4
Habbal, S. R., P-78
Hagenaar, H., P-8
Hahn, M., **P-45**
Hannah, I. G., **P-93**, P-115

Hansteen, V. H., IT-5, IT-12, CT-1, CT-23, **P-28**, **P-68**, **P-69**, P-70, P-77
Hao, J., **P-22**
Hara, H., **CT-33**, CT-35, CT-38, P-89, P-91, P-109
Harra, L. K., **CT-31**, CT-33, CT-35
Hayashi, Y., CT-26
Hazra, S., P-73
He, H., **CT-9**
He, J., P-78
Heinzel, P., **P-7**, P-18, P-39, **P-82**, P-94, P-102
Henriques, V. M. J., P-16
Hill, F., **IT-4**
Hillier, A., **CT-27**
Holman, G., CT-36
Hudson, H., **P-46**, P-74
Hurlburt, N., **P-29**
Ichimoto, K., CT-4, CT-6, CT-38, **P-30**, P-90, P-109
Ii, T., CT-26
Iida, Y., **P-8**
Imada S., **CT-35**, P-12, P-89
Inomoto, M., **CT-26**, P-71, P-76
Ishikawa, R., **IT-2**, CT-38, P-79, P-109
Isobe, H., CT-27
Ito, S., CT-26, P-71
Ito, T., CT-26, P-71
Jaeggli, S. A., **P-43**
Joshi, J., **P-31**
Kamio, S., **IT-8**
Kankelborg, C., IT-12
Kano, R., **CT-19**, CT-38, P-53, P-74, **P-109**
Kariyappa, R., **P-98**
Karlicky, M., P-64, P-101, P-102
Kashyap, V., P-96
Kasparova, J., P-102
Kato, Y., **P-70**
Katsukawa, Y., CT-38, **P-32**, P-109
Kawate, T., CT-16, P-104
Keller, C.U., P-27
Kim, T., CT-38
Kitagawa, H., P-104
Kitagawa, N., **P-47**
Kitai, R., **IT-6**, CT-4
Kitiashvili, I.N., **P-9**, **P-10**
Kliem, B., CT-29
Klimchuk, J., CT-21
Ko, Y.-K., **P-48**
Kobayashi, K. , **CT-38**, P-108, P-109
Kobelski, A., P-57, **P-106**
Kontar, E. P., P-93, P-115
Korreck, K. E., P-105, P-108, P-114
Kosovichev, A.G., P-9, P-10, P-37
Kotrc, P., P-18, P-94
Kozarev, K. A., **P-105**
Kubo, M., CT-38, **P-33**, P-109
Kucera, T. A., **P-34**, P-74
Kupryakov, Yu. A., P-18
Kusano, K., **CT-34**
Kuwahata, A., CT-26, **P-71**, P-76
Kuzin, S. V., CT-30, P-56
Lagg, A., CT-7
Landi, E., P-45
Lapenta, G., CT-3, P-49
Lee, E., CT-3, **P-49**
Lele, S.K., P-9
Lemen, J., IT-12, P-108
Li, Y., **P-83**
Lim, E.-K., **P-11**
Lin, H., P-43, **P-110**
Lin, J., **P-95**
Lites, B.W., P-27, **P-35**
Liu, W., P-80
Liu, W. J., **P-50**, **P-72**
Lobzin, V. V., P-105
Longcope, D. W., CT-32, P-41, P-50, P-72, P-108
Lu, M., P-99
MacKinnon, A., P-46
Malherbe, J. M., P-42
Mandrini, C.H., CT-24
Manso Sainz, R., CT-38, P-24
Mansour, N.N., P-9, P-10
Mariska, J., P-81
Martens, P., P-54
Martinez-Sykora, J., **CT-1**, CT-18, **P-36**, P-69, P-77, **P-111**
Mason, H. E., **CT-21**, P-62
Masuda, S., P-90
Matsui, Y., **P-12**
Matsumoto, T., **CT-25**

Matthews, S., P-14
McIntosh, S. W., CT-18, P-77, P-78, P-100
McKenzie, D. E., CT-32, CT-36, P-57, **P-84**, P-106, P-108
Mignone, A., CT-22
Minoshima, T., P-104
Miralles, M. P., **P-51**, P-85
Moore, R., **P-52**, P-87
Moravec, Z., P-101, P-102
Moreno-Insertis, F., CT-1
Mulu-Moore, F., P-66
Munoz-Jaramillo, A., **CT-10**
Murphy, N. A., **P-85**
Nagashima, K., **P-37**
Nakamura, T., CT-16
Nandy, D., **P-73**
Narukage, N., CT-38, **P-53**, P-109
Nishizuka, N., **CT-16**
Nordlund, A., P-20
O'Dwyer, B., CT-21, P-62
O'Hara, J., P-50
Ofman, L., CT-17, P-80
Oka, H., P-71, P-76
Okamoto, T. J., **CT-13**
Oliver, R., P-44, P-82
Olluri, K., **CT-23**
Ono, Y., CT-26, P-71, P-76
Opitz, A., CT-24
Orlando, S., CT-22
Orozco Suarez, D., CT-11, P-3, P-32
Ortiz, A., **CT-12**, P-28
Otsuji, K., **CT-4**
Parchevsky, K., P-37
Parenti, S., P-7
Pariat, E., CT-8
Pascoe, D. J., CT-20
Pearson, J., P-61
Peck, C., P-50
Pedram, E., **P-14**
Pereira, T. M. D., CT-1, **CT-14**, P-77
Peres, G., P-55
Plowman, J., **P-54**
Poletto, G., P-86, P-97
Pope, C. L., P-85
Posson-Brown, J., **P-96**
Prat, V., P-42
Pucci, S., **P-86**, **P-97**
Qiu, J., P-50, P-72
Ramelli, R., P-40
Ravindra, B., P-73
Raymond, J. C., P-51, P-85
Reale, F., CT-22, **P-55**, P-59
Reardon, K., P-79
Reeves, K., CT-36, P-65, **P-74**, P-85, P-103, P-106, P-108
Regnier, S., P-61, P-88
Rempel, M., P-43
Renon, N., P-42
Reva, A. A., CT-30, **P-56**
Rieutord, M., P-42
Ritchie, M., P-54
Robinson, B., CT-38
Romoli, M., P-86, P-97
Roudier, T., **P-42**
Rouillard, A., CT-24
Rouppe van der Voort, L., CT-5, CT-12, P-19, **P-38**, P-77
Saar, S., P-66, P-106, **P-113**, **P-114**
Sainz Dalda, A., **P-15**, P-77
Sakao, T., CT-38
Sako, N., CT-11, P-53
Savage, S., **CT-36**, P-84
Savcheva, A. S., **CT-8**, P-51
Savin, D. W., P-45
Scharmer, G. B., **P-16**
Schlichenmaier, R., P-6
Schmieder, B., **P-4**, P-7, **P-39**, P-65
Schmit, D., **P-17**, P-34
Schrijver, C.J., IT-12
Schwadron, N. A., P-105
Schwartz, P., **P-18**
Scott, J., P-54
Scullion, E., **P-19**
Seaton, D. B., CT-36, P-85
Sechler, M., CT-18
Sekii, T., **P-33**, P-37
Sekse, D., P-77
Severino, G., P-67
Sharma, R., P-54
Shestov, S. V., **CT-30**, P-56
Shibata, K., CT-4, CT-16, CT-27

Shimizu, T., **CT-6**, CT-35, CT-38, P-89, P-90
Shimojo, M., CT-11, P-53
Shiota, D., **CT-11**
Solanki, S. K., CT-7
Song, D., P-109
Stein, R., **P-20**
Steiner, O., **IT-1**, P-70
Stenborg, G., P-51
Stenflo, J.O., P-10
Stepan, J., CT-37, CT-38, **P-40**
Sterling, A. C., CT-31, P-52, P-86, **P-87**, P-97
Straus, T., P-67
Su, Yingna, **CT-29**, **P-21**, **P-99**
Su, Yang, CT-36
Suematsu, Y., CT-6, CT-38, **P-75**, P-109
Surges, V., CT-29
Suzuki, T. K., CT-25
Svanda, M., P-42
Takeda, A., **P-57**
Tanabe, H., CT-26, P-71, **P-76**
Tarbell, T.D., IT-12, P-15, **P-77**
Tarr, L., **P-41**
Terradas, J., **P-58**
Terzo S., **P-59**
Testa, P., **IT-11**, P-55, P-69, P-113
Tian, H., **CT-18**, **P-78**, **P-100**
Tian, Z., **P-60**
Title, A., IT-12, P-15
Tiwari, S. K., **CT-7**
Toriumi, S., **CT-2**
Tripathi, D., CT-21
Tsuneta, S., **IT-13**, CT-11, CT-19, CT-38, **P-79**, P-109
Ueda, K., CT-19, P-79
Uitenbroek, H., P-43
Uribe-Patarroyo, N., **P-107**
van Ballegooijen, A., CT-8, CT-29, P-21, P-99
van Driel-Gesztelyi, L., CT-24, CT-28, P-14
Varady, M., **P-101**, **P-102**
Veronig, CT-31
Verwichte, E., CT-5
Walsh, R. W., **P-61**, **P-88**
Wang, H., CT-9
Wang, T., **CT-17**, **P-80**
Wang, X., CT-18, P-100
Wang, Y.-M., P-48
Warren, H. P., P-48, **P-81**
Watanabe, H., CT-38, P-109
Watanabe, K., P-89, **P-90**
Watanabe, T., CT-33, CT-35, **P-89**
Webb, D. F., P-85
Weber, M.A., P-106, P-108
Wedemeyer, S., P-19
West, E., CT-38
Williams, D.R., **CT-3**, P-49
Winebarger, A., **IT-7**, CT-38, P-66, P-108
Winter, H., **P-103**
Woods, T., P-46
Wray, A.A., P-9, P-10
Wuelser, J.-P., IT-12
Yamada, T., CT-26
Yamamoto, T. T., CT-34
Yan, Y., CT-9
Yokoyama, T., CT-2, P-8, P-12, P-47, **P-104**
Yoshimura, K., P-57
You, S., P-76
Young, P. R., CT-33, P-48, **P-62**
Yurchyshyn, V., P-11
Zapior, M., P-39, P-82, **P-94**
Zhang, M., **IT-9**, P-22
Zhao, J., P-37